©2014

Gongping Sun

ALL RIGHTS RESERVED

HIPPO SIGNALING IN REGENERATION AND NEOPLASTIC TUMORS

by

GONGPING SUN

A dissertation submitted to the

Graduate School-New Brunswick

Rutgers, The State University of New Jersey

and

The Graduate School of Biomedical Sciences

University of Medicine and Dentistry of New Jersey

In partial fulfillment of the requirements

For the degree of

Doctor of Philosophy

Graduate Program in Cell and Developmental Biology

Written under the direction of

Kenneth D. Irvine

and approved by

_____

_____

_____

_____

New Brunswick, New Jersey

May, 2014

ABSTRACT OF THE DISSERTATION

HIPPO SIGNALING IN REGENERATION AND NEOPLASTIC TUMORS

by GONGPING SUN

Dissertation Director:

Kenneth D. Irvine

Hippo signaling controls organ size during development from *Drosophila* to humans. It limits tissue growth through regulation of cell proliferation and apoptosis. Deregulation of Hippo signaling leads to tissue overgrowth and tumor formation. An important characteristic of Hippo signaling is its connection to other pathways, through which Hippo signaling plays an indispensable role in diverse biological processes.

We found, in addition to regulating growth during development, Hippo signaling regulates growth during regeneration. The growth suppression effect of Hippo signaling is through inhibition of a transcriptional co-activator Yorkie (Yki). Yki can promote cell proliferation and suppress apoptosis. Using the *Drosophila* wing imaginal disc, a mono-layered epithelial tissue, as a model, we found Yki is activated in the wing discs in response to apoptosis induction. Yki remains active over the entire wing disc regeneration. Yki activation during regeneration requires c-Jun N-terminal kinase (JNK). JNK activation of Yki is independent of cell death, and through a Hippo pathway component, Jub (a fly Ajuba LIM domain protein). Both Yki and Jub are required for wing regeneration.

We also observed activation of Yki in the neoplastic tumors caused by disruption of epithelial apical-basal polarity. The growth of the neoplastic tumors is JNK-dependent. Like in regeneration, Yki activation in the neoplastic tumors also requires regulation of Jub by JNK. Reduction of Yki or Jub level suppresses tumor growth. Our work identified Jnk regulation of Hippo signaling as an important mechanism to drive the stress-responsive tissue growth, and established Jub and Yki as stress-responsive molecules.

JNK regulation of Yki is also conserved in mammalian cells. Using cultured epithelial cell lines, we found manipulation of JNK activity affects the activity of YAP (the mammalian homolog of Yki), like what we observed in flies. And JNK influences the binding of the mammalian Ajuba proteins to LATS (the mammalian homolog of Wts, a core kinase that suppresses Yki activity) through a phosphorylation-dependent mechanism. Ajuba proteins may serve as a hub connecting multiple pathways to the Hippo pathway as the binding between Ajuba proteins and LATS can also be regulated by other signaling pathways. The activity of Ajuba proteins may depend on their conformation.

ACKNOWLEDGEMENT

First, I would like to thank my advisor, Ken, for his support, training, and patience during these years. He always pointed out the key scientific questions in my projects, which gave the direction for the research, and also left me a lot of freedom to explore my own interests. He generously made suggestions when I met problems on the research and the career, and patiently encouraged me whenever I felt frustrated. I have learned a lot from him on how to view and approach scientific issues.

I would also like to thank my committee members, Dr. Richard Padgett, Dr. Ruth Steward, Dr. Vassiliki Karantza, and Dr. Kim Mckim, for their suggestions and help on my graduate research and my future career.

I am very grateful to my current and former labmates. My work could not go smoothly without their help. In particular, I want to thank: Cordelia, for training me with the confocal imaging, dissection, and immunostaining, which are the most essential techniques of my research; Guohui and Yongqiang, for teaching me how to make the genomic rescue constructs; Veronica, for sharing the tricks in mammalian cell culture; Venu, for suggestions in the biochemical experiments; Shuguo, for always sharing his thoughts and understanding on Hippo pathway and the general biological sciences with me, and for the collaboration in the labor-intensive discs dissection; Elmira and Ed, for providing the essential reagents; Shemeekah, for helping me set up everything when I joined the lab.

The work in this dissertation was funded by Howard Hughes Medical Institute and the Human Frontier Science Program. And I also want to thank the graduate program in Molecular Biosciences for the first year fellowship.

Finally, I want to thank my parents who are always there whenever I need help, suggestions, and support, and always have faith in my career. And special thank to my fiancé, who understands my pursuit, and always loves me even though we only have a little time to stay together during the six years.

TABLE OF CONTENTS

LIST OF TABLES

LIST OF ILLUSTRATIONS

CHAPTER I

General introduction

Section 2 in this chapter was published in *Curr Top Dev Biol 108 (2014): 95-120*.

The text for this section was written jointly by Gongping Sun and Kenneth D. Irvine.

1. *Drosophila* wing imaginal discs

The *Drosophila* imaginal discs are the larval precursors for adult appendages, and consist of undifferentiated, proliferating epithelial cells. They are a single cell layer thick, form at embryonic stages, and grow through cell proliferation during larval stages. One important characteristic of growth in the wing disc, which develops to the adult wing, is compartmentalization. Cells in the wing disc are organized into different compartments. Cell lineages are restricted within compartments, and never cross the boundary. At the boundary separating the anterior compartment and the posterior compartment (A/P boundary) is a stripe of cells expressing Decapentaplegic (Dpp). The dorsoventral boundary (D/V boundary at the interface of the dorsal compartment and the ventral compartment) is perpendicular to A/P boundary, and cells there express Wingless (Wg) (Fig 1). The establishment of the anterior compartment and the posterior compartment occurs at the embryonic stage under the control of a homeobox gene *engrailed* (*en*). The expression of En gives cells the posterior identity, and the cells not expressing En become anterior. En induces the expression of Hedgehog (Hh) from the posterior cells, which triggers the expression of Dpp in the anterior cells and formation of the A/P boundary. The dorsal cells are specified by the expression of *apterous* (*ap*), and the cells not expressing *ap* are the ventral cells. Dpp and Wg are secreted from the A/P and D/V boundary, and diffuse to form concentration gradients to control the fate of the cells in the wing disc[1, 2].

The wing disc forms not only the adult wing blade but also the hinge that connects the wing blade to the body, and the notum (Fig 1). The area that develops to the wing blade, called wing pouch, is defined by the expression of Vestigial (Vg) under the

control by Wg. The formation of the hinge region requires two transcription factors, Homothorax (Hth) and Teashirt (Tsh). Hth and Vg antagonize each other to keep the entity of the pouch and the hinge. The development of the notum requires Vein-EGFR signaling. Vein and Wg repel each other to separate the notum and the wing area[1].

The wing disc is a monolayered tissue, so the organization of the wing disc is limited to two dimensions with the distal part at the center surrounded by the proximal region. During the pupation, the wing disc evaginates at the D/V boundary, and the dorsal and the ventral part adhere together to form a three-dimensional structure. The D/V boundary forms the margin of the wing.

2. Regeneration in *Drosophila* wing imaginal discs

Regeneration enables animals to recover from severe organ damage or amputation by restoring fully formed and functional organs. Regeneration exists in all the metazoa but the capacity for regeneration varies from species to species. For example, Planaria and *Hydra* are famous for their incredible capacity for regeneration, which can restore the whole body from a small part. Amphibians can regenerate several functional organs depending upon the species, such as limbs, tails, and lens. By contrast mammals have only a very limited capacity to regenerate damaged organs. In 1901, Morgan classified regeneration into two types, epimorphosis and morphallaxis [3]. Morphallaxis is regeneration through remodeling of pre-existing cells, whereas epimorphosis is regeneration in which growth contributes to restoration of missing tissue [4, 5]. Regeneration in many animals is actually a combination of morphallaxis and epimorphosis. While epimorphic regeneration requires several steps, including wound closure, activation of pre-existing stem cells or de-differentiation of differentiated cells, cell proliferation, patterning of newly formed tissue, and differentiation [6, 7], a distinguishing feature is the reliance on precisely controlled proliferation to restore correctly sized organs.

The *Drosophila* wing imaginal disc is a widely used model to study regulatory mechanisms of cell proliferation during regeneration because of its high regenerative capacity and the ease of genetic manipulation [8]. Imaginal disc regeneration can be studied after surgical excision of part of the disc, and such studies have contributed to our understanding of how positional information influences regenerative growth [9]. More recently, regeneration has been studied after genetic ablation of a portion of a developing

imaginal disc, typically induced by localized, transient expression of pro-apoptotic genes like *reaper*, *hid*, or *eiger* [10-13].

Regeneration in wing discs involves two processes: clearance of damaged cells through apoptosis, and elevated proliferation near dying cells to compensate the loss of cells, which is referred to as compensatory cell proliferation[14]. Apoptosis is not only a way to remove damaged cells, but also an important trigger stimulating the proliferation of nearby healthy cells. In wing discs, stimulating apoptosis while blocking the execution of apoptosis leads to sustained compensatory proliferation, and consequently tissue overgrowth. This can occur in animals mutant for the effector caspase Drice/Dcp-1[15], or when a Drice inhibitor, the bacculovirus P35 protein, is expressed [16-18]. Conversely, if apoptosis is prevented at an earlier step, by mutation or down-regulation of the initiator caspase Dronc, then compensatory cell proliferation does not occur. These observations indicate that it is not simply the elimination of cells that triggers compensatory proliferation, but specific molecular events associated with induction of apoptosis.

c-Jun N-terminal kinase (JNK) is found among the first responding molecules after tissue damage and an essential modulator of regenerative growth. JNK activity appears at the leading edge of healing tissues quickly after genetic or surgical ablation, and persists and broadens during and after wound healing [19, 20]. JNK activation is also essential for apoptosis-induced compensatory cell proliferation [16]. As noted above, blocking effector caspase activity by over-expressing P35 blocks the removal of dying cells, but these ‘undead’ cells keep triggering compensatory proliferation, causing hyperplastic growth in discs [16, 21]. These observations revealed that compensatory cell proliferation is a response to molecular events associated with induction of apoptosis, and

consistent with this, JNK activation, which is required for hyperplastic disc growth induced by undead cells, can be induced by activation of the initiator Caspase Dronc [22]. There is also a potential for positive feedback between JNK and Dronc (Fig. 2), as activation of JNK can promote apoptosis through upregulation of *hid* and *reaper*, which leads to Dronc activation [23].

Lineage analysis experiments have revealed that a large proportion of the cells that contribute to regeneration after disc damage arise from cells with JNK-activation [24]. Moreover, blocking JNK activity significantly suppresses wing disc regeneration and compensatory proliferation in response to genetic ablation, amputation or irradiation [16, 20, 25]. The growth-promoting function of JNK during wing disc regeneration stems from its regulation of other growth control pathways (Fig. 2). Activation of JNK leads to localized elevation of Wg (*Drosophila* homolog of Wnt1) and Dpp (a *Drosophila* homolog of BMPs), and activation of the downstream effector of Hippo signaling, Yki [11, 13, 16-18].

The roles of Wg and Dpp upregulation in the wing disc damage response are complex, and context-dependent. When wing discs expressing P35 were subject to irradiation or co-expression of pro-apoptotic genes, ectopic Wg and Dpp expression were detected both in ‘undead’ cells and also in normal cells nearby [21]. Both Wg and Dpp are required for the hyperplastic growth caused by ‘undead’ cells [21, 26]. However, in the absence of P35 expression, though ectopic expression of Wg and Dpp is observed in irradiated discs[17], it is dispensible for compensatory cell proliferation [26]. When a portion of a disc is ablated by transient expression of pro-apoptotic genes in the absence of P35, different responses have been observed depending upon the pro-apoptotic gene

employed. When apoptosis is induced by expressing *eiger* or *reaper*, proliferation is stimulated at the edge of the wound, and Wg is required for this compensatory cell proliferation and for wing regeneration [10]. At least in part, this occurs through Wg down-regulating Notch, which leads to upregulation of Myc [10]. Intriguingly, when apoptosis is induced by expressing the pro-apoptotic gene, *hid*, Wg and Dpp expression patterns are not altered [12]. Moreover, knocking down *wg* does not block wing regeneration after *hid* expression [12]. But unlike the localized elevation of proliferation observed after *egr*- or *rpr*-induced ablation [10], or proliferation associated with 'undead' cells [16], after *hid*-induced ablation, elevated proliferation is induced uniformly throughout the regenerating disc [12]. The basis for these differences in patterns of cell proliferation during regeneration and requirement for mitogenic signals is not yet clear. They might in part reflect differences in the efficiency of genetic ablation, but it seems that there are multiple, distinct mechanisms that can promote cell proliferation during disc regeneration, which may be preferentially induced depending upon the nature of the tissue damage.

3. Neoplastic tumors in *Drosophila* imaginal discs

In *Drosophila*, the apical-basal polarity of the disc epithelia is determined during embryogenesis. Establishment of apical-basal polarity involves three complexes, the aPKC/Baz/Par-6 complex (atypical protein kinase C/Bazooka/Par-6), the Crb/Patj/Sdt (Crumbs/PALS1-associated tight junction protein/Stardust) complex, and the Lgl/Scrib/Dlg (Lethal giant larvae/Scribbled/Disc large). The aPKC/Baz/Par-6 complex and Crb/Patj/Sdt complex localize at the apical domain and repel the Lgl/Scrib/Dlg complex from the apical domain. The Lgl/Scrib/Dlg complex localizes at the basolateral region. Disruption of this complex causes expansion of the apical domain[27].

The imaginal discs of lgl^-, $scrib^-$, or dlg^- mutants are multilayered with disrupted epithelial structure, and fuse together to form an overgrown mass at the anterior of the larvae. The mutant animals finally die as giant larvae. Mutation of any component of the Lgl/Scrib/Dlg complex in the whole imaginal discs from embryo stage results in neoplastic tissue overgrowth and metastasis, thus these three proteins are categorized as neoplastic tumor suppressors[27, 28]. However, unlike mutation in some tumor suppressors that makes the mutant cells outcompete wild type cells, the lgl^-, or $scrib^-$ or dlg^- mutant cells are with growth disadvantage compared with wild type cells. Therefore, when mutant clones are induced in imaginal discs surrounding by wild type cells, they are eliminated through cell competition. The elimination of mutant clones requires JNK activity in two aspects: JNK activation in the mutant clones causes autonomous apoptosis; JNK activation in the neighboring wild type cells drives the engulfment of the mutant cells by the neighboring cells[29]. Combination of lgl^-, or $scrib^-$ or dlg^- with some oncogenic mutation like ras^{V12} or activated Notch transforms the mutant clones to

overgrown, invasive tumors, like what is observed in the whole tissue mutants[30]. Interestingly, the overgrowth in combined mutant clones and whole tissue mutants also requires JNK activity[31] (Fig 3). Thus the cell fate upon JNK activation is context-dependent, though the switch between the pro-proliferation and the pro-apoptosis function of JNK is elusive. Besides JNK, other growth control pathways are also involved in the neoplastic tumor growth, like JAK/STAT, which functions downstream of JNK[32]. In this study, we found Yki acts downstream of JNK to promote neoplastic tumor growth. In *Drosophila* midgut regeneration, Unpaired, the ligand for JAK/STAT pathway, is identified as a Yki target[33]. Thus in the neoplastic tumors, JNK-activated Yki may also drive activation of JAK/STAT pathway (Fig 3).

4. Hippo signaling

4.1 The core kinase cassette

Hippo signaling is an essential pathway that limits growth during development. It controls developmental and pathological growth through regulating cell proliferation, cell survival, and stem cell maintenance. The core of the pathway is composed of two kinases, Hippo (Hpo) and Warts (Wts), and two scaffold proteins Salvador (Sav) and Mob as tumor suppressor (Mats) (Fig 4A). These four proteins are all identified from genetic screening in *Drosophila* as tumor suppressors. Clones with mutation in any of these four genes exihibit overgrowth, increased proliferation, reduced apoptosis, delayed cell cycle exit, and elevated transcription of Cyclin E and DIAP1 [34-43].

The core kinase cassette is highly conserved in mammals (Fig 4B). Deficiency of LATS1/2 (mammalian homologs of Wts), MST1/2 (mammalian homologs of Hpo), WW45 (mammalian homolog of Sav), or MOB1 (mammalian homolog of Mats) are linked to cancers in human or mice [37, 44-47].

Hpo is the most upstream kinase in the cassette. Hpo activation requires phosphorylation at Thr-195[48]. Phosphorylation at this site can be promoted by dimerization of Hpo [49, 50]. And another Ste20 family kinase Tao1 is responsible for phosphorylation of Hpo at this site [51, 52].

The molecular interaction within the core cassette has been studied in both flies and mammals [38-42, 53-55]. Activated Hpo phosphorylates Sav, Wts and Mats. The phosphorylated Mats binds to Wts and promotes the autophosphorylation of a serine in the activation loop of Wts. Hpo phosphorylates Wts at a threonine in the hydrophobic

motif in C-terminal through the interaction with Sav. Activation of Wts requires phosphorylation on both sites (Fig 4).

4.2 Direct negative regulators of the core kinase cassette

The core kinase cassette conveys multiple extracellular and intracellular signals to transcription regulation, so the activity of the core kinases must be under precise control. Identification of the negative regulators of the core kinase cassette is of the same importance as elucidation of the kinase activation cascade.

The Ras association family (RASSF) proteins can bind to Hpo and negatively regulate Hpo activity [56]. Two mechanisms involved in the inhibition of Hpo activity by RASSF, competing with Sav for Hpo binding, and mediating the interaction between Hpo and a PP2A complex, dSTRIPAK, which is a phosphatase for Hpo [56, 57]. Recently, a serine/threonine kinase, Par-1, has been reported to interact with Hpo/Sav complex and inhibits Hpo through phosphorylation of Hpo [58]. Another suppressor of Hpo/Sav complex activity is the salt-inducible kinase (Sik), which inhibits Sav through phosphorylation [59] (Fig 5A).

The direct negative regulators of Wts/LATS identified are all from the Zyxin protein family. In mammals, the Zyxin protein family contains the LIM domain proteins Zyxin, Ajuba, LIMD1, WTIP, LPP, and TRIP6, all with three LIM domains at the C-terminus to mediate protein-protein interactions. The Zyxin family proteins localize to the adherens junctions and the focal adhesions[60], and link the cytoskeleton to cell junctions[61-63]. According to the sequence similarity, proteins in the Zyxin family can be further divided to two subgroups, the Zyxin proteins (Zyxin, LPP, and TRIP6), and the Ajuba proteins (Ajuba, LIMD1, WTIP). In *Drosophila*, there is only one Zyxin protein,

Zyxin, and one Ajuba protein, Jub. Both Zyxin and Jub suppress Wts, but through different mechanisms. Jub, and mammalian Ajuba proteins, Ajuba, LIMD1, and WTIP, inhibit Wts and LATS activity through their binding to Wts and LATS[64] (Fig 5B). Zyxin regulates Wts by affecting its stability, but the mechanism is not clear [65] (Fig 5C).

4.3 The downstream effector

The major effect of Hippo signaling on regulation of cell proliferation, cell death and cell cycle progression is transcriptional regulation. Activated Wts regulates transcription through inhibition of a transcription co-activator, Yorkie (Yki). The activity of Yki is closely related to its subcellular localization, as cytoplasmic Yki has no activity in transcription regulation. Yki was first identified as a Wts-binding protein. It interacts with Wts through its WW domain and the PPXY domain in Wts [66]. The WW domain in Yki can also interact with Hpo and Ex [67, 68]. These physical interactions contribute to cytoplasmic retention of Yki, but the major way Wts suppresses Yki is phosphorylating Yki. The phosphorylated Yki is held in the cytoplasm by protein 14-3-3 [66, 69-71]. The mammalian homologs of Yki are YAP and TAZ, which can be phosphorylated by LATS [72-74]. In mammalian cells, phosphorylation of YAP and TAZ affects not only their subcellular localization but also the protein stability. LATS phosphorylation of YAP or TAZ primes a subsequent phosphorylation by CKIδ/ε and the recruitment of $SCF^{\beta\text{-}TRCP}$ E3 ligase [75, 76]. The phosphorylation-dependent cytoplasmic retention, phosphorylation-independent cytoplasmic retention, and phosphorylation-dependent degradation are three major ways to regulate Yki/YAP/TAZ activity.

The Yki target genes can be divided to the following groups: anti-apoptosis genes, DIAP1[66], microRNA *bantam* (inhibitor of the pro-apoptotic protein Hid)[77, 78]; regulators of cell cycle and proliferation, dE2F1, Cyclin E[79], Myc[80]; ligands for other signaling pathways, Unpaired[33], Wg[81], EGFR ligands[82]; upstream regulators of Hippo pathway (for negative feedback), Ex, Mer[83], Kibra[84], Fj[85].

Activation of Yki resembles the phenotypes of *wts*, *hpo*, or *sav* mutant, as the clones overexpressing wild type or activated Yki exhibit overgrowth, increased proliferation and reduced apoptosis. And recently, Yki activity has also been related to expansion of intestinal stem cells in *Drosophila* midgut during regeneration[86, 87]. Like Yki in *Drosophila*, the major biological effect of mammalian YAP and TAZ is promoting proliferation. Overexpression of YAP in mice results in tumor in multiple tissues[47, 69, 88]. And high activity of YAP has been linked to human cancers[89, 90]. YAP and TAZ are also required for maintenance of stem/progenitor cells in many organs including intestine, liver, skin[91-94]. Mammalian YAP and TAZ have some other functions that have not been discovered for *Drosophila* Yki. YAP and TAZ can promote cell migration, and thus may participate in tumor metastasis[95, 96]. YAP is also considered as a promoter of apoptosis through its interaction with P73[97, 98], but so far this phenomenon has not been observed in animal models. And a recent study stating miR-29, a PTEN suppressor, as a YAP target links YAP to cell size control[99].

4.4 The upstream regulators of the core kinase cassette

Hippo pathway can be regulated by multiple upstream signals, including cell-cell contact, signals from cell junction, cell polarity, and as recently found, mechanical tension.

4.4.1 Cell junction

With more and more Hippo signaling upstream regulators revealed, the apical region and the cell junctions become critical regulatory regions for Hippo signaling. The first identified upstream regulators of Hippo signaling are two FERM (4.1, Ezrin, Radixin, Moesin) domain proteins, Expanded (Ex) and Merlin (Mer)[83]. Ex and Mer form a complex at the apical domain in epithelia and suppress cell proliferation through activation of Hippo signaling[83, 100]. The mammalian homolog of Mer, Neurofibromatosis-2 (NF2), is the first Hippo pathway component for which loss-of-function mutations were reported to cause human cancer[101]. Ex and Mer are genetically put upstream of Hpo, but how Ex and Mer activated Hpo is not clear. Ex and Mer form a complex with Kibra. Kibra can interact with the core kinase cassette as well as interact with Ex and Mer[84, 102, 103]. So Kibra may bring the core kinase complex to the Ex/Mer complex. Most recently, another model of Ex/Mer regulation of Hpo/Sav/Wts/Mats (H/S/W/M) complex has been proposed. In contrast with the classical model that Mer regulates H/S/W/M complex upstream of Hpo, in the new model, Wts and Hpo are recruited to the cell membrane by Mer and Sav, respectively; then, Hpo phosphorylates Wts at the membrane[104]. More studies are needed to elucidate the activation mechanism of H/S/W/M complex.

An apical-basal polarity determinant Crumbs (Crb) has been linked to Hippo signaling. In *Drosophila* imaginal discs, Crb localizes at apical membrane and overexpression of Crb causes tissue overgrowth through suppression of Hippo signaling. Crb interacts with Ex through its juxtamembrane FERM-binding motif and regulates the apical localization of Ex[105-108]. The interaction of Crb and Hippo signaling in

mammalian cells has also been reported, but the identified function of the mammalian homolog of Crb in Hippo signaing is to recruit YAP/TAZ to apical region[109].

One important role of Hippo signaling in mammalian epithelial cells is to mediate cell-cell contact inhibition. The adherens junction complex, E-cadherin/catenin complex activates Hippo signaling through the mammalian NF2, thus suppresses YAP activity to promote cell proliferation in mammalian epithelial cells[110]. α-catenin can also sequester YAP at the adherens junction through direct physical interaction, therefore blocks activation of YAP[110, 111].

Cell-cell contact also regulates Hippo signaling through the tight junction. The tight junction protein, Angiomotin (AMOT), interacts with YAP and increases the cytoplasmic retention of YAP[112, 113]. In addition, AMOT can also interact with LATS, thus may act as a scaffold protein to mediate phosphorylation of YAP by LATS[113].

4.4.2 Other signaling pathways

Fat (Ft), an atypical cadherin protein localized at the apical membrane, is a membrane receptor that is activated by its ligand, another cadherin protein Dachsous (Ds). Ft-Ds pathway regulates both planar cell polarity and cell proliferation. The proliferation regulation of Ft-Ds is through Hippo signaling. Ft may regulate Hippo signaling through two different mechanisms. Ft may activate Hippo signaling through regulating Ex localization[114-116], but *ft* and *ex* double mutants show severe phenotypes than *ft* or *ex* single mutation, suggesting Ft also works in parallel with Ex[117]. After activation, Ft interferes with the subcellular localization of Dachs, which promotes the interaction with Zyxin and Wts. And the formation of Zyxin/Wts complex

may cause degradation of Wts[65, 117], but how Zyxin participates in regulation of Wts stability is unclear.

In recent years, more and more signaling has been linked to Hippo signaling. The G-protein coupled receptor (GPCR) mediates serum-induced YAP activation through Rho GTPase and the subsequent F-actin polymerization [118]. In *Drosophila*, the epidermal growth factor receptor (EGFR) signaling suppresses Hippo signaling through Jub to regulate glial cell proliferation [119]. In mammalian epithelial cells, the cross-talk between EGFR signaling and Hippo signaling is also observed, but mechanism is different. In mammals, activation of EGFR leads to dissociation of the H/S/W/M complex and YAP activation through interaction between PDK1 (Phosphoinositide-dependent kinase-1) and Sav [120].

The stress-activated protein kinase JNK can directly phosphorylate YAP, but the effect of this phosphorylation on YAP activity is controversial[121, 122]. In *Drosophila*, JNK activation of Yki is found in adult midgut regeneration[33]. And in this study, we found JNK inhibits Hippo signaling through Jub during wing disc regeneration and in *lgl*$^{-}$ neoplastic tumors. However, other researchers have reported in *scrib*$^{-}$ or *src*-overexpressing clones, JNK promotes Hippo signaling activity to suppress cell proliferation[123, 124]. So it is most likely JNK regulation of Hippo signaling is context-dependent.

4.4.3 Cytoskeleton and mechanical signals

Cells *in vivo* undergo diverse mechanical stress, including stretching and compression from the neighboring cells and adhesion to the extracellular matrix (ECM). The mechanical signals influence cell proliferation, survival, differentiation and

migration. In recently years, the role of YAP and TAZ in mechanical signals transduction to growth has been brought to the focus. The activity of YAP and TAZ can be regulated by cell density, cell size, and the stiffness of ECM[125-127]. However, whether the mechanical regulation of YAP and TAZ requires Hippo signaling is controversial. In *Dupont et al* (2011) and *Aragona et al* (2013) papers, regulation of YAP/TAZ by cell morphology and ECM stiffness are considered independent of LATS. However, another group reported loss of attachment to ECM activates YAP through suppression of LATS activity [46]. This difference may be due to different cell types and different method to change the mechanical tension applied to cells.

The three studies mentioned above have all pointed out the requirement of rearrangement of actin cytoskeleton[46, 125, 126]. In *Drosophila*, F-actin has already been linked to Hippo signaling. Ectopic accumulation of F-actin at the apical region suppresses Hippo signaling and activates Yki[128, 129]. Actually F-actin also mediates GPCR signaling regulation of Hippo signaling in mammalian cells[118]. Thus, actin cytoskeleton is an important regulator of Hippo signaling that transduces extracellular physical and chemical signals to Hippo signaling.

Figures

Fig 1. *Drosophila* wing imaginal disc

Illustration of the anterior (A), posterior (P), dorsal (D), ventral (V) domains of the *Drosophila* wing disc, and regions that develop to the wing blade (pouch), the hinge and the notum. Adopted from ref[130].

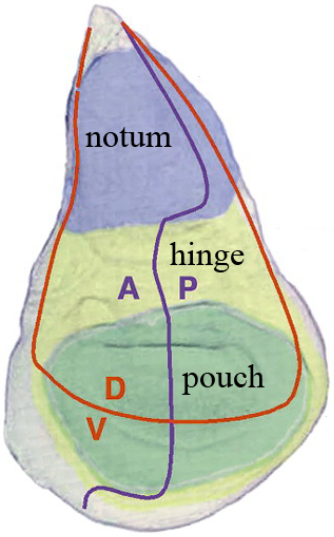

Fig 2 Signaling network promoting *Drosophila* wing disc regeneration

Schematic of regulatory interactions between components of signaling pathways involved in promoting *Drosophila* wing disc regeneration. The blue rectangles are two adjacent epithelial cells.

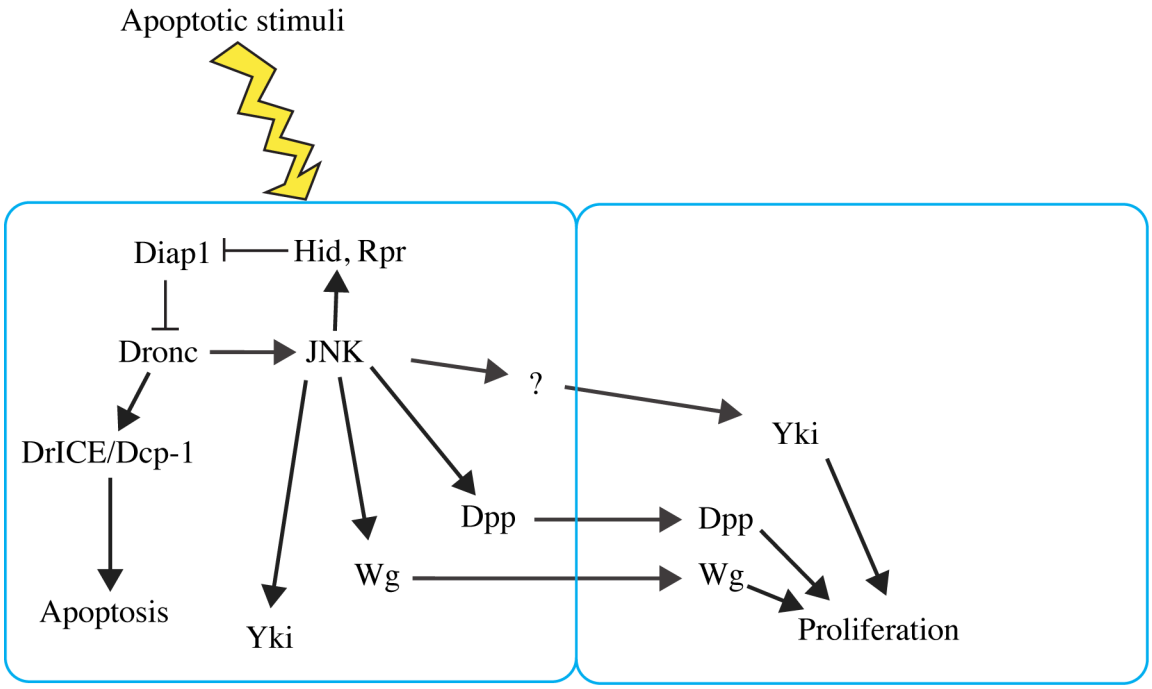

Fig 3. Signaling network regulates the neoplastic tumor growth.

A) The mechanism underlying the elimination of *lgl*$^{-}$, *scrib*$^{-}$, or *dlg*$^{-}$ clones in the imaginal discs. B) The signaling network involved in the overgrowth of *lgl*$^{-}$, *scrib*$^{-}$, or *dlg*$^{-}$ clones with oncogenic *Ras*^{V12}. Modified from ref [32]

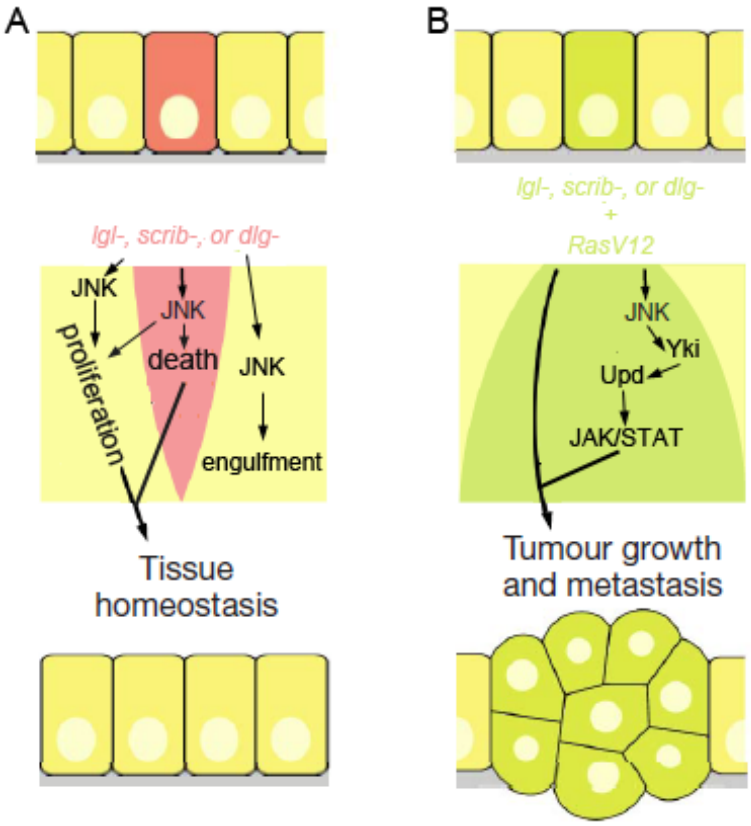

Fig 4. The core components of Hippo signaling in *Drosophila* and in mammals. Illustration of the core kinase cassette of Hippo signaling in *Drosophila* (A) and in mammals (B). Proteins that are homologs are indicated in the same color. The green "P" demonstrates phosphorylation that activates the protein.

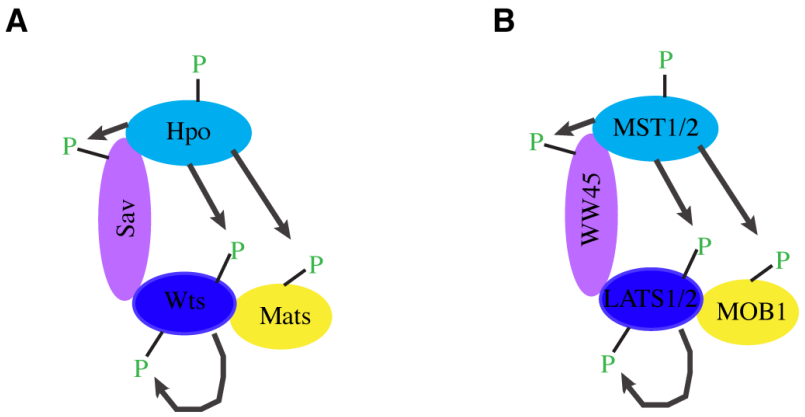

Drosophila Mammal

Fig 5. Direct regulation of the core kinase cassette of Hippo signaling in *Drosophila*. A) Illustration of the regulation of the core kinase cassette of Hippo signaling in *Drosophila* by the kinases and phosphatases. The green "P" indicates the phosphorylation site that activates the protein, and the red "P" indicates the phosphorylation site that suppresses the protein. B) Jub suppresses Hippo signaling through binding to Wts, possibly because of disruption of the kinase complex. C) Zyxin binds Wts to promote its degradation.

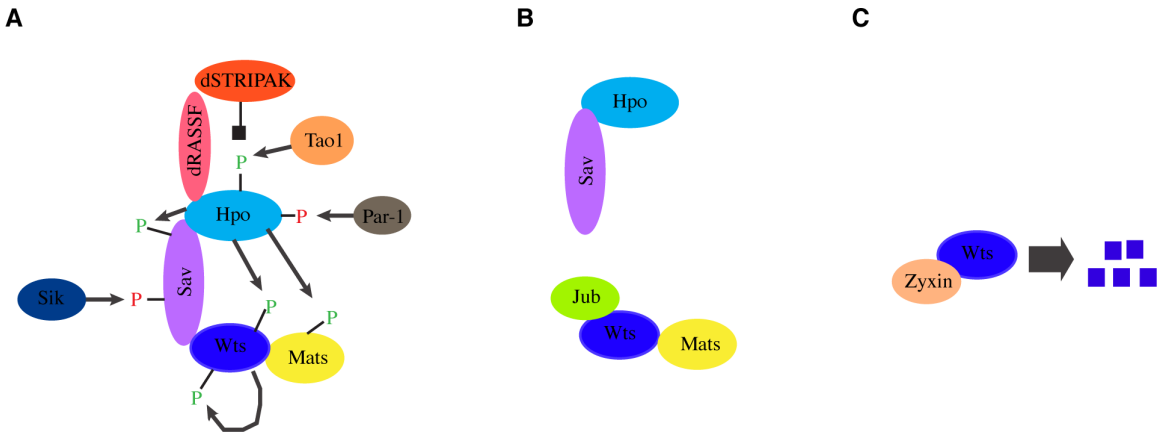

CHAPTER II

Regulation of Hippo signaling by Jun kinase signaling during compensatory cell proliferation and regeneration, and in neoplastic tumors

This chapter was published in *Dev Biol 350 (2011), 139-151*

Gongping Sun performed all of the experiments described. The chapter was written jointly by Gongping Sun and Kenneth D. Irvine.

Summary

When cells undergo apoptosis, they can stimulate the proliferation of nearby cells, a process referred to as compensatory cell proliferation. The stimulation of proliferation in response to tissue damage or removal is also central to epimorphic regeneration. The Hippo signaling pathway has emerged as an important regulator of growth during normal development and oncogenesis from *Drosophila* to humans. Here we show that induction of apoptosis in the *Drosophila* wing imaginal disc stimulates activation of the Hippo pathway transcription factor Yorkie in surviving and nearby cells, and that Yorkie is required for the ability of the wing to regenerate after genetic ablation of the wing primordia. Induction of apoptosis activates Yorkie through the Jun kinase pathway, and direct activation of Jun kinase signaling also promotes Yorkie activation in the wing disc. We also show that depletion of neoplastic tumor suppressor genes, including *lethal giant larvae* and *discs large*, or activation of aPKC, activates Yorkie through Jun kinase signaling, and that Jun kinase activation is necessary, but not sufficient, for the disruption of apical-basal polarity associated with loss of *lethal giant larvae*. Our observations identify Jnk signaling as a modulator of Hippo pathway activity in wing imaginal discs, and implicate Yorkie activation in compensatory cell proliferation and disc regeneration.

Introduction

When cells in a tissue are damaged, proliferation of neighboring cells can be induced, enabling tissue repair. This phenomenon is central to epimorphic regeneration, which enables the regrowth and replacement of body parts after injury or amputation. The capacity of tissues to undergo epimorphic regeneration has been known for centuries and exists throughout the metazoa, although it varies between organisms, organs, and developmental stages. An important insight into epimorphic regeneration was provided by the observation that when cells initiate apoptosis, they produce mitogenic signals, thereby stimulating the proliferation of neighboring cells. This process, termed compensatory cell proliferation, was first characterized in the developing imaginal discs of *Drosophila*, but similar phenomena occur in other systems [reviewed in 8, 131].

Compensatory cell proliferation has been observed in *Drosophila* imaginal discs upon induction of cell death by X-irradiation, by expression of pro-apoptotic genes, or by mutation of the anti-apoptotic gene *thread* (*Diap1*) [16-18, 132]. Compensatory cell proliferation is associated with the induction of signaling molecules that have been linked to the promotion of cell proliferation, including Wingless (Wg) and Decapentaplegic (Dpp) [16-18]. Another common and essential feature of compensatory cell proliferation is the activation of Jun-kinase (Jnk) signaling [16, 26, 131]. Jnk signaling is a MAPK signaling pathway regulated by diverse cellular stresses, including irradiation, reactive oxygen species, infection, aging, disruption of cell polarity, cytoskeletal changes, and induction of apoptosis [reviewed in 133, 134, 135]. Jnk signaling has distinct outcomes in different contexts. It is crucial for morphogenesis during embryogenesis and wound

healing [136], and has an important pro-apoptotic function [134, 137]. However, when apoptosis is blocked, Jnk signaling can promote cell proliferation [16, 31, 138, 139].

In addition to its role in compensatory cell proliferation, Jnk signaling has been linked to proliferative and metastatic features of tumors associated with disruptions of apical-basal polarity in epithelial cells [31, 140]. Genes that, when mutated, result in over-proliferation coupled to loss of normal tissue architecture are classified in *Drosophila* as neoplastic tumor suppressors [reviewed in 138]. Three of the best-studied neoplastic tumor suppressors, *lethal giant larvae* (*lgl*), *discs large* (*dlg*) and *scribbled* (*scrib*), form a junctional complex that contributes to apical-basal polarity in epithelial cells [141]. Their effects on growth are complex. When an entire disc is mutant for one of these genes, it can overgrow and form a tumorous mass of unpolarized cells [141, 142]. However, when clones of cells mutant for these genes are induced by mitotic recombination in wing discs, they generally fail to survive, and are eliminated by Jnk-dependent apoptosis. But if combined with other oncogenic mutations, such as expression of Myc or activated-Ras or Notch, clones of cells mutant for *lgl*, *dlg* or *scrib* can survive and form large tumors that are prone to metastasis; the growth and metastasis of these tumors also depends on Jnk signaling [30, 31, 143-145].

The Hippo pathway controls growth during normal development, and its dysregulation is associated with oncogenesis [reviewed in 146, 147]. Hippo signaling is mediated by a transcriptional co-activator protein, Yorkie (Yki) [reviewed in 148]. When Hippo signaling is active, Yki is kept inactive, retained in the cytoplasm through the action of upstream tumor suppressor genes in the Hippo pathway. The key, direct repressor of Yki activity is the kinase Warts (Wts), which phosphorylates Yki [66]. In the

absence of Wts, unphosphorylated Yki accumulates in the nucleus [69, 70], and in conjunction with DNA-binding proteins, regulates the transcription of downstream genes. Recently, mutation of *lgl*, or over-expression of Crumbs or aPKC, were reported to result in activation of Yki, and Yki was functionally linked to over-proliferation phenotypes in these genotypes [107, 149]. The mechanism by which Yki becomes activated by these manipulations is not known, although it was suggested that it might involve mis-localization of Hippo and a Hippo-interacting protein, RASSF [107].

Here, we characterize the regulation and role of the Hippo pathway in compensatory cell proliferation and regeneration. Damage to the epithelial cells of the *Drosophila* wing imaginal disc by expression of pro-apoptotic genes results in activation of Yki. This Yki activation is mediated by the Jnk signaling pathway. We further determined that disruption of apical-basal polarity by depletion of neoplastic tumor suppressor genes, or activation of aPKC, activates Yki through Jnk signaling, and that Yki is required for wing disc regeneration after genetic ablation of the wing primordia. Our results identify Jnk signaling as a mechanism for regulating Hippo pathway activity in wing imaginal discs, and establish a fundamental role for Hippo signaling in regenerative responses to tissue damage.

Results

Activation of Yki adjacent to apoptotic cells

To investigate the potential involvement of Hippo signaling in compensatory cell proliferation and regeneration, we examined the sub-cellular localization of Yki in wing imaginal discs after localized induction of cell death. In one approach, we adopted a system developed by Smith-Bolton et al [10] for analysis of regenerative growth in imaginal discs, which involves expressing pro-apoptotic genes throughout the wing primordia of the developing disc under the control of *rotund* (*rn-Gal*), and then controlling the timing of expression using a temperature-sensitive repressor of Gal4 ($Gal80^{ts}$). The pro-apoptotic genes expressed were *reaper* (*rpr*), an inhibitor of the *Drosophila* apoptosis inhibitor Diap1 [150-152], or *eiger* (*egr*), a *Drosophila* TNFα that is a ligand for the Jnk pathway [23, 137, 153].

Normally, Yki is predominantly cytoplasmic within imaginal disc cells (Fig 1A). However, if Hippo signaling is impaired, then Yki can be detected in the nucleus [69, 70]. When *rpr* or *egr* were expressed for 30 h under *rn-Gal4* control, most of the wing primordia was ablated, although a small, irregular region of *rn-Gal4* expression persists, which includes both dying cells in which relatively stable marker proteins (ß-galactosidase or GFP) are still detectable, and some cells that appear viable (Fig. 1B,C and data not shown)[10]. Wing discs in which wing pouch cells have been ablated by expression of *rpr* or *egr* exhibit a striking re-localization of Yki to the nucleus, both in cells adjacent to the *rn-Gal4* domain, as well as among surviving cells within the *rn-Gal4* domain (Fig. 1B,C). This re-localization implies that ablation of cells and/or induction of apoptosis results in local activation of Yki. Consistent with this inference, a downstream

target of Yki, *expanded (ex)* [83], was upregulated within cells exhibiting nuclear Yki (Fig. 1D).

To investigate whether the re-localization of Yki was effected through an influence on Hippo signaling, we took advantage of the observations that over-expression of wild-type Wts has relatively little effect on wing growth in wild-type flies, but can suppress the over-growth phenotypes associated with mutation of upstream tumor suppressors that activate Yki, including *fat*, *ex*, and dco^3 [117, 154]. Over-expression of Wts similarly reduced the influence of *rpr* and *egr* on Yki localization, as strong nuclear Yki was no longer detected (Fig 1E, F). This implies that the influence of *rpr* and *egr* on Yki is mediated through an effect on Hippo signaling. Wts expression not only reduced the activation of Yki within the *rn-Gal4* domain, but also in neighboring cells, which implies that the non-autonomous activation of Yki is dependent upon Yki activation within *rpr* or *egr*-expressing cells. This inhibition of nuclear Yki by Wts over-expression was not due to inhibition of cell death, because the wing primordia was still ablated in these animals, and nuclei that, based on their small size and basal location appeared apoptotic, were still detected (not shown).

Apoptosis activates Yki through the Jnk pathway

Jnk signaling is an important regulator of both cell death and compensatory cell proliferation [16, 23, 26, 137, 153]. Egr activates Jnk signaling through its receptor Wengen [155], and inhibition of Jnk signaling suppresses Egr-overexpression phenotypes [23, 153]. We confirmed activation of Jnk signaling in *rn-Gal4 UAS-egr* discs by examining a downstream target of the Jnk pathway (*puc-lacZ*) (Figs 2A, S1A) [156].

Notably, Caspase activation can also result in Jnk activation [134], and consistent with this we observed induction of *puc-lacZ* in *rn-Gal4 UAS-rpr* discs (Fig 2B). The observations that both Egr and Rpr induce Jnk pathway activation, together with its role in compensatory cell proliferation [16, 26, 139], suggested that activation of Yki upon expressing pro-apoptotic genes might be due to Jnk activation. To test this hypothesis, we inhibited Jnk activation by expressing the Jnk phosphatase *puckered* (*puc*) [156]. Overexpression of Puc blocked Egr-induced apoptosis, and inhibited Yki activation (Figs 2C, S2B). Rpr-induced apoptosis isn't blocked by Jnk inactivation, but over-expression of Puc inhibits Rpr-induced compensatory cell proliferation [16]. When *puc* was co-expressed with *rpr*, the developing wing pouch was still ablated (Fig 2D), and apoptotic nuclei were still detected (not shown), but Yki activation was dramatically reduced (Figs 2D, S2C, cf 1B). Although low levels of Yki activation (Figs. 2C, S2B), or rare nuclei with nuclear Yki (Figs. 2D, S2C), could be detected when Puc was over-expressed, this could reflect differences in the extent and pattern of activation versus inhibition of Jnk, and our experiments establish that Jnk activation makes a crucial contribution to the activation of Yki in and adjacent to Egr- and Rpr-expressing cells.

Expression of Egr induces non-autonomous activation of Yki, but Egr is a secreted ligand for the Jnk pathway. To assess the consequences of autonomous pathway activation, we compared expression of an activated form of the Jnk kinase hemipterous (Hep.CA) [157], with expression of Egr. For these experiments we used an enhancer from the *spalt* gene (*sal.PE-Gal4*) (Fig. 2E), previously used to express *hep.CA* in studies of compensatory proliferation [26]. Most cells expressing *hep.CA* or *egr* undergo apoptosis (Figs 2F,G, S1B). Nonetheless, nuclear localization of Yki was detected within

and adjacent to surviving cells (Figs 2F,G, S2D, S2F). When *egr* was expressed, a non-autonomous effect on Yki activation, in some cases extending for several cells, was clearly evident (Figs 2G, S2D). When *hep.CA* was expressed, the non-autonomous effect was more limited, but still detectable in some cells immediately adjacent to *hep.CA*-expressing cells (Figs. 2F, S2F). Because analysis of *egr*- or *hep.CA*-expressing discs is complicated by cell death and tissue folding, we further confirmed the existence of non-autonomous Yki activation by *hep.CA* in vertical sections through the disc epithelia (Fig. 2F",G"), and in clones of cells expressing *hep.CA* or *rpr* (Fig. S1D,E).

Activation of Jnk signaling has diverse effects, but one major consequence is activation of caspases and induction of apoptosis [134]. Induction of apoptosis, and more specifically activation of the initiator caspase Dronc, can induce compensatory proliferation in neighboring cells [18]. To investigate whether caspase activation and apoptosis contribute to the activation of Yki by Jnk, we expressed *hep.CA* or *egr* in animals mutant for a hypomorphic allele of *Dronc*, $Dronc^{129}$. It has been reported that when compensatory cell proliferation is induced by expression of pro-apoptotic genes, including *rpr*, *hid*, or *hep.CA*, while apoptosis is reduced by *Dronc* mutation, that overgrowth of wing tissue and induction of Wg and Dpp expression can still occur, even though caspase activation is reduced [15, 26, 158]. In our experiments, staining for cleaved caspase 3 (Cas3) confirmed that the number of apoptotic cells upon Jnk activation was reduced in $Dronc^{129}$ discs (Fig S1C). However, activation of Yki was not diminished (Figs 2H,I, S2E, S2G). In fact, many more cells with nuclear Yki were detected, both within and adjacent to the *sal.PE* expression domain, presumably because *Dronc* mutation inhibits the apoptosis of cells with activated Jnk. These observations

indicate that Jnk signaling does not require Dronc activation or apoptosis in order to promote Yki activation.

We also took advantage of the decreased apoptosis in *Dronc*^{129} discs to further investigate the linkage between Jnk and Hpo signaling. Hep.CA-mediated Yki activation could be efficiently repressed either by over-expression of Wts, or by over-expression of Hpo (Figs 2J,K).

Regulation of Yki during wing disc regeneration

The observation that Yki is activated after tissue damage, together with its importance for growth control, suggests that Yki activation could contribute to regeneration. To examine Yki activity during regeneration, we monitored Yki localization during recovery after conditional induction of Egr. *rn*-expressing cells were ablated by expressing Egr under *rn-Gal4* control for 30h, then Egr expression was removed by shift back to the non-permissive temperature for Gal80^{ts}, and the discs were allowed to recover. After 24 h of recovery, strong Yki activation remained detectable (Fig. 3B). Substantial Yki activation was also detected 48 h after removal of Egr expression (Fig. 3C), but by 72 h Yki localization appeared almost normal (Fig. 3D). This Yki localization profile correlates with active proliferation and regeneration of the wing disc after genetic ablation of *rn-Gal4* expressing cells [10].

Wg expression is also upregulated during regeneration, and Wg has been functionally linked to disc regeneration [10]. As both Wg and Yki can be associated with promotion of cell proliferation, we explored the relationship between them during regeneration. Activated Yki and upregulated Wg were mostly overlapping in discs

damaged by Rpr or Egr expression (Fig 3A and data not shown). However, during regeneration, Wg expression appeared to recover more quickly than Yki localization, as Wg expression was almost normal by 48 h, at which time significant nuclear Yki was still detected (Fig. 3C). This difference suggests that Yki and Wg are regulated independently. Nonetheless, since activated Yki and upregulated Wg initially overlapped (Fig. 3A), and inactivation of the Hippo pathway can normally upregulate Wg in the proximal wing disc [159, 160], we investigated whether upregulated Wg in regenerative cells might be due to activation of Yki. However, neither reduction of Yki protein by RNAi, nor reduction of Yki activity by Wts over-expression, blocked Wg expression (Fig. 3F,G). We also observed that *wg* RNAi substantially decreased Wg expression, but didn't visibly decrease nuclear Yki (Fig. 3E). These observations imply that Yki activation and Wg expression are induced in parallel by activation of Jnk during regeneration, rather than being dependent upon one another.

Yki is required for wing regeneration after tissue damage

The above results identify a correlation between Yki activation and epimorphic regeneration of the wing disc after elimination of cells by induction of apoptosis. Hippo signaling is very sensitive to the dose of Yki [114, 115, 161]. Thus, to determine whether the activation of Yki functionally contributes to regeneration after genetic ablation of the wing pouch, we induced a 30h pulse of Egr expression at mid-third instar in the *rn-Gal4* domain, and then allowed animals to recover and develop into adult flies. Because there is some variability in the efficiency of regeneration in this type of experiment [10], regenerated wings were measured and then classified according their percentage of

normal wing size. Under our experimental conditions, when the wing primordia was ablated by expression of Egr, complete regeneration (to >80% wild-type wing size) was observed in 1/4 of animals, partial regeneration (20-80% normal wing size) was observed in 2/5 of animals, and minimal regeneration (<20% normal wing size) was observed in 1/3 of animals (Fig. 3H,J,K). When the same experiment was performed in animals heterozygous for *yki*, then none of the wings fully regenerated, and 90% of animals exhibited only minimal regeneration (Fig. 3H,M). Since heterozygosity for *yki* did not affect the rate of development or the extent of initial ablation (Fig. S3), this impairment of wing disc regeneration indicates that the elevated activity of Yki observed after induction of tissue damage is functionally required for efficient regeneration. Co-expression of Wts had even stronger effects, as 100% of the animals failed to exhibit significant regeneration (Fig. 3H).

Activation of Yki in loss of neoplastic tumor suppressors

The results described above establish that Jnk signaling can influence Yki activity, and identify a role for this activation of Yki in regeneration after tissue damage. The loss of normal epithelial architecture associated with mutation of members of the neoplastic Lgl-Dlg-Scrib complex constitutes another type of epithelial cell damage. Indeed, Jnk signaling is activated in neoplastic tumor suppressor clones [30, 31, 140]. Thus, we investigated the relationship between activation of Jnk, activation of Yki, and tumorous overgrowths associated with cells in which the Lgl-Dlg-Scrib complex was disrupted. To investigate this in a system that would facilitate genetic manipulations, and to avoid the necessity of combining *lgl* loss-of-function with oncogenic mutations that

could complicate the analysis, we depleted *lgl* from large, contiguous domains of cells using RNAi by expressing UAS-hairpin transgenes under the control of broadly expressed Gal4 lines, and in conjunction with *UAS-dcr2*, which enhances the effectiveness of RNAi [162].

Depletion of *lgl* in the posterior half of the wing disc, under *en-Gal4* control, resulted in overgrowth of the posterior compartment and loss of apical-basal polarity (Figs 4A,C,E, 5C,D,I,J). Thus, in this situation *lgl* RNAi phenocopied *lgl* mutant discs, or *lgl* mutant clones co-expressed with oncogenes [30, 31, 140]. The overgrowth was apparent from the increased size of the posterior compartment, which often became multilayered, distorted and folded (Fig 5C,D,I,J), and was also reflected in elevated cell proliferation detected by EdU labeling (Fig 4E). The loss of polarity was apparent from the rounded morphology and multilayered appearance of cells (Fig. 5D,J). In addition, proteins that normally have discrete localizations within the cells, such as Fat or Dlg, instead became mis-localized such that they were equally distributed around the plasma membrane (Fig. 5C,D,I,J).

To investigate whether the overgrowth of these *lgl*-depleted cells was related to effects on Hippo signaling, we examined the sub-cellular distribution of Yki. A strong re-localization of Yki, from predominantly cytoplasmic to predominantly nuclear, was evident in posterior cells (Fig. 4A,C). A similar effect on Yki localization was induced by RNAi for *dlg* (Fig 4B), which indicates that this influence on Hippo signaling is not specific to *lgl*, but rather appears to be a property of the Lgl-Dlg-Scrib complex. To confirm that the relocalization of Yki to the nucleus is associated with Yki activation, we

examined *ex-lacZ*; it was strongly upregulated in posterior cells of *en-Gal4 UAS-RNAi-lgl* wing discs (Fig 4C).

To establish the relevance of this Yki activation to the tumorous overgrowth of *lgl*-depleted cells, we examined the consequences of simultaneous knockdown of both *yki* and *lgl*. Co-overexpression of *yki-RNAi* with *lgl-RNAi* blocked the overgrowth of the posterior compartment, and yielded discs in which the P compartment was reduced in size (Fig 4G), and posterior nuclei appeared apoptotic (not shown), which indicates that Yki is required for the growth and survival of *lgl* RNAi cells. To examine the relationship of *lgl*-induced overgrowths to Hippo signaling under milder conditions of reduced Yki activity, we over-expressed Wts. Using a *UAS-wts* line that only modestly reduced growth of the P compartment on its own (Fig. 4J), we observed a strong suppression of the *lgl* RNAi over-proliferation phenotype (Fig 4F), and also suppressed the influence of *lgl* on Yki localization and activity (Fig. 4I), resulting in relatively normal looking wing discs. These observations confirm that *lgl* acts as a tumor suppressor in the wing disc by limiting activation of Yki, and further suggest that the influence of *lgl* on Hippo signaling occurs at or upstream of Wts.

Lgl acts through Jnk signaling to regulate Hippo signaling in the wing

lgl depletion is associated with Jnk activation (Figs 5Q, 6A, S3D) [31, 140]. Both Jnk activation and Yki activation were largely confined to *lgl* depleted cells, but occasionally non-autonomous activation was observed (Figs 6A, S4D). This is consistent with the reported detection of non-autonomous Jnk activation adjacent to *scrib* mutant cells [31]. The general correspondance between Jnk activation and Yki activation in discs

with *lgl* depletion suggested they could be functionally linked. To directly examine this, we blocked Jnk activation by RNAi-mediated depletion of the *Drosophila* Jnk *bsk*, or by over-expression of the Jnk phosphatase Puc. Both of these approaches suppressed the overgrowth of *lgl* RNAi, the nuclear localization of Yki, the upregulation of downstream target genes, and the elevation of EdU labeling (Figs 6D,E,S4A). Thus, the influence of *lgl* on Hippo signaling and growth in the wing disc is dependent upon Jnk signaling.

Strikingly, expression of *puc* or *bsk* RNAi also appeared to rescue the cell polarity defect of *lgl* RNAi (Figs 6D, S4A). This was confirmed by the observation that the apical localization of Dlg and Fat proteins was restored (Fig. 5E,F,K,L). Thus, the loss of apical-basal polarity in *lgl* depleted wing cells depends on activation of the Jnk pathway. This observation, together with the general correspondance between polarity disruption and Jnk activation in lgl RNAi discs (Fig. 5Q), led us to investigate whether Jnk activation could be sufficient for polarity disruption. However, while some tissue folding was induced by Jnk activation, both Fat and Dlg maintained their normal apical localization in wing discs expressing *hep.CA* under *sal-Gal4* control (Fig. 5M-P).

In a recent study of *lgl* mutant clones in eye discs, activation of Yki was observed and attributed at least in part to activation of aPKC [107]. Thus, we investigated the relationships among aPKC activation, Jnk activation, and Yki activation in wing discs. Expression of an activated form of aPKC, $aPKC^{CAAX}$ [163], induced a modest activation of Yki in the wing disc (Fig. 7A). Using the *puc-lacZ* reporter, we observed that expression of $aPKC^{CAAX}$ is also associated with Jnk activation (Fig. 7C). Moreover, the *puc-lacZ* insertion, which is also a *puc* allele, dominantly enhanced the Yki activation associated with $aPKC^{CAAX}$ expression (Fig. 7C). Conversely, reducing Jnk activation by

expression of *puc* reduced Yki activation (Fig. 7B). Together, these observations indicate that in wing discs, aPKC activates Jnk, and activation of Yki by aPKC is a Jnk-dependent process.

Jnk activation has diverse effects in different contexts. Our observation that Yki activation in the wing is Jnk-dependent in neoplastic tumor suppressors and in response to tissue damage is consistent with oncogenic effects of Jnk that have been identified in neoplastic tumor suppressors and during regeneration and compensatory cell proliferation. However, under other conditions, Jnk acts as a tumor suppressor by promoting apoptosis. Indeed, in eye discs, mutation of *scrib* in clones can promote Jnk-dependent apoptosis, and blocking Jnk by expression of a dominant negative isoform promotes the proliferation of *scrib* mutant clones [30]. To directly compare the influence of Jnk activation on Yki activation in different *Drosophila* organs, we analyzed multiple imaginal discs from larvae in which clones of cells expressing *hep.CA* had been induced. Because these discs were isolated from the ame animals, the intensity and duration of Hep activation (induced by first making Flp-out clones expressing *tub-Gal4* and *tub-Gal80^{ts}*, and then inducing expression of *UAS-hep.CA* for 14 h by temperature shift) should be identical. Strong induction of Yki was observed in wing and haltere discs within and adjacent Hep.CA-expressing clones (Figs. S1E, S1F). By contrast, in leg discs, strong nuclear Yki was not detected, but instead we observed a relatively even distribution of Yki between nucleus and cytoplasm, indicative of a more modest level of Yki activation (Fig. S1G). Finally, in eye discs, most clones were not associated with any visible change in Yki localization (Fig. S1H). Although basis for the distinct

responsiveness of different imaginal discs to Jnk activation is not known, it re-emphasizes that how cells respond to Jnk activation depends on the cellular context.

Discussion

Participation of Yki in regeneration and compensatory cell proliferation

Many tissues have the capacity respond to the removal or death of cells by increasing proliferation of the remaining cells. In *Drosophila*, this phenomena has been characterized both in the context of imaginal disc regeneration and compensatory cell proliferation. Our studies implicate the Hippo signaling pathway as a key player in these proliferative responses to tissue damage. After genetically ablating the wing primordia by inducing apoptosis, we observed that Yki becomes activated to high levels in surrounding cells, based on its nuclear abundance and induction of a downstream target of Yki transcriptional activity. Moreover, high level Yki activation is crucial for wing disc regeneration, as even modest reduction of Yki levels, to a degree that has only minor effects on normal wing development, severely impaired wing disc regeneration. While it was known that Yki is required for wing growth during development [66], our observations establish that Yki is also required for wing growth during regeneration, and moreover that regeneration requires higher levels of Yki activation than during normal development.

Regulation of Yki by Jnk signaling

Our studies identify Jnk activation as a promoter of Yki activity in the wing disc. Most aspects of imaginal disc development, including imaginal disc growth, normally do not require Jnk signaling [134]. By contrast, Jnk signaling is both necessary and sufficient for Yki activation in response to wing damage. Jnk signaling has previously been linked to compensatory cell proliferation and regeneration in imaginal discs [16, 20,

25, 26], and we can now ascribe at least part of that requirement to activation of Yki. However, Jnk signaling also promotes the expression of other mitogens, including Wg, which were linked to regeneration and proliferative responses to apoptosis [10, 16, 17]. Wg and Yki are not required for each other's expression, suggesting that they are regulated and act in parallel to influence cell proliferation after tissue damage. The mechanism by which Jnk activation induces Yki activation is not known. The observation that it could be suppressed by over-expression of Wts or Hpo suggests that it might impinge on Hippo signaling at or upstream of Wts, but the possibility that Jnk-dependent Yki regulation occurs in parallel to these Hippo pathway components can not be excluded (Fig. 8).

We detected strong Yki activation within the wing and haltere discs in response to Jnk activation, but weaker or non-existent effects in leg or eye discs. Jnk activation has previously been linked to oncogenic effects of neoplastic tumor suppressors in eye discs [30, 31, 140], and it’s possible that Yki activation might be induced by a distinct Jnk activation regimes in eye discs. Nonetheless, since we employed identical conditions in both wings and eyes, isolating discs from the same animals, our studies emphasize the important context-dependence of responses to Jnk activation. The link between Jnk activation and Yki activation is not limited to the wing however, as a connection between these pathways was recently discovered in the adult intestine [33].

There was a general correspondence between activation of Jnk and activation of Yki under multiple experimental conditions, including expression of Rpr, direct activation of Jnk signaling by Egr or Hep.CA, and depletion of *lgl*. However, some experiments, most notably direct activation of Jnk by Hep.CA, appear to argue for a non-

autonomous effect of Jnk on Yki, which would imply that the influence of Jnk on Yki activity is indirect. Nonetheless, we favor the hypothesis that this indirect effect is actually mediated through Jnk signaling, as it has been reported that under some conditions that Jnk activation can propagate from cell to cell [32]. Consistent with this possibility, we observed that a non-autonomous activation of Jnk adjacent to *lgl* depleted cells was blocked by depletion of *bsk* solely within the *lgl* RNAi cells. Alternative signals implicated in compensatory cell proliferation do not appear to be good candidates for mediating Yki activation, as Wg is not required for Yki activation in regenerating discs, and prior studies did not detect a direct influence of Dpp pathway activity on Yki activation [164].

Activation of Yki adjacent to Egr- or Rpr-expressing cells was also reduced by over-expression of Wts. This might reflect an influence of Yki on signaling from these cells, but because expression of Wts inhibits Yki activity, and activated Yki promotes expression of an inhibitor of apoptosis (Diap1), it is also possible that this effect could be explained simply by Wts over-expression resulting in reduction or more rapid elimination of Egr- or Rpr-expressing cells; the reduced survival of these cells would then limit their ability to signal to neighbors.

Although Jnk has been implicated in compensatory cell proliferation and regeneration [16, 20, 25], it is better known for its ability to promote apoptosis [23, 137, 153]. The dual, opposing roles of Jnk signaling as a promoter of apoptosis and a promoter of cell proliferation raise the question of how one of these distinct downstream outcomes becomes favored in cells with Jnk activation (Fig. 8). Given the links between Jnk activation and human diseases, including cancer [133, 135], defining mechanisms that

influence this is an important question, and our identification of the role of Yki activation in Jnk-mediated proliferation and wing regeneration should facilitate future investigations into how the balance between proliferation or apoptosis is regulated.

Regulation of Yki activity by neoplastic tumor suppressors

Hippo signaling is regulated by proteins that exhibit discrete localization at the subapical membrane, e.g. Fat, Ex, and Merlin [147]. The observation that disruption of apical-basal polarity is associated with disruption of Hippo signaling emphasizes the importance of this localization to normal regulation. Moreover, our observations, together with other recent studies [107, 149], establish that Hippo signaling is not only inhibited by neoplastic tumor suppressor mutations, resulting in Yki activation, they also establish that this activation of Yki is required for the tumorous overgrowths associated with these mutations.

Although our results agree with Grzeschik et al. [107] in linking *lgl* to Hippo signaling, there are some notable differences. Grzeschik et al. [107] examined *lgl* mutant clones in the eye imaginal disc, under conditions where cells retained apical-basal polarity, whereas we examined a more extreme condition in wing imaginal discs, where apical-basal polarity was lost. Intriguingly we found that conditions associated with activation of Yki by Jnk in the wing disc were not sufficient to activate Yki in the eye disc. This observation, together with the discovery that loss of polarity in lgl depleted cells requires Jnk activation, suggests as a possible explanation for why *lgl* null mutant clones retain apical-basal polarity in eye discs is that eye discs have a distinct, and apparently reduced, sensitivity to Jnk activation as compared to wing discs.

We also identified distinct processes linked to Yki activation in the absence of *lgl*. Grzeschik et al. [107] reported an effect of *lgl* on Hpo protein localization. In wing discs, we did not detect the discrete apical localization of Hpo reported by Grzeschik et al. [107] in their studies of eye discs. Thus, their proposed mechanism, involving activation of Yki via mis-localization of Hpo and dRassf, might not be relevant to the wing. By contrast, we identified an essential role for Jnk signaling in regulating Yki activation in *lgl*-depleted cells in the wing. Because we did not detect an effect of direct Jnk activation on Yki in eye discs, it's possible that Lgl can act through multiple pathways to influence Yki, including a Jnk-dependent pathway that is crucial in the wing disc, and a Jnk-independent pathway that is crucial in the eye disc. Grzeschik et al. [107] also linked the influence of *lgl* in the eye disc to its antagonistic relationship with aPKC. Our observation that the influence of aPKC in the wing depends on Jnk activation is consistent with an Lgl-aPKC link, while providing new mechanistic insight into the action of aPKC.

Our observation that the loss of polarity in *lgl* RNAi discs is dependent upon Jnk signaling was unexpected, but a related observation was recently reported by Zhu et al. [165]. These results suggest that the established role of the Lgl-Dlg-Scrib complex in maintaining epithelial polarity [141, 166] can be ascribed in part to a critical role in repressing Jnk activity. However, the observation that Jnk activation on its own was not sufficient to disrupt polarity supports a model in which multiple polarity complexes need to be disturbed in order for wing cells to lose apical-basal polarity, including both Lgl and additional, Jnk-regulated polarity complexes. The observation that eye disc cells were

relatively resistant to Hep.CA suggests that the apparently normal polarity of *lgl* mutant clones in the eye disc could be due to a relative insensitivity to Jnk activation.

The discovery of the role of Jnk signaling in Yki activation provides a unifying mechanism for the overgrowths observed in conjunction with mutations of neoplastic tumor suppressors, and those associated with compensatory cell proliferation, because in both cases a proliferative response is mediated through the ability of Jnk to induce Yki activation. Although the molecular basis for the linkage of these two pathways is not understood yet, it operates in multiple *Drosophila* organs, and thus may define a novel regulatory input into Hippo signaling, of particular importance in abnormal or damaged tissues. Moreover, Jnk activation has also been observed in conjunction with regeneration of disc fragments after surgical wounding [25], and thus its participation in regeneration is not limited to paradigms involving induction of apoptosis. It is also noteworthy that under conditions of widespread *lgl* depletion (ie *lgl* mutant or *lgl* RNAi), and consequent Jnk activation, the balance between induction of apoptosis and induction of cell proliferation is shifted towards a proliferative response. By contrast, in the wing disc clones of cells mutant for *lgl* fail to survive, unless oncogenic co-factors are expressed [30, 31, 143-145, 149], which suggests that the choice between proliferative versus apoptotic responses to Jnk activation might be influenced by the Jnk activation status of neighboring cells. Consistent with this hypothesis, the loss of *lgl* mutant clones in wing discs was recently attributed to cell competition, and the rescuing activity on oncogenic *ras* mutations to an ability to decrease cell competition by enabling the formation of larger clusters of *lgl* mutant cells.

Materials and methods

Drosophila genetics

Stocks used included *ex-lacZ en-Gal4 UAS-GFP/CyO; UAS-dcr2/TM6b*, *UAS-lgl-RNAi (VDRC 51249), UAS-dlg-RNAi (VDRC 41136), UAS-bsk-RNAi (VDRC 104569), UAS-yki-RNAi (VDRC 104532), UAS-wg-RNAi (VDRC 104579), rn-Gal4 UAS-egr tub-Gal80^{ts}/TM6b,Gal80* [10], *rn-Gal4 UAS-rpr tub-Gal80^{ts}/TM6b,Gal80* [10], *puc-lacZ[A251.1F3],ry/TM3 (Bloomington 11173)*, *UAS-myc:wts.2*, *FRT42D yki^{B5}/CyO,Act-GFP, UAS-puc, salPE-Gal4 UAS-GFP/CyO; Dronc^{129} FRT2A/TM6b* [26], *UAS-hep.CA/CyO; Dronc^{129} FRT2A/TM6b* [26], *UAS-wts:myc[2-2]gift of Tian Xu), UAS-GFP[T-2](Bloomington 1521), UAS-aPKC:CAAX [163], UAS-yki:V5* [71], *tub-Gal80^{ts}/TM6B, tub>CD2>Gal4 UAS-CD8:GFP/CyO; tub-Gal80^{ts}/TM6B* [167], *UAS-hep.CA (Bloomington 6406), UAS-rpr[14] (Bloomington 5824), rn-lacZ^{89}, ry^{+}, ry^{506}/TM3, Sb* (St Pierre et al., 2002), *UAS-egr* [23], *UAS-lacZ* [168]. The specificity of *lgl* RNAi has been described previously [107]. The specificity *yki* RNAi was confirmed by rescue using a *UAS-yki* line to over-express Yki. Because we lacked a direct test for *bsk* RNAi specificity, all experiments with *bsk* RNAi were repeated using *UAS-puc*, which gave similar results.

Larvae from crosses of *rn-Gal4 UAS-egr tub-Gal80^{ts}/TM6b,Gal80* or *rn-Gal4 UAS-rpr tub-Gal80^{ts}/TM6b,Gal80* were kept at 18°C for 8 days and shifted to 30°C for 30h to induce cell death. After cell death induction, larvae were either dissected or put back to 18°C for 24h, 48h, 72h recovery. To make *rpr* or *hep.CA* clones, *y w hs-flp; UAS-rpr/CyO,GFP* or *y w hs-flp; UAS-hep.CA/CyO,GFP* flies were crossed to

tub>CD2>Gal4 UAS-CD8:GFP/CyO; tub-Gal80^{ts}/TM6B. Larvae were maintained at 25°C for 3 days and clones were induced by heat shock at 38°C for 10 min. Larvae were then kept at 18°C for 3 days to let clones grow larger, and then cell death was induced by temperature shift to 30°C for 12-14h.

To evaluate the effect of *yki^{B5}*/+ on development timing, *rn-Gal4 UAS-egr tub-Gal80^{ts}/TM6b,Gal80* females were crossed to oregon R or *FRT42D yki^{B5}/CyO,Act-GFP* males. Eggs were collected at 25°C in 8h intervals on grape juice plates covered with yeast, and subsequently kept at 18°C. The dates of larvae hatching and pupa formation were recorded.

For adult wings, larvae were maintained at 18°C after tissue damage until eclosion. Wings were mounted in Gary's Magic Mountant, and measured using NIH ImageJ software.

Immunofluorescent staining

Wing discs of third instar larvae were fixed in 4% paraformaldehyde and stained as described previously. Primary antibodies used include rabbit anti-Yki (1:400), mouse anti-Wg (1:800, 4D4, Developmental Studies Hybridoma Bank (DSHB), mouse anti-DLG (1:400, 4F3, DSHB), rat anti-Fat (1:800) [154], goat anti-β-gal (1:1000, Biogenesis), rabbit anti-GFP (1:400, Molecular Probes), rat anti-DE-cadherin (1:450, DCAD2, DSHB), rabbit anti-active Caspase 3 (1:200, Asp175, Cell Signaling Technology), rabbit anti-phospho-JNK (1:100), mouse anti-Myc (1:400, 9E10,Babco) , mouse anti-Nubbin (1:100, gift from Steve Cohen). EdU labelling was performed using

Click-it™ EdU Alexa Fluor Imaging Kit (Molecular Probes). Images were captured on a Leica TCS SP5 confocal microscope.

Figures

Fig 1. Yki activation induced by expression of pro-apoptotic genes.

Third instar wing discs, stained for Yki (red). Panels marked prime show separate channels of the stain to the left. Examples of nuclear Yki are highlighted by arrows. A) Wild-type expression of *rn* (visualized using *rn-lacZ*, blue), Wg (green) and Yki. B) *rn-Gal4 UAS-rpr tub-Gal80^{ts} UAS-lacZ*, 30h after induction of *rpr*. The rn domain (anti-ß-gal, green) is small and irregular, and nuclear Yki is detected. C) *rn-Gal4 UAS-egr tub-Gal80^{ts} UAS-GFP*, 30h after induction of *egr*. The rn domain (GFP, green) is small and irregular, and nuclear Yki is detected. D) *rn-Gal4 UAS-egr tub-Gal80^{ts}*, 30h after induction of *egr*. *ex-lacZ* (Cyan) is upregulated in cells with nuclear Yki. E) *rn-Gal4 UAS-egr tub-Gal80^{ts} UAS-Wts:Myc*, 30h after induction. Nuclear Yki is suppressed. F) *rn-Gal4 UAS-rpr tub-Gal80^{ts} UAS-GFP UAS-Wts:Myc*, 30h after induction. Nuclear Yki is suppressed.

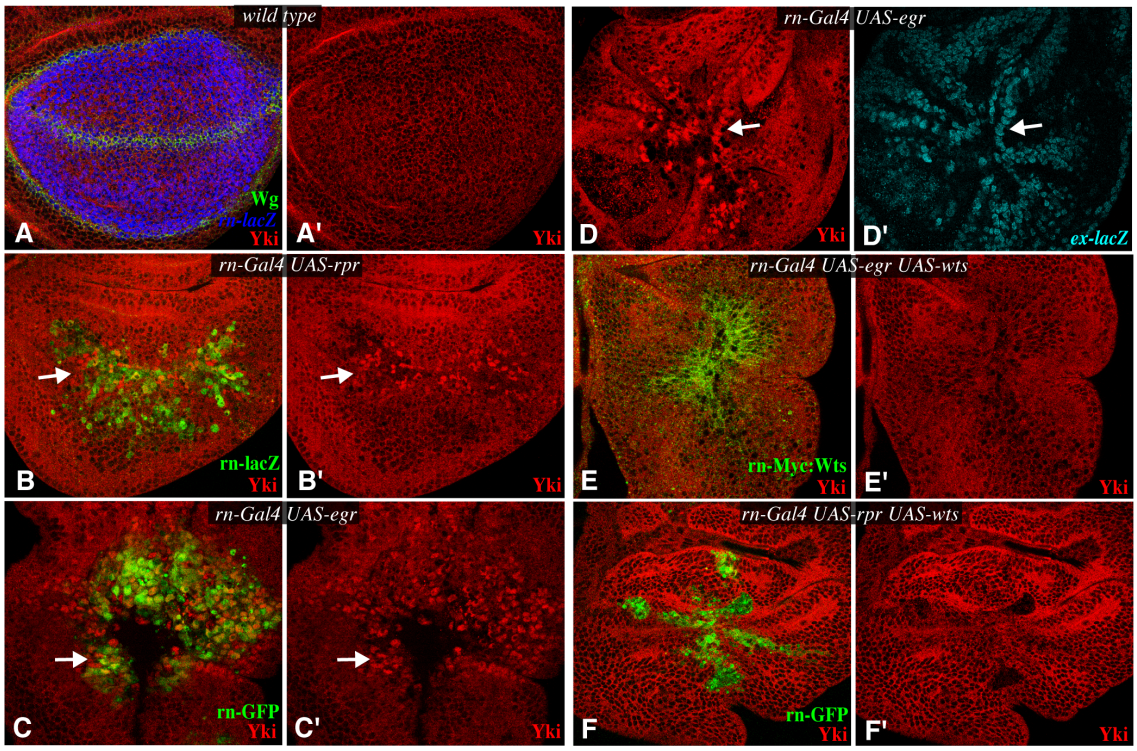
wild type
Wg
ex-lacZ
Yki
A
A'
Yki
rn-Gal4 UAS-egr
D
Yki
D'
ex-lacZ
rn-Gal4 UAS-rpr
rn-lacZ
Yki
B
B'
Yki
rn-Gal4 UAS-egr UAS-wts
rn-Myc:Wts
Yki
E
E'
Yki
rn-Gal4 UAS-egr
rn-GFP
Yki
C
C'
Yki
rn-Gal4 UAS-rpr UAS-wts
rn-GFP
Yki
F
F'
Yki

Fig 2. Jnk activates Yki

Third instar wing discs, stained for Yki (red). Panels marked prime show separate channels of the stain to the left. Panels marked by double prime symbols show vertical sections through these discs. Examples of nuclear Yki are highlighted by arrows. A) *rn-Gal4 UAS-egr tub-Gal80^{ts} puc-lacZ*, 30h after induction. Nuclear Yki and *puc-lacZ* (magenta) are detected. B) *rn-Gal4 UAS-rpr tub-Gal80^{ts} puc-lacZ*, 30h after induction. Nuclear Yki and *puc-lacZ* (magenta) are detected.C) *rn-Gal4 UAS-egr tub-Gal80^{ts} UAS-puc*, 30h after induction. Nuclear Yki is reduced, and Wg (green) appears normal. D) *rn-Gal4 UAS-rpr tub-Gal80^{ts} UAS-puc*, 30h after induction. Nuclear Yki is reduced (compare with Figs 1B, 2B). E) *sal.PE-Gal4 UAS-GFP*, GFP (green) indicates the *sal* expression domain. F) *sal.PE-Gal4 UAS-GFP UAS-hep.CA Dronc^{129}*/+. The *sal* domain is reduced and irregular, and nuclear Yki is detected. G) *sal.PE-Gal4 UAS-GFP UAS-egr Dronc^{129}*/+. The *sal* domain is reduced and irregular, and nuclear Yki is detected. H) *sal.PE-Gal4 UAS-GFP UAS-hep.CA Dronc^{129}/ Dronc^{129}*. Nuclear Yki is increased. I) *sal.PE-Gal4 UAS-GFP UAS-egr Dronc^{129}/ Dronc^{129}*. Nuclear Yki is increased. J) *sal.PE-Gal4 UAS-GFP UAS-hep.CA UAS-wts Dronc^{129}/ Dronc^{129}*. Nuclear Yki is lost. K) *sal.PE-Gal4 UAS-GFP UAS-hep.CA UAS-hpo Dronc^{129}/ Dronc^{129}*. Nuclear Yki is lost.

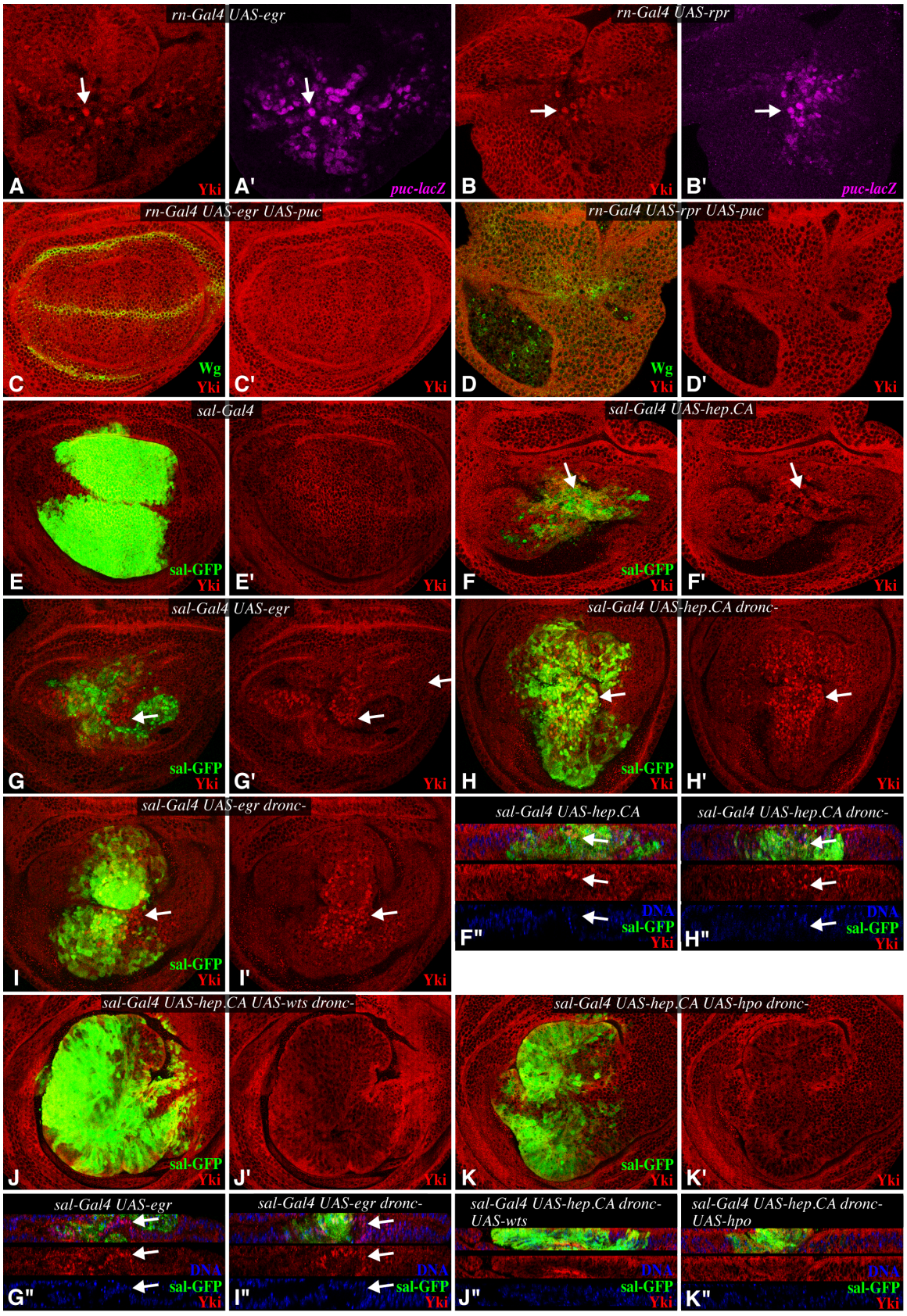
rn-Gal4 UAS-egr
A
Yki
A'
puc-lacZ
rn-Gal4 UAS-rpr
B
Yki
B'
puc-lacZ
rn-Gal4 UAS-egr UAS-puc
C
Wg
Yki
C'
Yki
rn-Gal4 UAS-rpr UAS-puc
D
Wg
Yki
D'
Yki
sal-Gal4
E
sal-GFP
Yki
E'
Yki
sal-Gal4 UAS-hep.CA
F
sal-GFP
Yki
F'
Yki
sal-Gal4 UAS-egr
G
sal-GFP
Yki
G'
Yki
sal-Gal4 UAS-hep.CA dronc-
H
sal-GFP
Yki
H'
Yki
sal-Gal4 UAS-egr dronc-
I
sal-GFP
Yki
I'
Yki
sal-Gal4 UAS-hep.CA
F"
DNA
sal-GFP
Yki
sal-Gal4 UAS-hep.CA dronc-
H"
DNA
sal-GFP
Yki
sal-Gal4 UAS-hep.CA UAS-wts dronc-
J
sal-GFP
Yki
J'
Yki
sal-Gal4 UAS-hep.CA UAS-hpo dronc-
K
sal-GFP
Yki
K'
Yki
sal-Gal4 UAS-egr
G"
DNA
sal-GFP
Yki
sal-Gal4 UAS-egr dronc-
I"
DNA
sal-GFP
Yki
sal-Gal4 UAS-hep.CA dronc-
UAS-wts
J"
DNA
sal-GFP
Yki
sal-Gal4 UAS-hep.CA dronc-
UAS-hpo
K"
DNA
sal-GFP
Yki

Fig 3. Yki activation during wing regeneration

A-G) Third instar wing discs, stained for Yki (red) and Wg (green). Panels marked prime show separate channels of the stain to the left. A-D) *rn-Gal4 UAS-egr tub-Gal80^{ts} ,* after 30h of *egr* expression at 30°C, and A) 0 h, B) 24 h, C) 48 h, and D) 72 h of recovery at 18°C. Nuclear Yki gradually diminishes as the disc regenerates. E) *rn-Gal4 UAS-egr UAS-RNAi-wg UAS-dcr2 tub-Gal80^{ts},* 30h after induction. Wg is severely reduced, but strong nuclear Yki is still detected. E) *rn-Gal4 UAS-egr UAS-RNAi-yki UAS-dcr2 tub-Gal80^{ts},* 30h after induction. Yki is severely reduced in the *rn* domain, but strong Wg is still detected. G) *rn-Gal4 UAS-egr UAS-wts tub-Gal80^{ts},* 30h after induction. Nuclear Yki is suppressed, but Wg is still detected. H) Distribution of adult wing sizes in *wild type (wt), yki^{b5}/+, rn-Gal4 UAS-egr tub-Gal80^{ts}, rn-Gal4 UAS-egr tub-Gal80^{ts} yki^{b5}/+, rn-Gal4 UAS-wts tub-Gal80^{ts},* or *rn-Gal4 UAS-egr UAS-wts tub-Gal80^{ts}* flies, after a 30h temperature pulse during mid-third instar followed by recovery at 18°C. I-M) Representative examples of wings of each size category, with measurement indicated at top left and actual genotype indicated at top right.

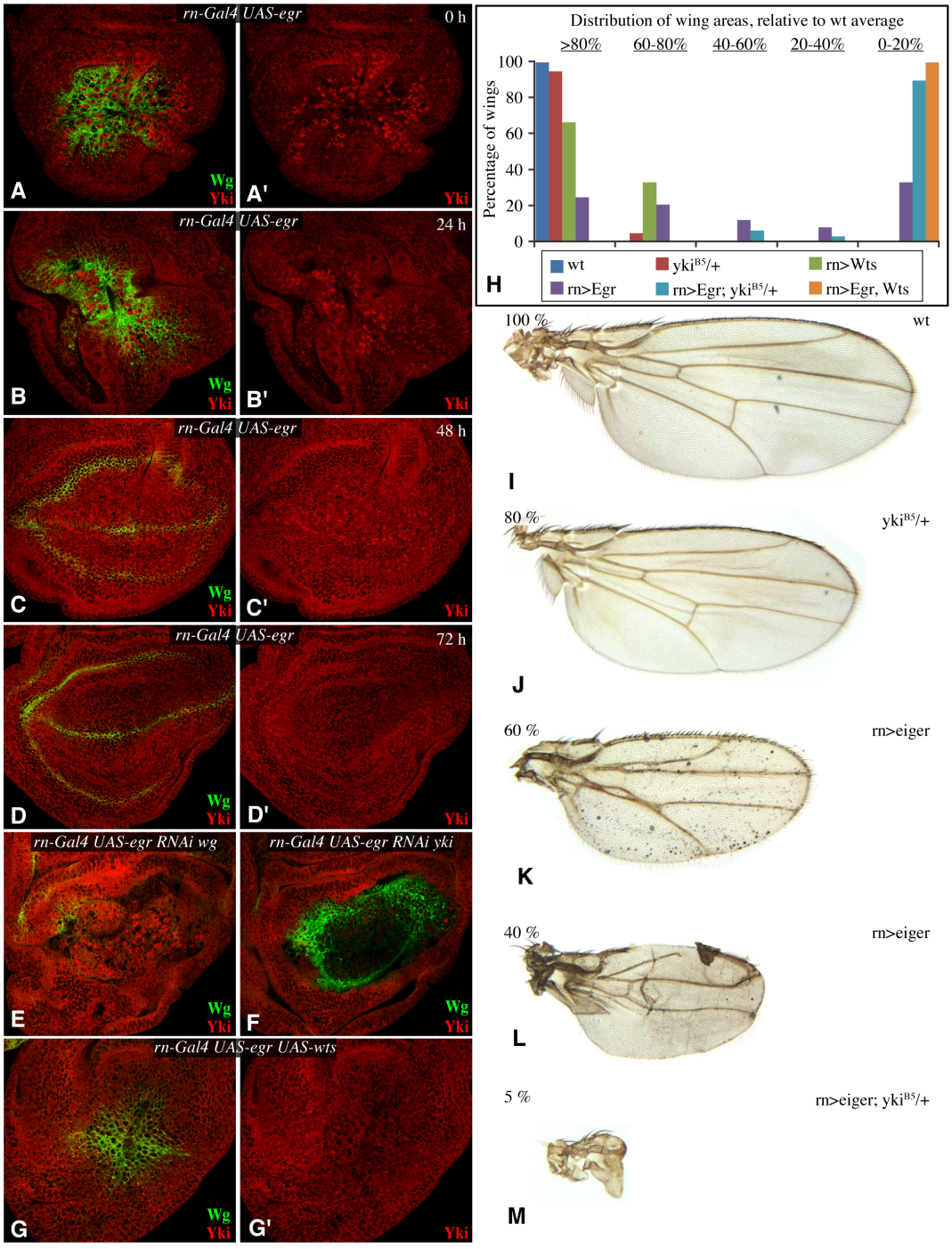
rn-Gal4 UAS-egr
0 h
A
Wg
Yki
A'
Yki
rn-Gal4 UAS-egr
24 h
B
Wg
Yki
B'
Yki
rn-Gal4 UAS-egr
48 h
C
Wg
Yki
C'
Yki
rn-Gal4 UAS-egr
72 h
D
Wg
Yki
D'
Yki
rn-Gal4 UAS-egr RNAi wg
E
Wg
Yki
rn-Gal4 UAS-egr RNAi yki
F
Wg
Yki
rn-Gal4 UAS-egr UAS-wts
G
Wg
Yki
G'
Yki
Distribution of wing areas, relative to wt average
≥80%
60-80%
40-60%
20-40%
0-20%
Percentage of wings
100
80
60
40
20
0
wt
yki^B5/+
rn>Wts
rn>Egr
rn>Egr; yki^B5/+
rn>Egr, Wts
H
100 %
wt
I
80 %
yki^B5/+
J
60 %
rn>eiger
K
40 %
rn>eiger
L
5 %
rn>eiger; yki^B5/+
M

Fig 4. Yki activation by depletion of neoplastic tumor suppressors

Third instar wing discs, stained for Yki (red), GFP (green), *ex-lacZ* (cyan) or EdU (magenta), as indicated. Panels marked prime show separate channels of the stain to the left. A) *en-Gal4 UAS-RNAi-lgl UAS-dcr2 UAS-GFP*. B) *en-Gal4 UAS-RNAi-dlg UAS-dcr2 UAS-GFP*. C) *en-Gal4 UAS-RNAi-lgl UAS-dcr2 UAS-GFP ex-lacZ*. D) *en-Gal4 UAS-dcr2 UAS-GFP*. E) *en-Gal4 UAS-RNAi-lgl UAS-dcr2 UAS-GFP*. F) *en-Gal4 UAS-RNAi-lgl UAS-dcr2 UAS-myc:wts.2 UAS-GFP*. G) *en-Gal4 UAS-RNAi-lgl UAS-yki-RNAi UAS-dcr2 UAS-GFP*. H) *en-Gal4 UAS-yki-RNAi UAS-dcr2 UAS-GFP*. I) *en-Gal4 UAS-RNAi-lgl UAS-dcr2 UAS-myc:wts.2 UAS-GFP ex-lacZ.* J) *en-Gal4 UAS-myc:wts.2 UAS-GFP*.

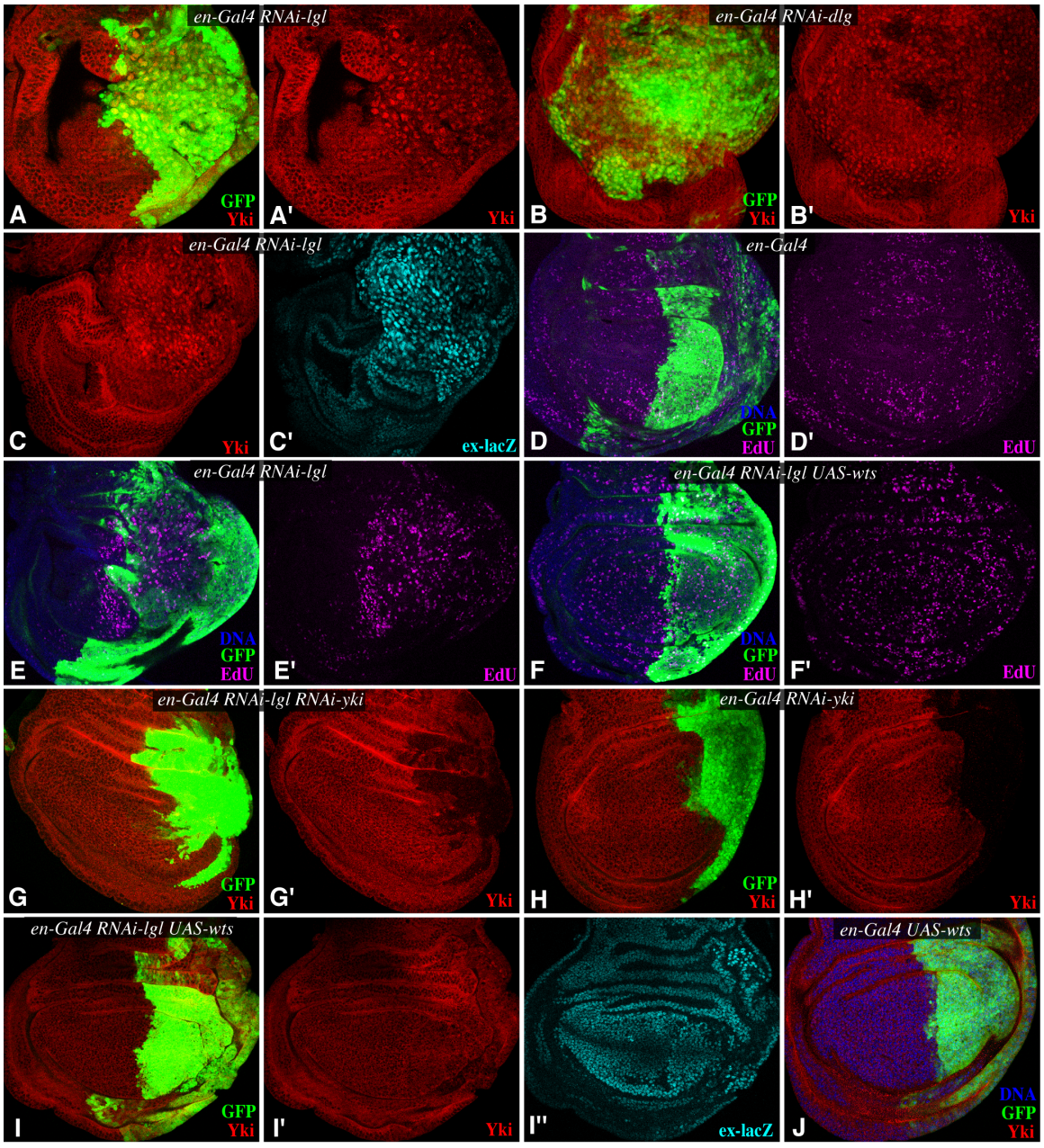
en-Gal4 RNAi-lgl
GFP
Yki
A
A'
Yki
en-Gal4 RNAi-dlg
GFP
Yki
B
B'
Yki
en-Gal4 RNAi-lgl
C
Yki
C'
ex-lacZ
en-Gal4
DNA
GFP
EdU
D
D'
EdU
en-Gal4 RNAi-lgl
DNA
GFP
EdU
E
E'
EdU
en-Gal4 RNAi-lgl UAS-wts
DNA
GFP
EdU
F
F'
EdU
en-Gal4 RNAi-lgl RNAi-yki
GFP
Yki
G
G'
Yki
en-Gal4 RNAi-yki
GFP
Yki
H
H'
Yki
en-Gal4 RNAi-lgl UAS-wts
GFP
Yki
I
I'
Yki
I''
ex-lacZ
en-Gal4 UAS-wts
DNA
GFP
Yki
J

Fig 5. Jnk is required for disruption of polarity upon *lgl* depletion

Third instar wing discs, stained for GFP (green) and Fat (red) or Dlg (red), or as indicated. For A-L, panels marked prime show separate channels of the stain to the left, A,C,E,G,I,K show horizontal sections, B,D,F,H,J,L show verticle sections of the disc above. A,B,G,H) *en-Gal4 UAS-dcr2 UAS-GFP*. C,D,I,J) *en-Gal4 UAS-RNAi-lgl UAS-dcr2 UAS-GFP*. E,F,K,L) *en-Gal4 UAS-RNAi-lgl UAS-RNAi-bsk UAS-dcr2 UAS-GFP*. For M-Q, panels marked prime show vertical sections. M) *sal.PE-Gal4 UAS-GFP* $Dronc^{129}/Dronc^{129}$. N) *sal.PE-Gal4 UAS-GFP UAS-hep.CA* $Dronc^{129}/Dronc^{129}$. O) *sal.PE-Gal4 UAS-GFP* $Dronc^{129}/Dronc^{129}$. P) *sal.PE-Gal4 UAS-GFP UAS-hep.CA* $Dronc^{129}/Dronc^{129}$. Q) *en-Gal4 UAS-RNAi-lgl UAS-dcr2 puc-lacZ*.

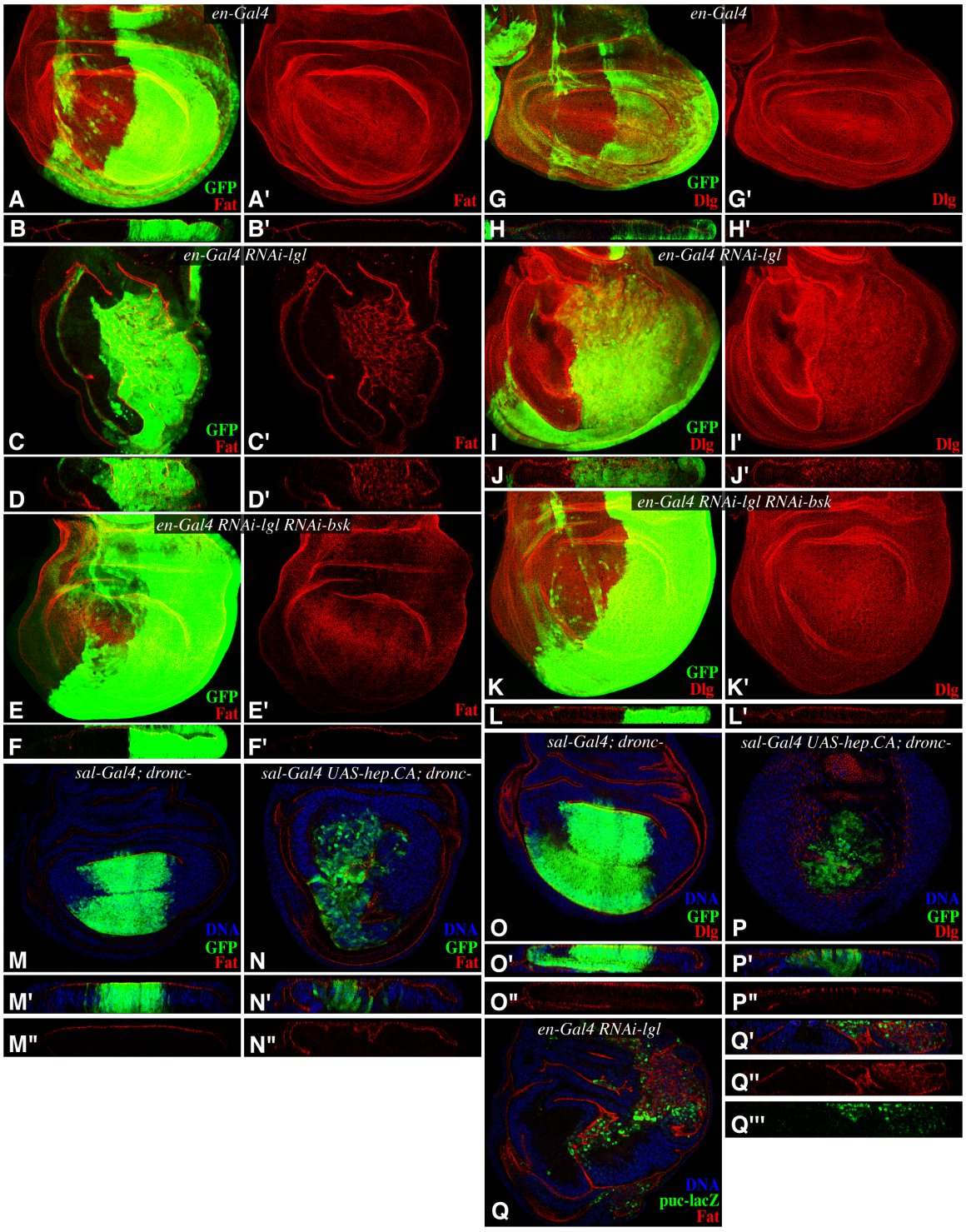
en-Gal4
GFP
Fat
A
A'
B
B'
en-Gal4
GFP
Dlg
G
G'
H
H'
en-Gal4 RNAi-lgl
GFP
Fat
C
C'
D
D'
en-Gal4 RNAi-lgl
GFP
Dlg
I
I'
J
J'
en-Gal4 RNAi-lgl RNAi-bsk
GFP
Fat
E
E'
F
F'
en-Gal4 RNAi-lgl RNAi-bsk
GFP
Dlg
K
K'
L
L'
sal-Gal4; dronc-
DNA
GFP
Fat
M
M'
M"
sal-Gal4 UAS-hep.CA; dronc-
DNA
GFP
Fat
N
N'
N"
sal-Gal4; dronc-
DNA
GFP
Dlg
O
O'
O"
sal-Gal4 UAS-hep.CA; dronc-
DNA
GFP
Dlg
P
P'
P"
en-Gal4 RNAi-lgl
DNA
puc-lacZ
Fat
Q
Q'
Q"
Q'''

Fig 6. *lgl* Depletion activates Yki through Jnk

Third instar wing discs, stained for Yki (red), p-Jnk (red), DNA (using Hoechst, blue), GFP (green), *ex-lacZ* (cyan) or EdU (magenta), as indicated. Panels marked prime show separate channels of the stain to the left. A) *en-Gal4 UAS-RNAi-lgl UAS-dcr2 UAS-GFP*. pJnk indicates staining for activated Jnk, using a phospho-specific antibody. B) *en-Gal4 UAS-RNAi-lgl UAS-RNAi-bsk UAS-dcr2 UAS-GFP*, pJnk staining is close to background levels. C) *wild type* D) *en-Gal4 UAS-RNAi-lgl UAS-RNAi-bsk UAS-dcr2 UAS-GFP*, Yki localization and ex-lacZ staining are almost normal (cf Fig 4A,B). E) *en-Gal4 UAS-RNAi-lgl UAS-RNAi-bsk UAS-dcr2 UAS-GFP*, EdU labeling is similar between anterior and posterior (cf Fig 4E).

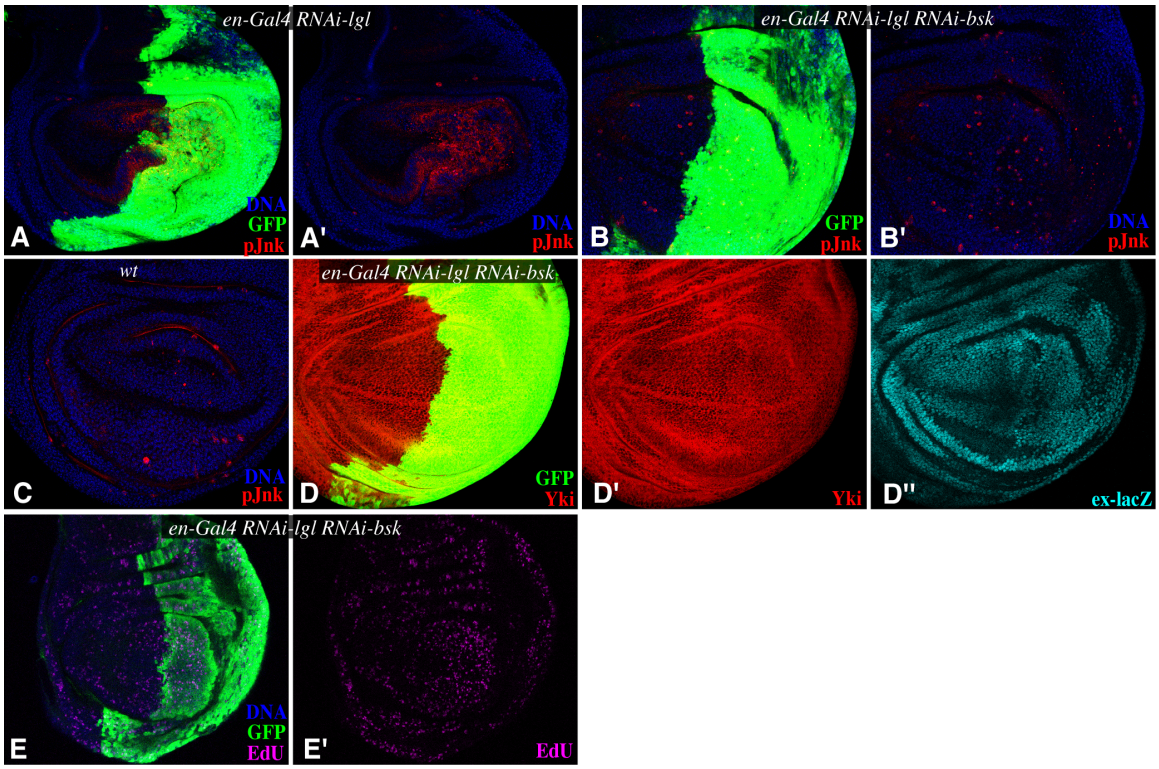
en-Gal4 RNAi-lgl
DNA
GFP
pJnk
A
A'
DNA
pJnk
en-Gal4 RNAi-lgl RNAi-bsk
GFP
pJnk
B
B'
DNA
pJnk
wt
C
DNA
pJnk
en-Gal4 RNAi-lgl RNAi-bsk
D
GFP
Yki
D'
Yki
D''
ex-lacZ
en-Gal4 RNAi-lgl RNAi-bsk
E
DNA
GFP
EdU
E'
EdU

Fig 7. aPKC activates Yki through Jnk

Third instar wing discs, stained for Yki (red), puc-lacZ (green), GFP (green/blue), as indicated. Panels marked prime show separate channels of the stain to the left. A) *en-Gal4 UAS-aPKC^{CAAX} UAS-GFP*. B) *en-Gal4 UAS-aPKC^{CAAX} UAS-puc UAS-GFP*. C) *en-Gal4 UAS-aPKC^{CAAX} puc-lacZ UAS-GFP*.

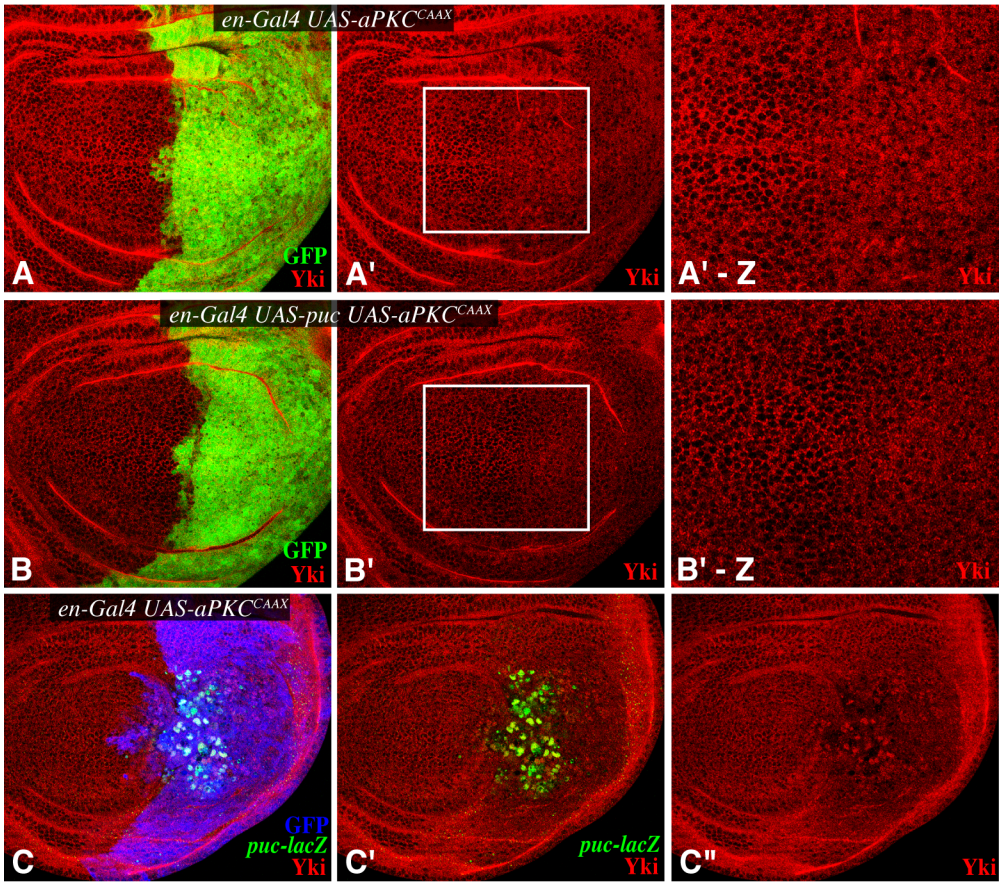
en-Gal4 UAS-aPKC^CAAX
GFP
Yki
A
A'
Yki
A' - Z
Yki
en-Gal4 UAS-puc UAS-aPKC^CAAX
GFP
Yki
B
B'
Yki
B' - Z
Yki
en-Gal4 UAS-aPKC^CAAX
GFP
puc-lacZ
Yki
C
C'
puc-lacZ
Yki
C"
Yki

Fig 8. Diverse inputs and outputs of Jnk signaling

Jnk, a stress activated protein kinase, is activated by diverse stimuli, including caspase activation, ligands for Jnk signaling pathways (Egr), cellular stresses (reactive oxygen species, infection, cytoskeletal changes), and loss of apical-basal polarity [134, 135]. Jnk activates apoptosis, but also cell proliferation. Activation of proliferation is mediated through Hippo signaling. The immediate target of Jnk signaling within the Hippo pathway is not known, it could act upstream of Wts, but might act in parallel to Wts (dashed lines and question mark). Yki both promotes cell proliferation and inhibits apoptosis through transcriptional regulation of downstream target genes.

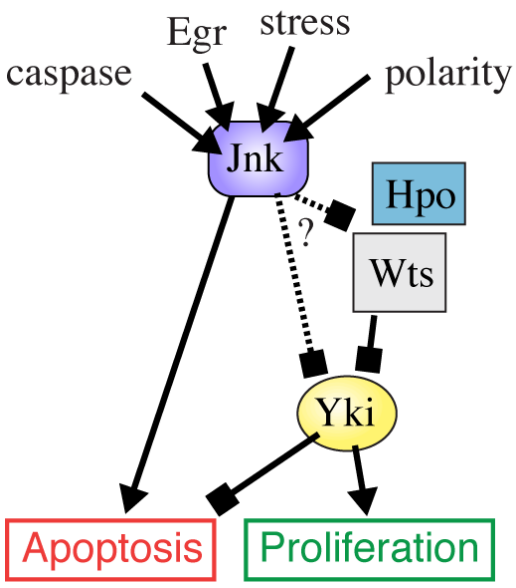

Supplementary figures

Fig S1. Activation of Yki by Jnk

Third instar discs, stained for Yki (red), GFP (green/blue), *puc-lacZ* (green) or cas3 (yellow), as indicated. Panels marked prime show separate channels of the stain to the left. A) *rn-Gal4 UAS-egr tub-Gal80^{ts} puc-lacZ*. B) *sal.PE-Gal4 UAS-GFP UAS-hep.CA Dronc^{129}*/+. Extensive cleaved Caspase3 staining (yellow) is detected, nuclei are stained with DAPI (blue). C) *sal.PE-Gal4 UAS-GFP UAS-hep.CA Dronc^{129}/ Dronc^{129}*. Cleaved Caspase3 staining (yellow) is restricted to scattered cells. D-H Show discs with clones of cells expressed under tub-Gal4 control, by making flip-out clones expressing tub-Gal4 in animals with tub-Gal80ts transgenes. Because of the lethlaity of these clones, clones were allowed to grow for 3 days at 18 C, and then expression was induced at 30C. D) Wing disc with *tub>CD2>Gal4 tub-Gal80^{ts} UAS-CD8:GFP UAS-rpr* clones, induced for 12 h. E-H) E)Wing, F) haltere, G) leg, H) eye, imaginal discs with *tub>CD2>Gal4 tub-Gal80^{ts} UAS-CD8:GFP UAS-hep.CA* clones, induced for 14 h.

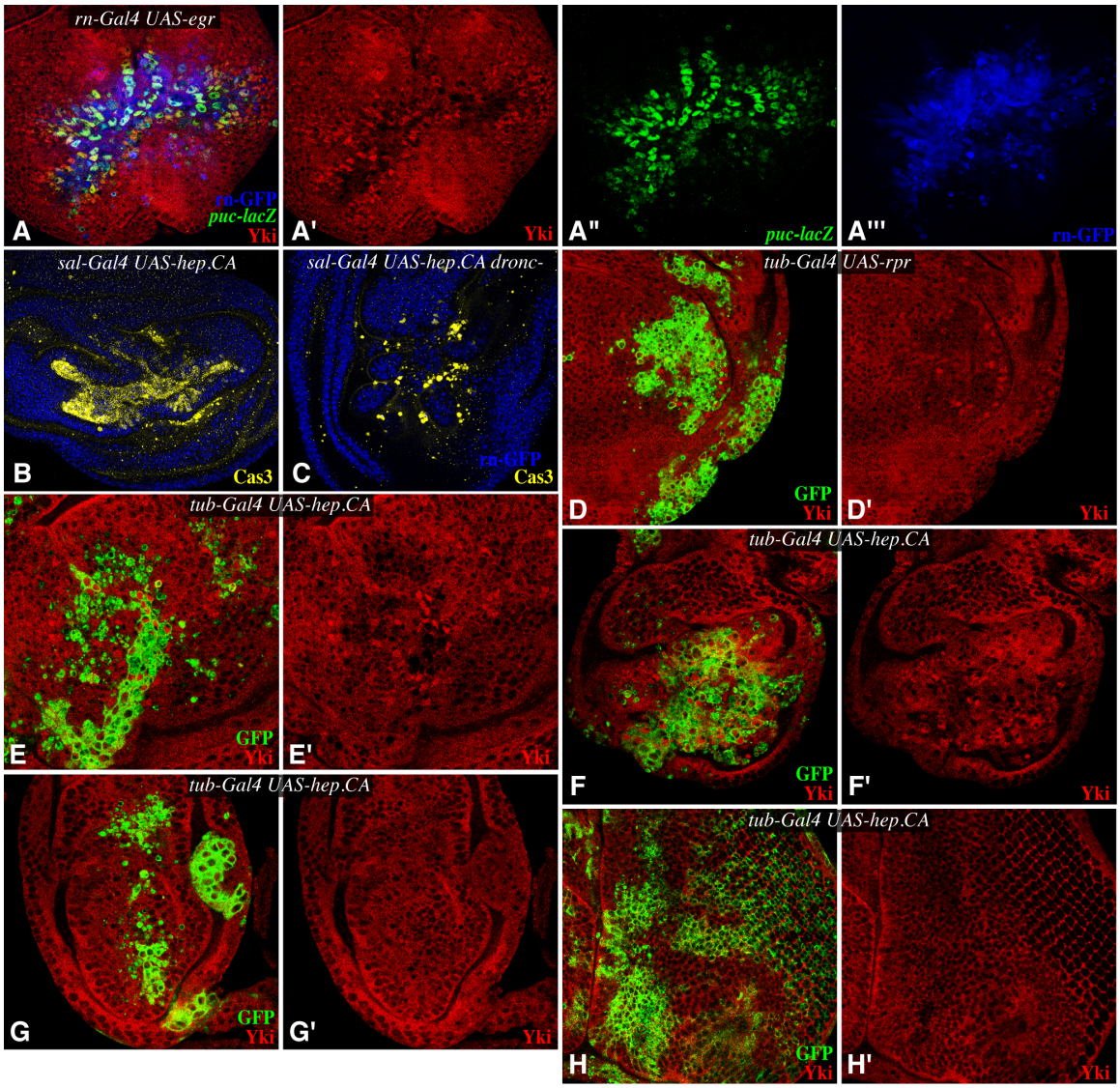
rn-Gal4 UAS-egr
rn-GFP
puc-lacZ
Yki
A
A'
Yki
A"
puc-lacZ
A'''
rn-GFP
sal-Gal4 UAS-hep.CA
B
Cas3
sal-Gal4 UAS-hep.CA dronc-
rn-GFP
C
Cas3
tub-Gal4 UAS-rpr
GFP
Yki
D
D'
Yki
tub-Gal4 UAS-hep.CA
E
GFP
Yki
E'
Yki
tub-Gal4 UAS-hep.CA
F
GFP
Yki
F'
Yki
tub-Gal4 UAS-hep.CA
G
GFP
Yki
G'
Yki
tub-Gal4 UAS-hep.CA
H
GFP
Yki
H'
Yki

Fig S2. High Magnification images showing Activation of Yki by Jnk

Close-ups of third instar wing discs, stained for Yki (red). Panels marked prime show separate channels of the stain to the left. A) wild type. B) *rn-Gal4 UAS-egr tub-Gal80^{ts} UAS-puc*, 30h after induction. C) *rn-Gal4 UAS-rpr tub-Gal80^{ts} UAS-puc*, 30h after induction. D) *sal.PE-Gal4 UAS-GFP UAS-egr Dronc^{129}*/+. E) *sal.PE-Gal4 UAS-GFP UAS-egr Dronc^{129}/ Dronc^{129}*. F) *sal.PE-Gal4 UAS-GFP UAS-hep.CA Dronc^{129}*/+. G) *sal.PE-Gal4 UAS-GFP UAS-hep.CA Dronc^{129}/ Dronc^{129}*.

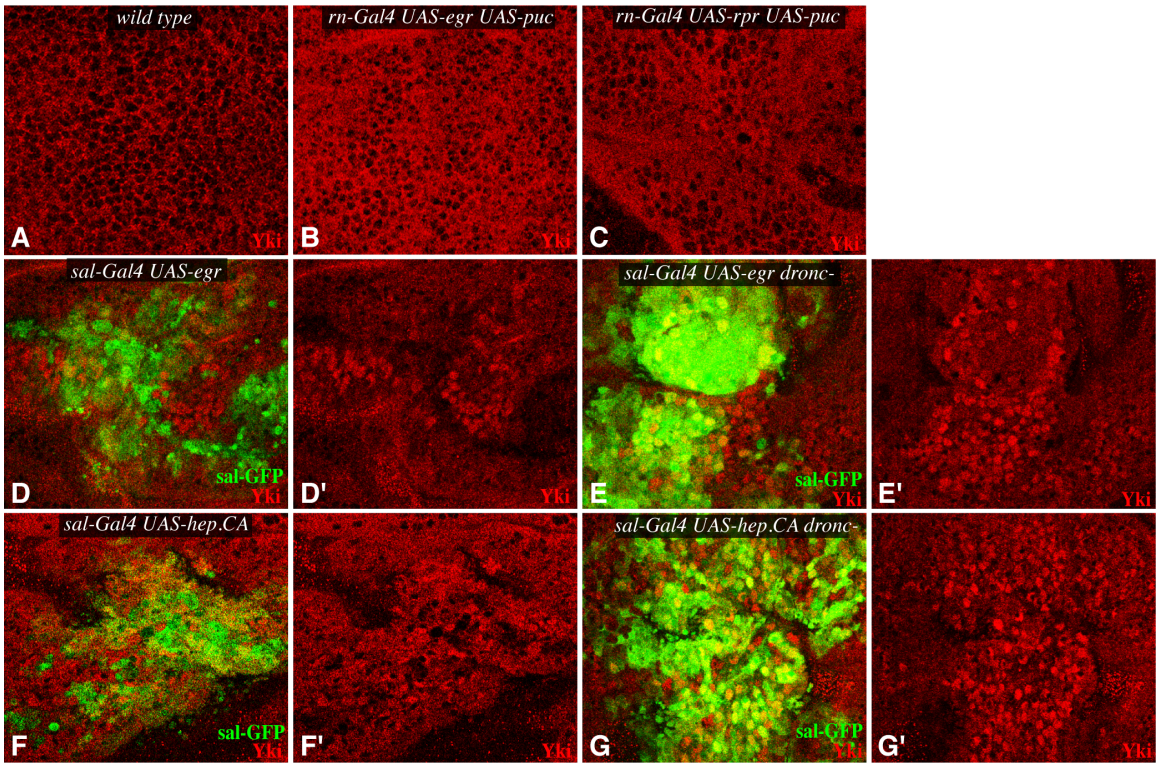
wild type
A
Yki
rn-Gal4 UAS-egr UAS-puc
B
Yki
rn-Gal4 UAS-rpr UAS-puc
C
Yki
sal-Gal4 UAS-egr
D
sal-GFP
Yki
D'
Yki
sal-Gal4 UAS-egr dronc-
E
sal-GFP
Yki
E'
Yki
sal-Gal4 UAS-hep.CA
F
sal-GFP
Yki
F'
Yki
sal-Gal4 UAS-hep.CA dronc-
G
sal-GFP
Yki
G'
Yki

Fig S3. Influence of yki on regeneration.

A-C show examples of wing discs, stained for DNA (blue), Nub (green), and *rn-lacZ* (red, A only). A) *wild type* B) *rn-Gal4 UAS-egr tub-Gal80^{ts},* C) *rn-Gal4 UAS-egr tub-Gal80^{ts} yki^{b5}/+,* D) Quantitation of developmental rate in the genotypes depicted in B,C, based on number of days required for pupation. E) Quantitation of wing pouch size immediately after 30h ablation, based on Nub staining for the genotypes depicted in A-C.

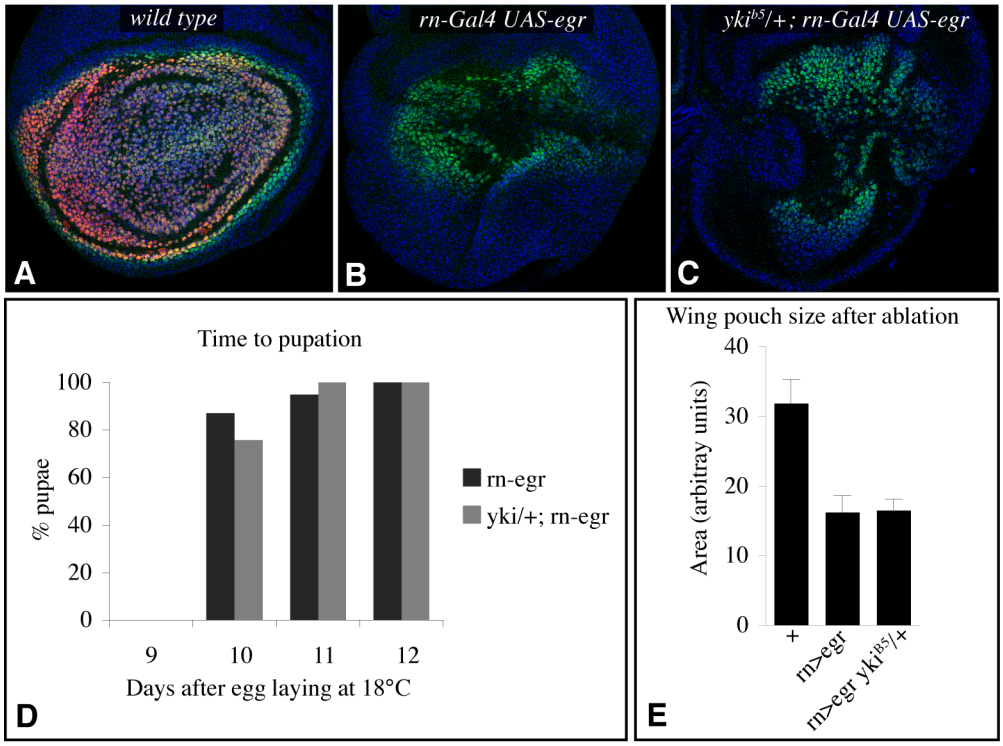
wild type
rn-Gal4 UAS-egr
yki^b5/+; rn-Gal4 UAS-egr
A
B
C
Time to pupation
% pupae
100
80
60
40
20
0
9
10
11
12
Days after egg laying at 18°C
rn-egr
yki/+; rn-egr
D
Wing pouch size after ablation
Area (arbitray units)
40
30
20
10
0
+
rn>egr
rn>egr yki^b5/+
E

Fig S4. Relationship between *lgl* and Jnk

Third instar wing discs, stained for Yki (red), puc-lacZ (red/green), DNA (using Hoechst, blue), GFP (green/blue), as indicated. Panels marked prime show separate channels of the stain to the left. A) *en-Gal4 UAS-RNAi-lgl UAS-dcr2 UAS-puc UAS-GFP*. Yki activation is blocked. B) *en-Gal4 UAS-RNAi-lgl UAS-dcr2 UAS-wts UAS-GFP*, puc-lacZ staining is not blocked by Wts over-expression, even though over-growth is blocked. C) *en-Gal4 UAS-RNAi-lgl UAS-dcr2 UAS-RNAi-bsk UAS-GFP*, puc-lacZ staining is blocked. D) *en-Gal4 UAS-RNAi-lgl UAS-dcr2 UAS-GFP*. A limited degree of non-autonomous induction of *puc-lacZ* and Yki is detected (arrow). Thin panels below each image show a vertical section.

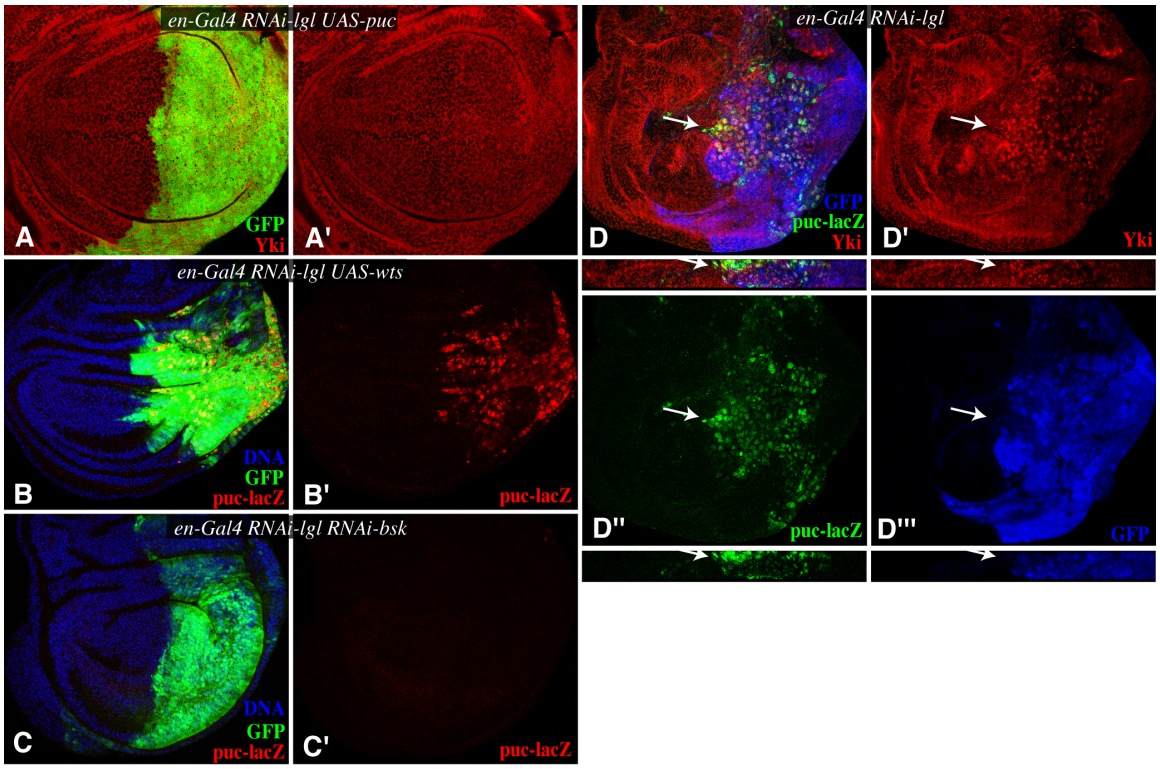
en-Gal4 RNAi-lgl UAS-puc
A
GFP
Yki
A'
en-Gal4 RNAi-lgl UAS-wts
B
DNA
GFP
puc-lacZ
B'
puc-lacZ
en-Gal4 RNAi-lgl RNAi-bsk
C
DNA
GFP
puc-lacZ
C'
puc-lacZ
en-Gal4 RNAi-lgl
D
GFP
puc-lacZ
Yki
D'
Yki
D''
puc-lacZ
D'''
GFP

CHAPTER III

Ajuba family proteins link JNK to Hippo signaling

This chapter was published in *Sci Signal 6 (292): ra81 (2013)*

Gongping Sun performed all of the experiments described. The chapter was written jointly by Gongping Sun and Kenneth D. Irvine.

Summary

Wounding, apoptosis, or infection can trigger a proliferative response in neighboring cells to replace damaged tissue. Studies in *Drosophila* have implicated Jun kinase (JNK)-dependent activation of Yorkie (Yki) as essential to regeneration-associated growth, as well as growth associated with neoplastic tumors, but the mechanism by which this occurs was unknown. Yki is a transcriptional co-activator that is inhibited by Hippo signaling, a conserved pathway that regulates growth. We found that JNK regulation of Hippo signaling is conserved in mammalian cells, and defined a conserved molecular mechanism by which JNK impinges on Hippo signaling. Genetic studies in *Drosophila* identified the Ajuba LIM protein (Jub) as required for JNK-mediated activation of Yki, and showed that Jub contributed to wing regeneration after wounding and to neoplastic tumor growth. Biochemical studies revealed that JNK promoted phosphorylation of Ajuba family proteins in both *Drosophila* and mammalian cells. Binding studies in mammalian cells indicated that JNK increased binding between the Ajuba family proteins LIMD1 or WTIP and LATS1, a kinase within the Hippo pathway that inhibits the Yki homologue YAP, and moreover that JNK promoted LIMD1 and LATS1 binding through direct phosphorylation of LIMD1. These results identify Ajuba family proteins as a conserved link between JNK and Hippo signaling, and imply that JNK increases Yki and YAP activity by promoting the binding of Ajuba family proteins to Warts and LATS.

Introduction

Many forms of tissue damage, including wounding, apoptosis or infection, can trigger a proliferative response in neighboring cells to replace damaged tissue [14, 169]. This regenerative growth requires activation of the c-Jun N-terminal kinase (JNK) signaling pathway [14, 20, 170]. JNK is a stress-activated kinase, which is stimulated by diverse signals such as wounding, irradiation, or oxidation, and which induces diverse biological responses, including cytoskeleton modulation, apoptosis, and cell proliferation, leading to modulation of morphogenesis, inflammation, regeneration, and tumorigenesis [170, 171]. Induction of apoptosis enables tissues to get rid of stressed or damaged cells, and is a frequent response to JNK activation. Nonetheless, JNK activity is also indispensable in some contexts for maintaining tissue homeostasis by triggering compensatory cell proliferation or stem cell activation in response to injury [20, 170, 172, 173]. Moreover, in some contexts JNK-promoted growth can promote tumorigenesis. For example, avoidance of cell competition or activation of the Ras oncogene in *Drosophila* enables cellular insults associated with JNK activation and apoptosis to instead trigger JNK-dependent tumorigenesis [11, 31, 119, 174-177], and JNK activation has also been associated with tumorigenesis in mammals [170, 178, 179].

JNK can influence several signaling pathways, some of which have been implicated in JNK-promoted cell proliferation [180]. One essential response for JNK-promoted proliferation in several contexts is activation of Yorkie (Yki in *Drosophila*, YAP in vertebrates) [181, 182]. Yki is a transcriptional co-activator controlled by Hippo signaling, a conserved pathway that regulates growth during development, regeneration, and oncogenesis [181, 183]. Within the Hippo pathway (Fig 1A), Yki and YAP are

inhibited by the kinase Warts (Wts in *Drosophila* and LATS in vertebrates), which suppress Yki and YAP activity by keeping it in cytoplasm. Several factors that regulate Wts have been identified, including the kinase Hippo (Hpo in *Drosophila* and MST in vertebrates) which gives the pathway its name. Activation of Yki and YAP leads to tissue overgrowth and tumor formation, whereas loss of Yki and YAP impairs growth and can lead to apoptosis [181, 183]. JNK-dependent activation of Yki is required for regenerative growth in multiple *Drosophila* tissues, including larval imaginal discs and adult intestines [11, 13, 33, 184], and is also required for growth associated with certain neoplastic tumor suppressors [11, 174, 177]. However, the mechanism by which JNK signaling promotes Yki activation has been unknown. Here, we have employed a combination of genetic and biochemical approaches to elucidate a molecular mechanism linking JNK activity to Yki regulation. Moreover, we establish that JNK can promote YAP activity in mammalian cells, and that it does so through a conserved molecular mechanism.

Results

JNK regulation of *Drosophila* Hippo signaling requires Ajuba LIM protein

To investigate the mechanism by which JNK regulates Hippo signaling, we took advantage of genetic approaches available in *Drosophila*. Expression of an activated form of the JNK kinase hemipterous (Hep.CA) in *Drosophila* wing discs, under the control of a Gal4 line expressed in the center of the wing (*sal.PE-Gal4*), results in strong Yki activation [11]. Strong JNK activation normally promotes apoptosis; to reduce the apoptosis associated with Hep.CA expression, these flies also carry a mutation in the initiator caspase Dronc ($Dronc^{I29}$) [104]. Yki activation is reflected in these experiments both by the nuclear accumulation of Yki protein, and by the increased activity of a reporter of Yki's transcriptional activity, *ex-lacZ* (Fig. 1B-E, S1H); this Yki activation was visible both in Hep.CA-expressing and neighboring cells. The biological effects of JNK activation are achieved through phosphorylation of target proteins [180], one of which is the transcription factor AP-1, a heterodimer of Fos and Jun proteins. RNAi directed against *Drosophila* Jun did not suppress the ability of Hep.CA expression to promote Yki activation (Figs 1F, S1A, S1H), suggesting that alternate targets of JNK were involved in mediating regulation of Yki activity. Although induction of Wingless and Decapentaplegic can contribute to proliferation in response to JNK activation [16, 175], prior studies suggest that these pathways do not contribute to autonomous activation of Yki [11, 185].

Because JNK promotes Yki activity, we introduced transgenes that should reduce Yki activity into flies with Hep.CA expression to examine the epistatic relationship between JNK and Hippo pathway components. The activation of Yki induced by Hep.CA

expression was suppressed by activating the Hippo pathway through overexpressing Hpo or Wts, suggesting that Jnk promotes Yki activity at or upstream of Hpo and Wts (Fig. S1B-E, S1H) [11]. Autonomous Yki activation was reduced by Hpo or Wts over-expression, although non-autonomous Yki activation was not completely blocked. We then examined whether depletion of components of the Hippo pathway that normally promote Yki activity could suppress Jnk-mediated Yki activation (Fig. 1A). Ras association family member (Rassf) interacts with a phosphatase complex and antagonizes Hippo activation [56, 186]. RNAi directed against Rassf failed to suppress Yki activation (Figs 1G, S1F,S1H). Zyxin (Zyx) is a LIM domain protein that acts upstream of Wts within the Fat branch of the Hippo pathway [65]; Zyx RNAi also failed to prevent activation of Yki by Jnk (Figs 1H, S1G,S1H). This lack of requirement for *Zyx* is consistent with observations that two other genes within the Fat branch of the Hippo pathway, *dachs* and *fat*, are not required for Yki activation induced by expression of Eiger [13]. Ajuba LIM protein (Jub) is a LIM domain protein that interacts with both Wts and the scaffolding protein Salvador (Sav) [64]. Knockdown of Jub by RNAi reduced the autonomous activation of Yki by Hep.CA (Fig 1I,J, S1H). Thus, JNK activation of Yki requires Jub, but not Zyx or Rassf.

Jub is required during wing regeneration and tumor growth

Regenerating wings are sensitive to reductions in Yki activity. For example, *yki* is normally recessive, because loss of one copy of *yki* has no discernible effects on normal wing growth, but heterozygosity for *yki* impairs wing regeneration after genetic ablation of the developing larval wing [11, 13]. If Jub is normally important for Jnk-mediated Yki

activation in vivo, then, given the essential role of Jnk in regeneration, regenerating wings might also exhibit sensitivity to Jub abundance. Indeed, heterozygosity for *jub* had no effect on wing growth or rates of development (Fig S2); however, loss of one copy of *jub* reduced the growth of regenerating wings (Fig. 2A-F).

Loss of Lethal giant larvae (Lgl) in wing discs causes disruption of apical-basal cell polarity and formation of neoplastic tumors. These tumors are associated with activation of both Jnk and Yki, which are required for the associated over-proliferation (Figs 2G-K)[11, 107, 174]. Because Jnk promotes Yki activation in Lgl-depleted cells (Fig 2G, I, and J)[11], we used this as an independent model to confirm the requirement for Jub in Jnk-mediated Yki activation in vivo. Indeed, *jub* RNAi in Lgl-depleted cells suppressed both Yki activation and tissue overgrowth (Fig 2G, H, and L).

JNK regulation of Hippo signaling is conserved in mammalian cells

Because both Jnk and Hippo signaling are conserved from *Drosophila* to humans, and JNK-triggered cell proliferation has also been implicated in repair of tissue damage and tumor growth in mammals [170, 172, 178, 179], we investigated whether JNK regulation of Yki is conserved. Basal JNK activity is required for cell proliferation in mammalian cell lines [187]. When we treated the human mammary epithelial cell line MCF10A with the JNK inhibitor SP600125 [188], phosphorylation of the mammalian Yki homolog YAP on a key regulatory site, Ser^{127}, was increased (Fig. 3A). Treatment of cultured cells with the JNK activator Anisomycin [189] significantly decreased phosphorylation of Ser^{127} at YAP (Fig 3A), an effect that was reversed by SP600125 (Fig. 3A). Characterizion of the phosphorylation of the JNK substrate c-Jun (Fig. S3A)

confirmed the expected effects of these treatments on JNK activity, and the same conditions were used in all drug treatment experiments. Phosphorylation of Ser^{127} in YAP by the kinase LATS is a key step in Hippo signaling, which promotes cytoplasmic localization of YAP through interaction with 14-3-3 proteins [183]. Conversely, loss of phosphorylation at Ser^{127} activates YAP by increasing its nuclear localization. Thus, these effects suggest that JNK can promote YAP activation in mammalian cells, just as it can promote Yki activation in *Drosophila*. This notion was further supported by assaying expression of the YAP target gene *CTGF*, which encodes connective tissue growth factor. *CTGF* expression was reduced by Jnk inhibition and increased by Jnk activation (Fig 3B).

The ability of JNK to reduce phosphorylation of Ser^{127} in YAP implies that Hippo signaling is being inhibited, because most upstream components of Hippo signaling ultimately impinge on LATS, the mammalian homologues of *Drosophila* Wts. LATS is activated by phosphorylation, and one key regulatory site in LATS1 is Thr^{1079}, which is phosphorylated by the MST family of kinases [54, 55], the mammalian homologues of *Drosophila* Hpo. In MCF10A cells, LATS phosphorylation on Thr^{1079} was increased by treatment with SP600125 and decreased by treatment with Anisomycin (Fig 3C). These results suggest that JNK activity inhibits phosphorylation of LATS1 by MST. We extended these studies by examining the influence of two distinct JNK isoforms on Hippo signaling in HEK293 cells transfected with plasmids expressing the JNK kinase MKK7 fused with either JNK1 (MKK7B2:FLAG:JNK1) or JNK2 (MKK7B2:FLAG:JNK2), which results in constitutive activation of JNK [190]. The JNK activity of the transfected fusion proteins was confirmed by phosphorylation of JNK (Fig. S3B). Phosphorylation of

both Ser^{127} in endogenous YAP and Thr^{1079} in endogenous LATS1 was reduced when activated JNK1 or JNK2 were expressed in HEK293 cells (Fig S3C,D). Altogether, our results establish that JNK signaling regulates Hippo signaling in mammalian cells, and impinges upon the pathway at or upstream of the phosphorylation and activation of LATS, which is consistent with our genetic experiments in *Drosophila*.

JNK increases the binding of LIMD1 and WTIP to LATS1

Because genetic studies implicated Jub as essential to JNK-mediated regulation of Yki, we considered the possibility that JNK might influence the activity of Ajuba family proteins. Ajuba proteins can bind to both Wts and Sav in *Drosophila* cells, and their homologues LATS and WW45 in mammalian cells [64]. The ability of Ajuba family proteins to promote Yki and YAP activity implies that they inhibit Wts and LATS activity through this binding [64]. Thus we examined whether JNK could influence the binding between Ajuba family proteins and LATS through co-precipitation experiments in cultured cells. There are three mammalian Ajuba family proteins: Ajuba, LIM domain-containing protein 1 (LIMD1), and Wilms tumor protein 1-interacting protein (WTIP). Expression of constitutively activated-JNK significantly increased binding of LIMD1 and WTIP, but not that of Ajuba, to LATS1 (Fig. 3D,E,F). For LIMD1, we also confirmed that binding between endogenous LIMD1 and endogenous LATS1 was increased in MCF10A cells upon JNK activation by Anisomycin treatment (Fig. 3G). Thus, JNK activation increases binding between LIMD1 or WTIP and LATS1, which could in principle account for the decreased LATS activity associated with JNK activation.

To identify the protein that is targeted by JNK activation, we affinity-purified V5-tagged LIMD1 from HEK293 cells co-transfected or not with plasmids expressing activated-JNK, and then mixed purified LIMD1 with lysates either from cells expressing LATS1, or from cells expressing LATS1 and activated JNK. Co-transfection of activated JNK2 with LIMD1 resulted in a robust (nine-fold) increase in LIMD1 binding to LATS1 (Fig. 3H). Conversely, co-expression of constitutively-activated JNK2 with LATS1 did not increase binding between LIMD1 and LATS1 (Fig. 3H). Thus, the enhanced binding between LIMD1 and LATS1 is due to an influence of JNK2 on LIMD1 rather than on LATS1. Co-expression of constitutively activated JNK1 with LIMD1 gave a similar increase in binding to LATS1, confirming that either JNK protein can increase LATS1-LIMD1 binding. (Fig S3E). Similar experiments established that JNK also increased WTIP-LATS1 binding through an effect on WTIP (Fig S3F).

We also examined the influence of JNK activation on binding between Ajuba family proteins and WW45. However, the binding between Ajuba, LIMD1, or WTIP and WW45 was unaffected by JNK activation (Fig S3G, H, I).

JNK induces phosphorylation of Ajuba family proteins

Activation of JNK reduced the mobility of LIMD1 (Figs 3, S3), suggesting that it induces a post-translational modification. To examine whether Ajuba family proteins could be subject to JNK-promoted phosphorylation, lysates from HEK293 cells expressing an epitope-tagged Ajuba family protein, along with activated forms of JNK1 or JNK2 or negative controls, were analyzed by standard SDS-PAGE gradient gels and Phos-tag gels, which contain a phosphate-binding moiety that specifically retards the

mobility of phosphorylated proteins [70, 191]. Activation of JNK resulted in efficient phosphorylation of LIMD1, visible as a clear mobility shift of most protein on both standard gels and Phos-tag gels (Fig. 4A). For WTIP, a fraction of the protein was phosphorylated, based on the mobility shift observed on both standard and Phos-tag gels (Fig. 4A), although the phosphorylation profile of a substantial fraction of the protein was not altered. Ajuba was the least affected, because Phos-tag gels did not identify any new species with decreased mobility (namely, increased phosphorylation), although there was a modest shift in the proportions of faster and slower migrating isoforms on Phos-tag gels (Fig. 4A). The extent of phosphorylation of Ajuba family proteins by JNK thus correlated with the degree of increased binding to LATS1. Similar analysis for *Drosophila* Jub indicated that activation of Basket (Bsk), the *Drosophila* homolog of JNK, induced phosphorylation of Jub in S2 cells (Fig. S4A). To investigate whether the phosphorylation of Ajuba family proteins was direct, we also performed in vitro kinase assays, using LIMD1 purified from HEK293 cells or Jub purified from S2 cells, and a commercially-available active JNK. These experiments confirmed that Jub and LIMD1 could be directly phosphorylated by JNK in vitro (Fig 4B and S4B).

Direct JNK phosphorylation of LIMD1 increases LIMD1-LATS1 binding

To investigate whether JNK enhances LIMD1-LATS1 binding directly through phosphorylating LIMD1, we incubated purified LIMD1 phosphorylated in vitro by JNK with cell lysates containing Myc-tagged LATS1. LIMD1-LATS1 binding was significantly increased by JNK-mediated phosphorylation of LIMD1 in vitro (Fig 4B).

We then identified candidate JNK phosphorylation sites on V5-tagged LIMD1 purified from cells with or without JNK2 activation by using mass spectrometry (LC-MS/MS). Eleven sites had increased phosphorylation in the presence of JNK activation (Fig S4C), nine of which conform to the minimal JNK site consensus (serine or threonine followed by proline). Of these, Ser^{272}, Ser^{277}, Ser^{421}, and Ser^{424} have been reported to be phosphorylated in cells [192]. A mutant version of LIMD1 with Ser^{272} and Ser^{277} changed to alanine ($LIMD1^{2SA}$) did not show a significant difference in binding to LATS1 without JNK activation, but with JNK activation, LATS1 binding was significantly but not completely reduced compared to wild-type LIMD1 (Fig. 4C). Thus, JNK phosphorylation of Ser^{272} and Ser^{277} accounts for roughly 40% of the JNK-dependent increase in LIMD1-LATS1 binding. A $LIMD1^{4SA}$ mutant (in which Ser^{272}, Ser^{277}, Ser^{421}, and Ser^{424} were changed to alanine) behaved similarly to $LIMD1^{2SA}$ in these experiments (Fig. S4D). We also constructed a $LIMD1^{8A}$ mutant (containing the mutations S187A, S197A, S211A, S255A, S272A, S277A, T294A, and S384A), and these mutations significantly reduced, but did not eliminate the increased LIMD1-LATS1 binding caused by JNK activation (Fig S4E).

Ser^{272} and Ser^{277} are within the N-terminal half of LIMD1, but Ajuba family proteins are reported to bind LATS proteins through their LIM domains [193], which are in the C-terminal half. To further investigate how JNK influences LIMD1-LATS1 binding, we assayed the influence of JNK on binding of a C-terminal LIMD1 polypeptide comprising the three LIM domains to LATS1. This polypeptide bound LATS1, but this binding was not affected by JNK activation (Fig S4F). This observation implies that the

ability of JNK to increase the binding of LATS1 to the C-terminal half of LIMD1 requires JNK phosphorylation sites in the N-terminal half of LIMD1.

Discussion

JNK signaling has been implicated in proliferative responses to tissue damage during regeneration, compensatory cell proliferation, and tumorigenesis. In many cases, these proliferative responses depend upon activation of Yki, but mechanisms by which JNK activation promotes Yki activation have been unknown. Here, we have combined genetic and biochemical approaches to identify and characterize a molecular mechanism that links JNK to Yki regulation. Moreover, we have discovered that the ability of JNK to activate YAP is conserved in mammalian cells. Considering the important roles for both JNK and YAP activity in regeneration and tumorigenesis, the discovery that they can be linked in mammalian cells as they are in *Drosophila* suggests that a JNK-YAP link could contribute to tumorigenesis and proliferative responses to tissue damage. JNK signaling also has pro-apoptotic activity, and the factors that control the balance between apoptotic and proliferative responses have remained unknown. Our identification of a key role for Ajuba family proteins and their regulation of Yki and YAP in the proliferative response provides a basis for further investigations of Ajuba family proteins as potential contributors to the divergent responses to JNK activation in different contexts.

Our results support a model in which JNK promotes Yki and YAP activity by phosphorylating Ajuba family LIM proteins and increasing their binding to Wts and LATS proteins, thereby preventing their activation by Hpo and MST (Fig. 4D). Although we have not yet identified the sites that completely account for the influence of JNK on LIMD1-LATS1 binding, our results show that the influence of JNK is mediated through an effect that ultimately impinges on LIMD1 rather than on LATS1, and that this effect could be at least partially recapitulated by in vitro phosphorylation of LIMD1 by JNK,

and partially blocked by preventing phosphorylation of two Ser residues in the N-terminus. Thus, although we do not exclude the possibility of additional mechanisms, at least part of the effect of JNK can be ascribed to direct phosphorylation of the N-terminus. Because the C-terminus is the LATS1 binding region, these observations suggest a model in which phosphorylation of LIMD1 promotes formation of an "open" conformation in which the LIM domains are more accessible (Fig 4E). Intriguingly, direct evidence for a similar mechanism has been obtained for a related LIM-domain protein, Zyxin: phosphorylation of sites in the N-terminus of Zyxin reduces interaction of the N-terminus with the C-terminal LIM domains, and enhances the ability of the LIM domains to associate with other binding partners [126, 128]. Our results also indicate that the responsiveness to JNK varies amongst the three mammalian family members, with LIMD1 being the most responsive and Ajuba the least responsive. Considering the requirement for *jub* in the regulation of Yki by JNK in *Drosophila*, it is noteworthy that amongst the three mammalian Ajuba family proteins, LIMD1 is the most closely related to *Drosophila* Jub, whereas Ajuba is the most divergent [64].

EGFR-Ras-ERK signaling has been linked to Yki activation [129]. ERK can also connect to Hippo signaling through phosphorylation of Ajuba family proteins. Thus, these combined studies implicate Ajuba family proteins as a key regulatory node within the Hippo pathway for cross-regulation by other signaling pathways. The biochemical mechanisms are distinct: JNK promotes both LIMD1 and WTIP binding to LATS1 whereas ERK only promotes WTIP binding to LATS1, JNK promotes binding to LATS1, whereas ERK promotes binding to both LATS1 and WW45 or Sav, and JNK acts through sites in the N-terminus, whereas ERK acts through a site within the C-terminal LIM

domains of WTIP [129]. Nonetheless, there is a general conceptual similarity, in which phosphorylation influences the ability of Ajuba family proteins to bind to partners within the Hippo pathway, which might in all cases stem from a phosphorylation-induced conformational change. The observation that both pathways impinge upon Ajuba family proteins is particularly intriguing in light of the synergy between Ras and JNK activation in promoting tumorigenesis [31, 119, 174, 176, 177], which might thus be at least partially explained by their impinging upon a shared biochemical mechanism for Yki and YAP regulation.

Materials and Methods

Fly stocks

The fly stocks used were as follows: *salPE-Gal4 UAS-GFP UAS-hep.CA /CyOGFP;UAS-dcr2 Dronc^{I29}/TM6BGal80*, *ex-lacz salPE-Gal4 UAS-GFP UAS-hep.CA /CyOGFP; UAS-dcr2 Dronc^{I29}/TM6BGal80*, *ex-lacz en-Gal4 UAS-GFP/CyO; UAS-dcr2/TM6B, UAS-lglRNAi* (vdrc 51249), *UAS-bskRNAi* (vdrc 104569), *UAS-dRASSFRNAi* (vdrc 110203), *UAS-jubRNAi* (vdrc 38442), *UAS-zyxinRNAi* (vdrc 104169), *UAS-myc:wts.2*, *UAS-hpo*, *rn-Gal4 UAS-egr Gal80^{ts}/TM6BGal80*[10], and *jub^{E1}/FM7* [194].

Plasmids

V5-tagged human Ajuba, LIMD1, and LIMD1-C were generated by PCR using Ajuba or LIMD1 cDNA (Open Biosystems) as templates and inserting into pCDNA3.1-V5:His B vector (Life Technologies). Other plasmids used in this paper includes pCDNA3-MKK7B2:flag:Jnk1a1 (Addgene 19731), pCDNA3-MKK7B2:flag:Jnk1a1(APF) (Addgene 19730), pCDNA3-MKK7B2:flag:Jnk2a2(Addgene 19727), pCDNA3-myc:lats1 [54], pCDNA3-GFP:V5, pCDNA3-WTIP:V5, pUAST-3Xflag:jub [129]. MKK7B2:flag:Jnk1a1(APF) is a kinase dead form of JNK1 fused with MKK7, in which the activation motif Thr^{1959}-Pro-Tyr^{1965} is replaced with Ala-Pro-Phe [190]. LIMD1:V5 mutants were made using Quickchange lightning multi site-directed mutagenesis kit (Agilent Technologies).

Cell culture, transfection and treatment

Drosophila S2 cells were cultured in Schneider's *Drosophila* medium (Life Technologies) supplemented with 10% FBS (Sigma) and Antibiotic-Antimycotic (Life Technologies) at 25°C. HEK293 cells were cultured in DMEM medium (Life Technologies) supplemented with 10% FBS and Antibiotic-Antimycotic, and MCF10A cells were cultured in DMEM/F12 medium (Life Technologies) supplemented with 5% horse serum, 20μg/ml EGF, 10μg/ml insulin, 0.1μg/ml chloratoxin, 0.5μg/ml hydrocortisone and Antibiotic-Antimycotic at 37°C and 5% CO_2. S2 cells were transfected with Cellfectin II (Life Technologies), and HEK293 and MCF10A cells were transfected with Lipofectamine 2000 (Life Technologies) according to manufacturer's protocols, and harvested 24h after transfection. 50μM SP600125 (Santa Cruz Biotechnology) and/or 50ng/ml Anisomycin (Abcam) were applied to MCF10A cells for 4h after 24h serum starvation, for co-treatments cells were pretreated with DMSO (-) or 50μM SP600125 for 1h, followed by treatment with 50ng/ml Anisomycin and/or 50μM SP600125 for 4h.

Immunoblotting and immunoprecipitation

Cells were lysed in lysis buffer (50mM Tris·HCl pH7.4, 150mM NaCl, 1% Triton X-100, 0.1% CHAPS, 0.1% NP-40, 1mM EDTA, 5% glycerol) supplemented with protease inhibitor cocktail (Roche) and phosphatase inhibitor cocktail (Calbiochem). Protein samples were applied to 4-15% gradient gels (Bio-rad). For immunoprecipitation, protein samples were incubated with mouse anti-V5 agarose affinity gel (Sigma) overnight or rabbit anti-Lats1 (1:150, Cell signaling Technology) overnight followed by incubation with protein G sepharose (GE Healthcare) for 1h at 4°C. Antibodies used for immunoblotting include rabbit anti-Lats1 (1:2000, Cell Signaling Technology), rabbit

anti-phospho-Lats1(T1079) (1:2000, Cell Signaling Technology), rabbit anti-phospho-Yap(S127) (1:4000, Cell Signaling Technology), rabbit anti-Yap (1:2000, Epitomics), rabbit anti-phospho-c-Jun (S73) (1:1000, Cell Signaling Technology), rabbit anti-Myc (1:2000, Santa Cruz Biotechnology), mouse anti-V5 (1:10000, Life Technologies), rabbit anti-LIMD1 (1:2000, Bethyl Laboratories). Blots were visualized and quantified using fluorescent-conjugated secondary antibodies (Li-Cor Biosciences) and Odyssey Imaging System (Li-Cor Biosciences).

Statistical Analysis

Statistical significance was determined using paired two-tailed t test for two sample comparisons or ANOVA for multiple samples analysis, after logarithm transformation of normalized or ratio values, with $P<0.05$ set as the criteria for significance. The Tukey test was used to derive adjusted P values for multiple comparisons. Error bars on figure panels show standard error of the mean.

Phos-tag gel

For Phos-tag gel, cells were lysed in 50mM Tris·HCl pH7.5, 150mM NaCl, 1% Triton X-100, 0.1% NP-40. Lysates containing transfected *Drosophila* Jub or human LIMD1 were applied to 6% SDS-PAGE containing 25μM Phos-tag Acrylamide AAL-107 (NARD Institute) and 50μM $MnCl_2$. Lysates containing transfected human Ajuba or WTIP were applied to 8% SDS-PAGE containing 25μM Phos-tag Acrylamide AAL-107 and 50μM $MnCl_2$.

In vitro kinase assay

Flag tagged Jub was expressed in S2 cells in 6-well plates and purified using EZviewRed Anti-flag M2 Affinity Gel (Sigma). After washing with lysis buffer, beads with purified proteins were added to kinase buffer (50mM Tris·HCl pH7.5, 1mM DTT) supplemented with protease inhibitor cocktail, phosphatase inhibitor cocktail, and magnesium/ATP cocktail (1:5, Millipore). For each reaction, 500ng JNK1a1 (to phosphorylate *Drosophila* Jub) or JNK2a2 (to phosphorylate LIMD1, Millipore) was added. The mixture was incubated at 15°C for 1h.

In vitro binding assay

V5-tagged LIMD1, LIMD1-C, WTIP, or GFP were transfected into HEK293 cells with or without MKK7B2:FLAG:Jnk2a2. Cells were lysed in lysis buffer (50mM Tris·HCl pH7.4, 150mM NaCl, 1% Triton X-100, 0.1% CHAPS, 0.1% NP-40, 1mM EDTA, 5% glycerol) supplemented with protease inhibitor cocktail (Roche) and phosphatase inhibitor cocktail (Calbiochem). Lysates were incubated with mouse anti-V5 agarose (Sigma) for 3h at 4°C, then washed with lysis buffer 4 times. The beads with V5-tagged proteins were incubated with cell lysates containing Myc-tagged Lats1 with or without MKK7B2:FLAG:Jnk2a2 or MKK7B2:FLAG:Jnk1a1 overnight at 4°C. Beads were then washed with lysis buffer 6 times, and applied to SDS-PAGE.

Mass spectrometry

V5-tagged LIMD1 was transfected into HEK293 cells with or without MKK7B2:FLAG:Jnk2a2. After protein extraction, LIMD1:V5 was purified using anti-V5

agarose (Sigma), and applied to 4-15% gradient gel. Gels were stained using Gelcode blue stain reagent (Pierce). Bands were cut from gel and analyzed by the Biological Mass Spectrometry Facility of the UMDNJ- Rutgers for LC-MS/MS analysis.

Quantitative RT-PCR

RNA was extracted from MCF10A cells treated with different drugs using Trizol reagent (Life Technologies). SuperScript III reverse transcriptase (Life Technologies) was used for reverse transcription. Quantitative PCR was conducted using QuantiTect SYBR green PCR kit (Qiagen).

Immunostaining

Inverted anterior part of *Drosophila* larvae were fixed in 4% PFA for 20min at room temperature, then washed with PBS containing 1% BSA and 0.1% Triton X-100 and blocked by 5% Donkey serum. Antibodies used for immunostaining include rabbit anti-Yki (1:400), mouse anti-β-gal (1:400, DHSB). The intensity of ex-lacZ staining and compartment area were quantified using Image J software, comparing GFP-expressing to non-GFP expressing cells within the wing pouch.

Wing regeneration experiment

Larvae were raised at 18°C for 8 days after egg laying then transferred to 29°C for 40h to ablate the developing larval wing by inducing pro-apoptotic gene expression through inactivation of $Gal80^{ts}$. After ablation, larvae were shifted back to 18°C and maintained at 18°C until eclosion. Adult wings were mounted in Gary's magic mountant and

photographed using ProgRes Mac Capture Pro software. Wing sizes were quantified using ImageJ software.

Figures

Fig 1. Jnk activation of Yki in *Drosophila* wing discs requires Jub

A) Simplified schematic of the *Drosophila* Hpo pathway. Proteins that inhibit Yki activity are indicated by dark shading and proteins that promote Yki activity are indicated by light shading. B-J) Wing discs stained for *ex-lacZ* (magenta) or Yki (red) and DNA (Hoechst, blue) with the *salPE-Gal4* expression domain identified by expression from *UAS-GFP* (green). The right part of each panel shows a single channel from the stain to the left. White dashed lines outline the *salPE-Gal4* expressing domain. Arrows point to examples of nuclear Yki. Discs are from animals with $Dronc^{I29}$ mutation, *salPE-Gal4* and *UAS-GFP* transgenes, and B) control, C) *ex-lacZ*, D) *UAS-hep.CA*, E) *ex-lacZ UAS-hep.CA*, F) *UAS-hep.CA UAS-RNAi-jun,* G) *UAS-hep.CA UAS-RNAi-Rassf*, H) *UAS-hep.CA UAS-RNAi-zyx*, I) *UAS-hep.CA UAS-RNAi-jub*, J) *ex-lacZ UAS-hep.CA UAS-RNAi-jub*. Images are representative of at least eight animals per genotype.

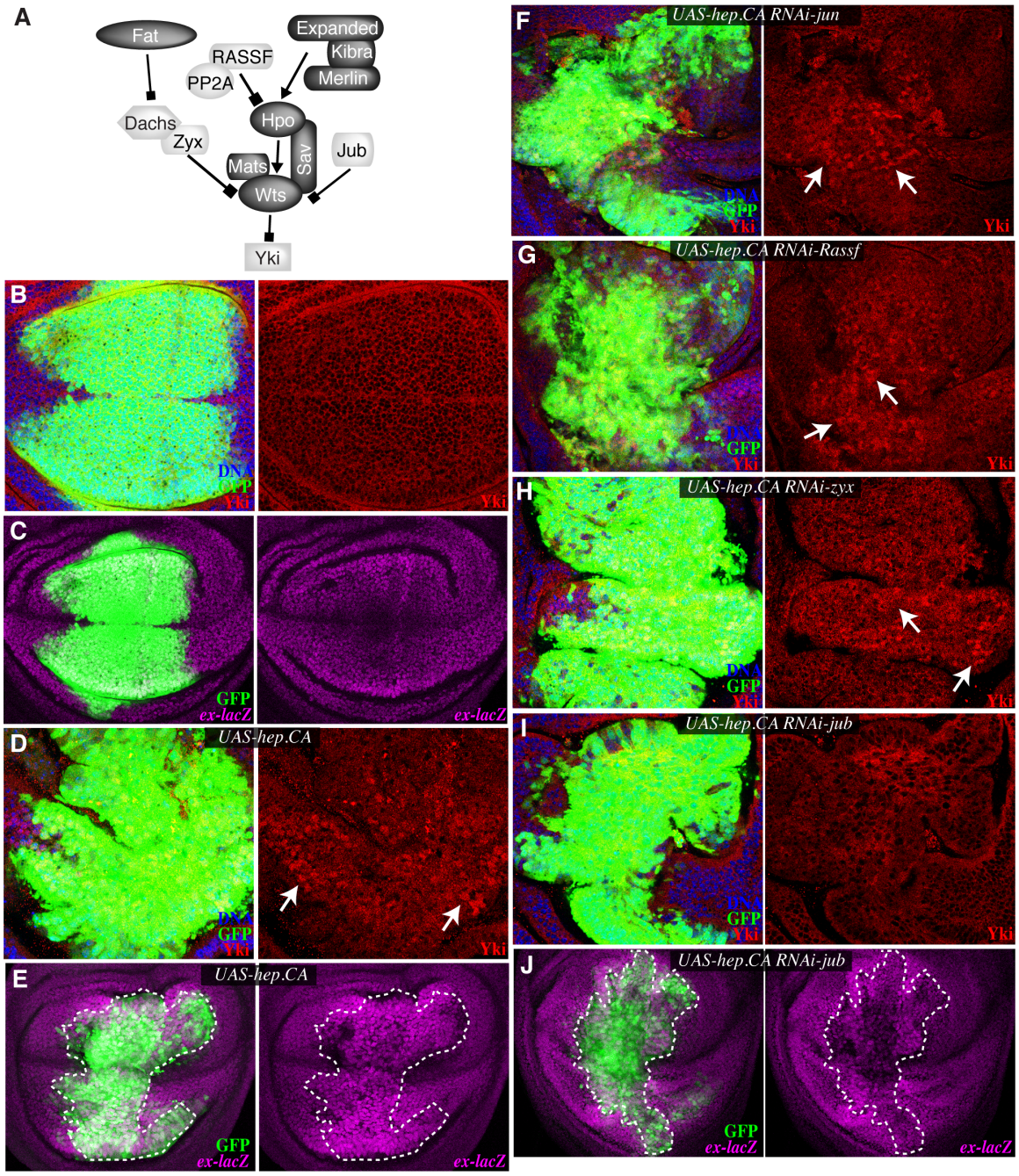
A
Fat
Expanded
Kibra
Merlin
RASSF
PP2A
Dachs
Zyx
Hpo
Sav
Mats
Wts
Jub
Yki
B
DNA
GFP
Yki
Yki
C
GFP
ex-lacZ
ex-lacZ
D
UAS-hep.CA
DNA
GFP
Yki
Yki
E
UAS-hep.CA
GFP
ex-lacZ
ex-lacZ
F
UAS-hep.CA RNAi-jun
DNA
GFP
Yki
Yki
G
UAS-hep.CA RNAi-Rassf
DNA
GFP
Yki
Yki
H
UAS-hep.CA RNAi-zyx
DNA
GFP
Yki
Yki
I
UAS-hep.CA RNAi-jub
DNA
GFP
Yki
Yki
J
UAS-hep.CA RNAi-jub
GFP
ex-lacZ
ex-lacZ

Fig 2. Jub is required for *Drosophila* wing regeneration and for neoplastic tumor growth in wing discs with *lgl* knock-down.

A) Distribution of adult wing sizes in *rn-Gal4 UAS-egr tubGal80^{ts}* (N=78) or *rn-Gal4 UAS-egr tubGal80^{ts} jub^{E1}/+* (N=105) flies after larval wing ablation and recovery. B-F) Representative wings of 100% (B), 70% (C), 50% (D), 30% (E) and 10% (F) wild-type size. G-J) Wing discs stained for *ex-lacz* (ß-gal, magenta) and with the posterior marked by expression of *en-Gal4 UAS-GFP* (green). The right part of each panel shows the *ex-lacZ* only stain from the image to the left. Discs are from animals with *ex-lacZ*, *en-Gal4* and *UAS-GFP* transgenes and G) *UAS-lglRNAi*, H) *UAS-lglRNAi UAS-jubRNAi*, I) *UAS-lglRNAi UAS-bskRNAi*, J) *UAS-lglRNAi UAS-myc:wts*. K) Quantification of the ratios of mean intensity of ex-lacZ expression in posterior to anterior compartments for the indicated genotypes (N=3 discs per genotype). L) Quantification of the ratios of mean area of the posterior to anterior compartments for the indicated genotypes (N=3 discs per genotype). Error bars indicate standard error, and P values less than 0.05 are shown.

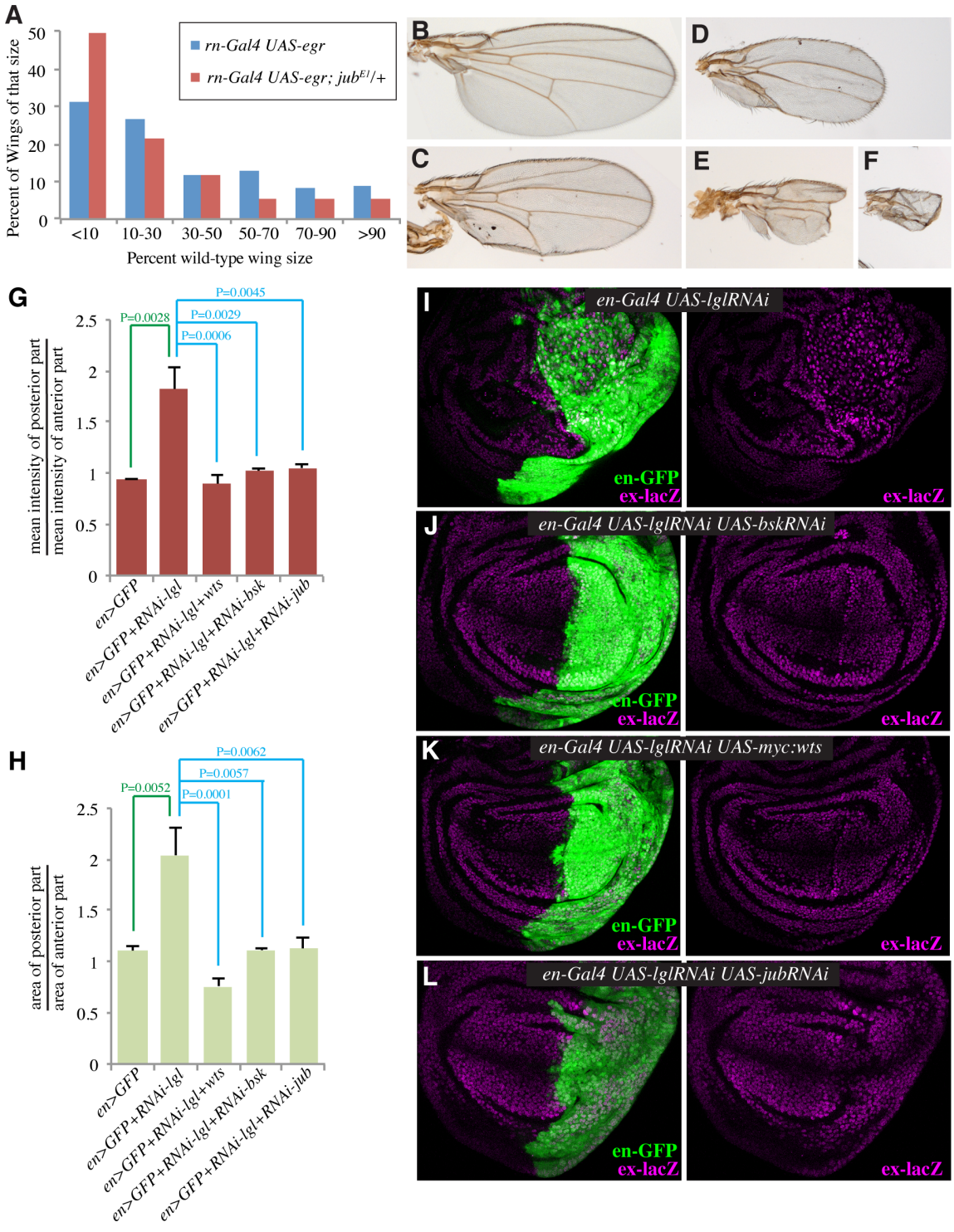
A
Percent of Wings of that size
50
40
30
20
10
0
rn-Gal4 UAS-egr
rn-Gal4 UAS-egr; jub^E1/+
<10
10-30
30-50
50-70
70-90
>90
Percent wild-type wing size
B
C
D
E
F
G
mean intensity of posterior part / mean intensity of anterior part
P=0.0028
P=0.0045
P=0.0029
P=0.0006
2.5
2
1.5
1
0.5
0
en>GFP
en>GFP+RNAi-lgl
en>GFP+RNAi-lgl+wts
en>GFP+RNAi-lgl+RNAi-bsk
en>GFP+RNAi-lgl+RNAi-jub
H
area of posterior part / area of anterior part
P=0.0052
P=0.0062
P=0.0057
P=0.0001
2.5
2
1.5
1
0.5
0
en>GFP
en>GFP+RNAi-lgl
en>GFP+RNAi-lgl+wts
en>GFP+RNAi-lgl+RNAi-bsk
en>GFP+RNAi-lgl+RNAi-jub
I
en-Gal4 UAS-lglRNAi
en-GFP
ex-lacZ
ex-lacZ
J
en-Gal4 UAS-lglRNAi UAS-bskRNAi
en-GFP
ex-lacZ
ex-lacZ
K
en-Gal4 UAS-lglRNAi UAS-myc:wts
en-GFP
ex-lacZ
ex-lacZ
L
en-Gal4 UAS-lglRNAi UAS-jubRNAi
en-GFP
ex-lacZ
ex-lacZ

Fig 3. JNK inhibits the Hippo pathway in mammalian cells and enhances LIMD1 and WTIP binding to LATS1

A) Western blots on lysates of MCF10A cells treated with DMSO (control, indicated by -), SP600125, and/or Anisomycin as indicated (+), blotted using the indicated antisera. TUB is a loading control. Histograms show quantitation of the pYAP over YAP ratio from three biological replicates, normalized to the ratio in mock treated cells. B) Quantitation of *CTGF* mRNA abundance (N=3 biological replicates) by RT-PCR on MCF10A cells treated with DMSO (-), SP600125, and/or Anisomycin (+). GAPDH was used as an internal control. The CTGF over GAPDH ratio was normalized to the ratio in mock treated cells. C) Western blots on lysates of MCF10A cells treated with DMSO (-), SP600125, and/or Anisomycin (+), blotted using the indicated antisera. TUB is a loading control. Histograms show quantitation of the pLATS1 over LATS ratio from three biological replicates, normalized to the ratio in mock treated cells. D-F) Co-immunoprecipitation experiments from HEK293 cells co-transfected with Myc:LATS1 and Ajuba:V5 (D), WTIP:V5 (E), or LIMD1:V5 (F), in the presence or absence of a plasmid expressing activated-JNK2, as indicated. Blots marked “input” show relative amounts of the indicated proteins in cell lysates. Blots marked “IP V5” show relative amounts of protein precipitated by anti-V5 beads. Histograms show average ratio of LATS1/Ajuba family proteins from three biological replicates, normalized to the ratio in controls. G) Co-immunoprecipitation experiments from MCF10A cells treated or not with Anisomycin. Blots marked “Input” show relative amounts of endogenous LATS1 and LIMD1 in cell lysates. Blots marked “IP LATS1” show relative amounts of protein immunoprecipitated with anti-LATS1. Histogram shows average ratio of LIMD1/LATS1

from three biological replicates, normalized to the ratio in controls. H) In vitro binding experiments comparing the influence of JNK2 activation on LATS1 and LIMD1. Blot of anti-V5 beads shows amounts of LIMD1 or GFP (control) on beads, co-IP shows amounts of Myc:LATS1 precipitated by these beads. LIMD1 Lysates shows the relative amounts of LIMD1:V5 and JNK2 fusion protein in the lysates applied to V5 beads for purification, and LATS1 Lysates shows Myc:LATS1 and JNK2 fusion protein in the lysates added to beads. Histogram shows average ratio of LATS1/LIMD1 from three biological replicates, normalized to the ratio in controls. In all histograms, error bars indicate standard error, and P values less than 0.05 are shown.

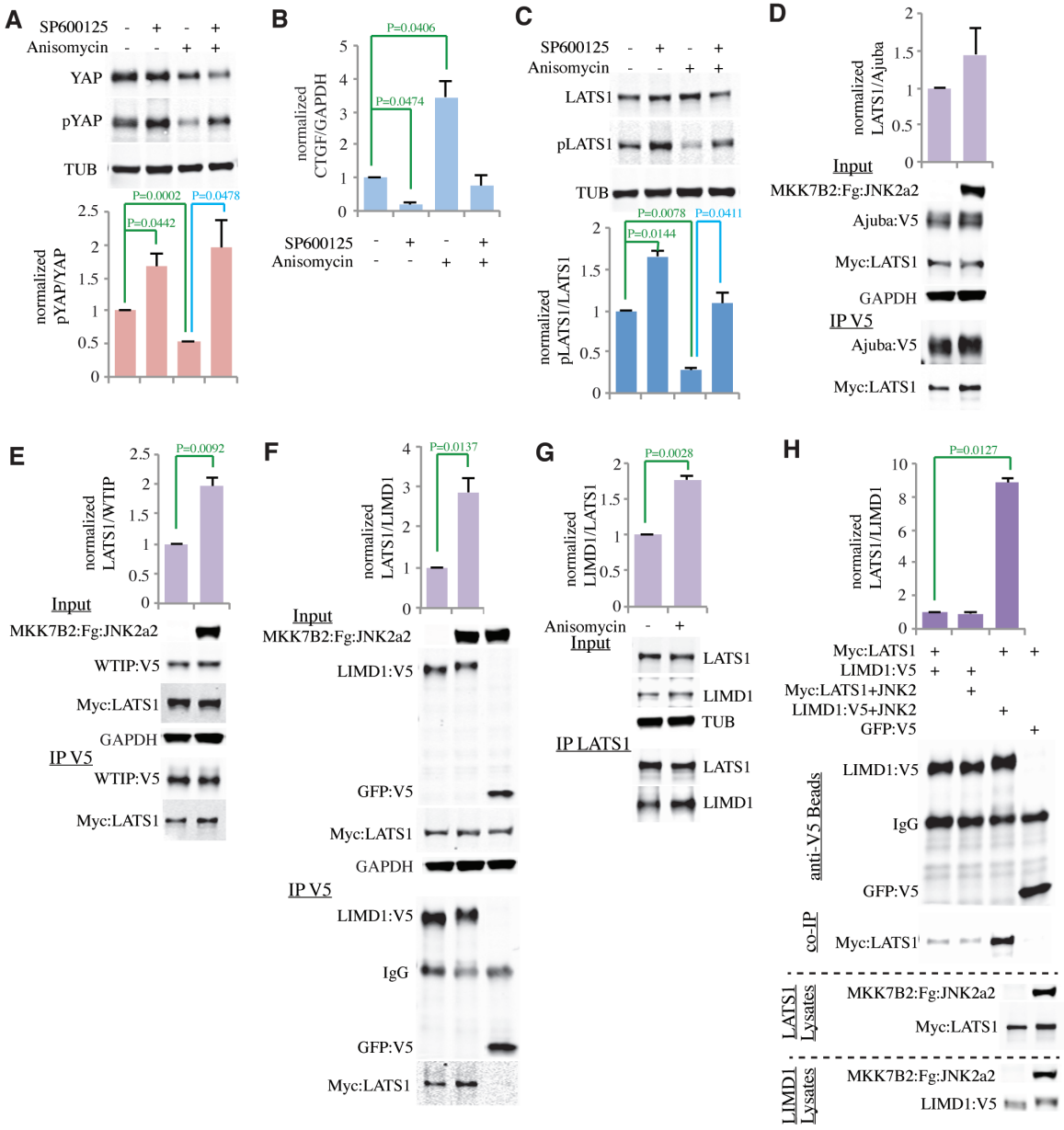
A
SP600125 - + - +
Anisomycin - - + +
YAP
pYAP
TUB
P=0.0002
P=0.0478
P=0.0442
normalized pYAP/YAP
B
P=0.0406
P=0.0474
normalized CTGF/GAPDH
SP600125 - + - +
Anisomycin - - + +
C
SP600125 - + - +
Anisomycin - - + +
LATS1
pLATS1
TUB
P=0.0078
P=0.0411
P=0.0144
normalized pLATS1/LATS1
D
normalized LATS1/Ajuba
Input
MKK7B2:Fg:JNK2a2
Ajuba:V5
Myc:LATS1
GAPDH
IP V5
Ajuba:V5
Myc:LATS1
E
P=0.0092
normalized LATS1/WTIP
Input
MKK7B2:Fg:JNK2a2
WTIP:V5
Myc:LATS1
GAPDH
IP V5
WTIP:V5
Myc:LATS1
F
P=0.0137
normalized LATS1/LIMD1
Input
MKK7B2:Fg:JNK2a2
LIMD1:V5
GFP:V5
Myc:LATS1
GAPDH
IP V5
LIMD1:V5
IgG
GFP:V5
Myc:LATS1
G
P=0.0028
normalized LIMD1/LATS1
Anisomycin - +
Input
LATS1
LIMD1
TUB
IP LATS1
LATS1
LIMD1
H
P=0.0127
normalized LATS1/LIMD1
Myc:LATS1 + + +
LIMD1:V5 + +
Myc:LATS1+JNK2 +
LIMD1:V5+JNK2 +
GFP:V5 +
anti-V5 Beads
LIMD1:V5
IgG
GFP:V5
co-IP
Myc:LATS1
LATS1 Lysates
MKK7B2:Fg:JNK2a2
Myc:LATS1
LIMD1 Lysates
MKK7B2:Fg:JNK2a2
LIMD1:V5

Fig 4. JNK induces phosphorylation of Ajuba family proteins to increase binding to LATS1

A) Western blots on lysates of HEK293 cells co-transfected with Ajuba:V5, LIMD1:V5, or WTIP:V5 and, as indicated, MKK7B2:FLAG:JNK1a1 (activated JNK1), MKK7B2:FLAG:JNK1a1(APF) (inactive JNK1), or MKK7B2:FLAG:JNK2a2 (activated JNK2). The expression of transfected JNK constructs is shown in Flag blots. For each Ajuba family protein, the upper blot shows a standard gel, and the lower blot shows a Phos-tag gel. Blots are representative of 3 biological replicates. B) In vitro binding of LIMD1 to LATS1 after in vitro phosphorylation of LIMD1 by active JNK2. The upper blot shows amount of LIMD1 on beads, and the lower blot shows Myc:LATS1 bound to the beads. The histogram shows the average LATS1/LIMD1 ratio from three biological replicates, normalized to the ratio without JNK2 phosphorylation. C) In vitro binding assays comparing wild-type LIMD1 and LIMD1^{2SA} mutant binding to LATS1. Anti-V5 beads blot shows LIMD1, LIMD1^{2SA} or GFP (control) protein on beads. Co-IP shows Myc:LATS1 bound to wild-type or mutant LIMD1. Expression of constitutively active JNK2 is shown in LIMD1 Lysates blot. The histogram shows the average LATS1/LIMD1 ratio from three biological replicates, normalized to the ratio in wild-type LIMD1 control. Error bars in B,C show standard error. P values less than 0.05 are indicated. D) Model illustrating influence of JNK on Hippo signaling, active proteins are outlined in black, P indicates phosphorylation. In the absence of JNK activation, MST (Hpo), MOB (Mats), and WW45 (Sav) can activate LATS (Wts), which then represses YAP (Yki) by phosphorylating it. When JNK is active, it promotes phosphorylation of Ajuba family proteins (LIMD1, WTIP, or Jub), which then bind more strongly to LATS.

This binding inhibits LATS phosphorylation and consequent activation of LATS, possibly by occluding the phosphorylation site, or by inhibiting binding of WW45 or MOB. E) Model illustrating the proposed conformational change of Ajuba family proteins caused by JNK that enhances LATS binding. Without JNK activation, Ajuba family proteins stay as a ‘closed’ form and cannot be accessed by LATS (left). When JNK is activated, the N-terminus of Ajuba family proteins get phosphorylated which result in exposure of C-terminus to LATS (right).

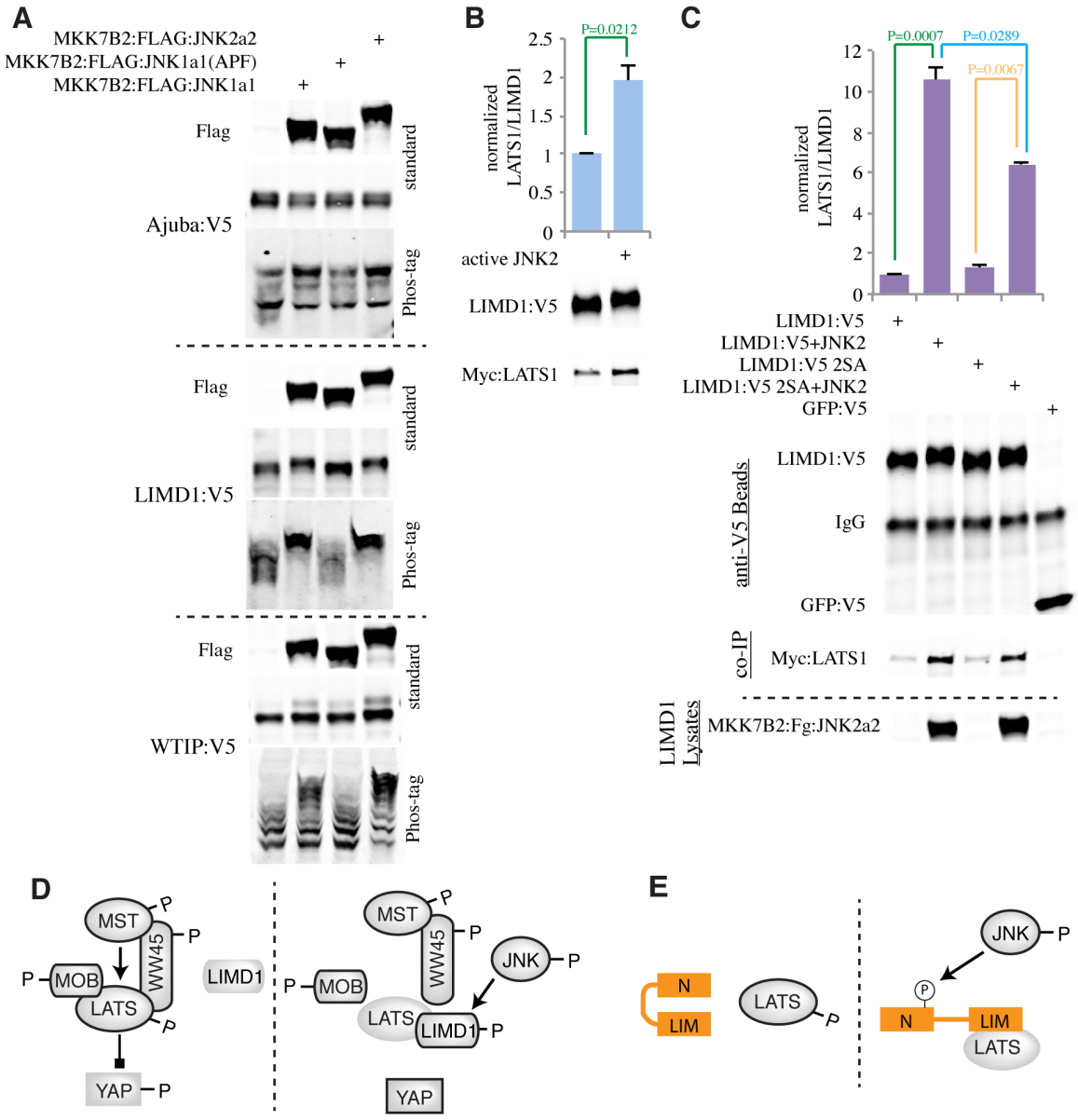
A
MKK7B2:FLAG:JNK2a2
MKK7B2:FLAG:JNK1a1(APF)
MKK7B2:FLAG:JNK1a1
Flag
standard
Ajuba:V5
Phos-tag
Flag
standard
LIMD1:V5
Phos-tag
Flag
standard
WTIP:V5
Phos-tag
B
P=0.0212
normalized LATS1/LIMD1
active JNK2
LIMD1:V5
Myc:LATS1
C
P=0.0007
P=0.0289
P=0.0067
normalized LATS1/LIMD1
LIMD1:V5
LIMD1:V5+JNK2
LIMD1:V5 2SA
LIMD1:V5 2SA+JNK2
GFP:V5
anti-V5 Beads
LIMD1:V5
IgG
GFP:V5
co-IP
Myc:LATS1
LIMD1 Lysates
MKK7B2:Fg:JNK2a2
D
MST
WW45
MOB
LATS
YAP
LIMD1
JNK
E
N
LIM
LATS

Supplementary figures

Fig S1. Epistasis between JNK and Hippo pathway components in regulation of Yki

Wing discs stained for *ex-lacz* (ß-gal, magenta) or Yki (red) and DNA (Hoechst, blue) with the *salPE-Gal4* expression domain identified by expression from *UAS-GFP* (green). The right part of each panel shows a single channel of the stain to the left, and white dashed lines outline the *salPE-Gal4* expressing domain. Discs are from animals homozygous mutant for $Dronc^{I29}$ and with *salPE-Gal4 UAS-hep.CA* and *UAS-GFP* transgenes, and A) *ex-lacZ UAS-RNAi-jun*, B) *ex-lacZ UAS-Myc:wts*, C) *ex-lacZ UAS-hpo*, D) *UAS-Myc:wts,* E) *UAS-hpo*, F) *ex-lacZ UAS-RNAi-Rassf,* G) *ex-lacZ UAS-RNAi-zyx*. H) Quantification of the ratio of the mean (N=3 discs for each genotype) *ex-lacZ* intensity within the *salPE* domain compared to that outside the *salPE* domain in discs of the indicated genotypes. Error bars indicate standard errors. P values less than 0.05 are listed.

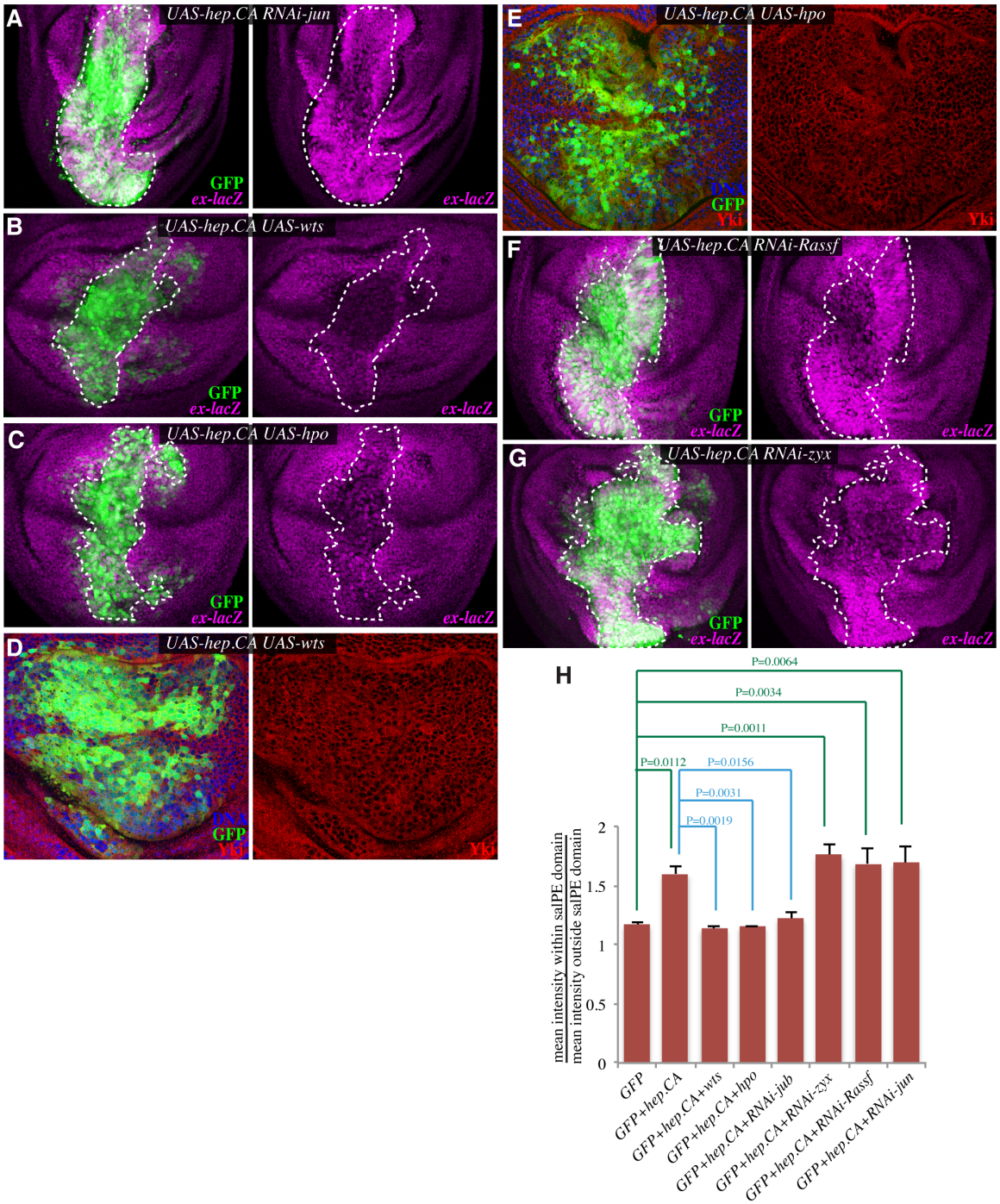
A
UAS-hep.CA RNAi-jun
GFP
ex-lacZ
ex-lacZ
B
UAS-hep.CA UAS-wts
GFP
ex-lacZ
ex-lacZ
C
UAS-hep.CA UAS-hpo
GFP
ex-lacZ
ex-lacZ
D
UAS-hep.CA UAS-wts
DNA
GFP
Yki
Yki
E
UAS-hep.CA UAS-hpo
DNA
GFP
Yki
Yki
F
UAS-hep.CA RNAi-Rassf
GFP
ex-lacZ
ex-lacZ
G
UAS-hep.CA RNAi-zyx
GFP
ex-lacZ
ex-lacZ
H
P=0.0064
P=0.0034
P=0.0011
P=0.0112
P=0.0156
P=0.0031
P=0.0019
mean intensity within salPE domain
mean intensity outside salPE domain
2
1.5
1
0.5
0
GFP
GFP+hep.CA
GFP+hep.CA+wts
GFP+hep.CA+hpo
GFP+hep.CA+RNAi-jub
GFP+hep.CA+RNAi-zyx
GFP+hep.CA+RNAi-Rassf
GFP+hep.CA+RNAi-jun

Fig S2 Heterozygosity for *jub* does not affect the rate of development or adult wing size without ablation

A) To assess rates of development, days until eclosion were scored under our experimental paradigm for wild-type and jub^{E1} heterozygotes, with and without the expression of *egr* in the wing to induce transient wing ablation and regeneration. Graph shows the fraction of animals eclosing in days after egg laying of wild-type (WT, n=198), $jub^{E1/+}$ (n=111), *rn-Gal4 UAS-egr tubGal80*^{ts} (n=160) or *rn-Gal4 UAS-egr tubGal80*^{ts}$jub^{E1/+}$ (n=110) flies. B) Average wing size (in arbitrary units) of wild type (WT, n=198) and $jub^{E1/+}$ (n=111) flies.

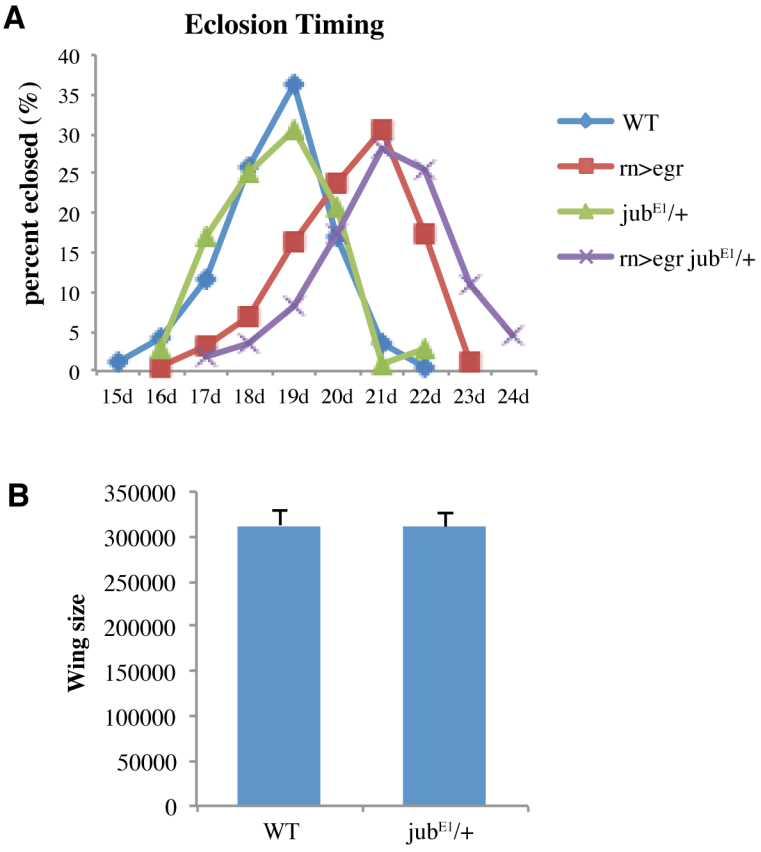
A
Eclosion Timing
percent eclosed (%)
40
35
30
25
20
15
10
5
0
15d 16d 17d 18d 19d 20d 21d 22d 23d 24d
WT
rn>egr
jub^E1/+
rn>egr jub^E1/+
B
Wing size
350000
300000
250000
200000
150000
100000
50000
0
WT
jub^E1/+

Fig S3 JNK regulates Hippo signaling and enhances LIMD1 and WTIP binding to LATS1

A) Western blots on lysates of MCF10A cells treated with DMSO (control, indicated by -), SP600125, and/or Anisomycin as indicated (+), blotted as indicated. Blots are representative of 3 biological replicates. B) Western blots on lysates of HEK293 cells transfected with control vector (no label), or plasmid expressing activated JNK1 (MKK7B2:FLAG:JNK1a1), kinase-dead JNK1 (MKK7B2:FLAG:JNK1a1(APF)), or activated JNK2 (MKK7B2:FLAG:JNK2a2), as indicated, blotted as indicated. Blots are representative of 3 biological replicates. C-D) Western blots on lysates of HEK293 cells transfected with control vector (no label), or plasmids expressing activated JNK1 or JNK2, as indicated. C) pYAP, YAP and TUB levels, histogram shows quantitation of the pYAP over YAP ratio from three biological replicates, normalized to the ratio in cells transfected with control vector. D) pLATS1 and LATS1 levels, histogram shows quantitation of the pLATS1 over LATS1 ratio from three biological replicates, normalized to the ratio in cells transfected with control vector. E) Results of in vitro binding experiments testing the influence of JNK1 and JNK2 activation on LIMD1 binding to LATS1. The upper blot shows LIMD1 on beads, the blot in middle shows Myc:LATS1 bound to these beads. Expression of transfected activated JNK2 in LIMD1 lysates is shown in LIMD1 Lysates blot. Histogram above shows average ratio of LATS1/LIMD1 from three independent experiments, normalized to the ratio in controls. F) Results of in vitro binding experiments testing the influence of JNK2 activation on WTIP binding to LATS1. Anti-V5 beads shows WTIP or GFP (control) on beads, co-IP shows Myc:LATS1 bound to these beads. Expression of transfected activated JNK2 in

LIMD1 lysates is shown in LIMD1 Lysates blot. Histogram above shows average ratio of LATS1/WTIP from three independent experiments, normalized to the ratio in controls. G-I) Results of in vitro binding assay testing the influence of JNK2 on LIMD1 (G), Ajuba (H), or WTIP (I) binding to WW45. In each panel, the upper blot shows Ajuba family proteins on beads, the blot in middle shows the amount of GFP:WW45 bound to beads, and expression of transfected activated JNK2 in lysates containing Ajuba family proteins is shown in Lysates blot. Histograms show average ratio of WW45/Ajuba family protein from three independent experiments, normalized to the ratio in controls. In all panels, error bars indicate standard error, and P values less than 0.05 are listed.

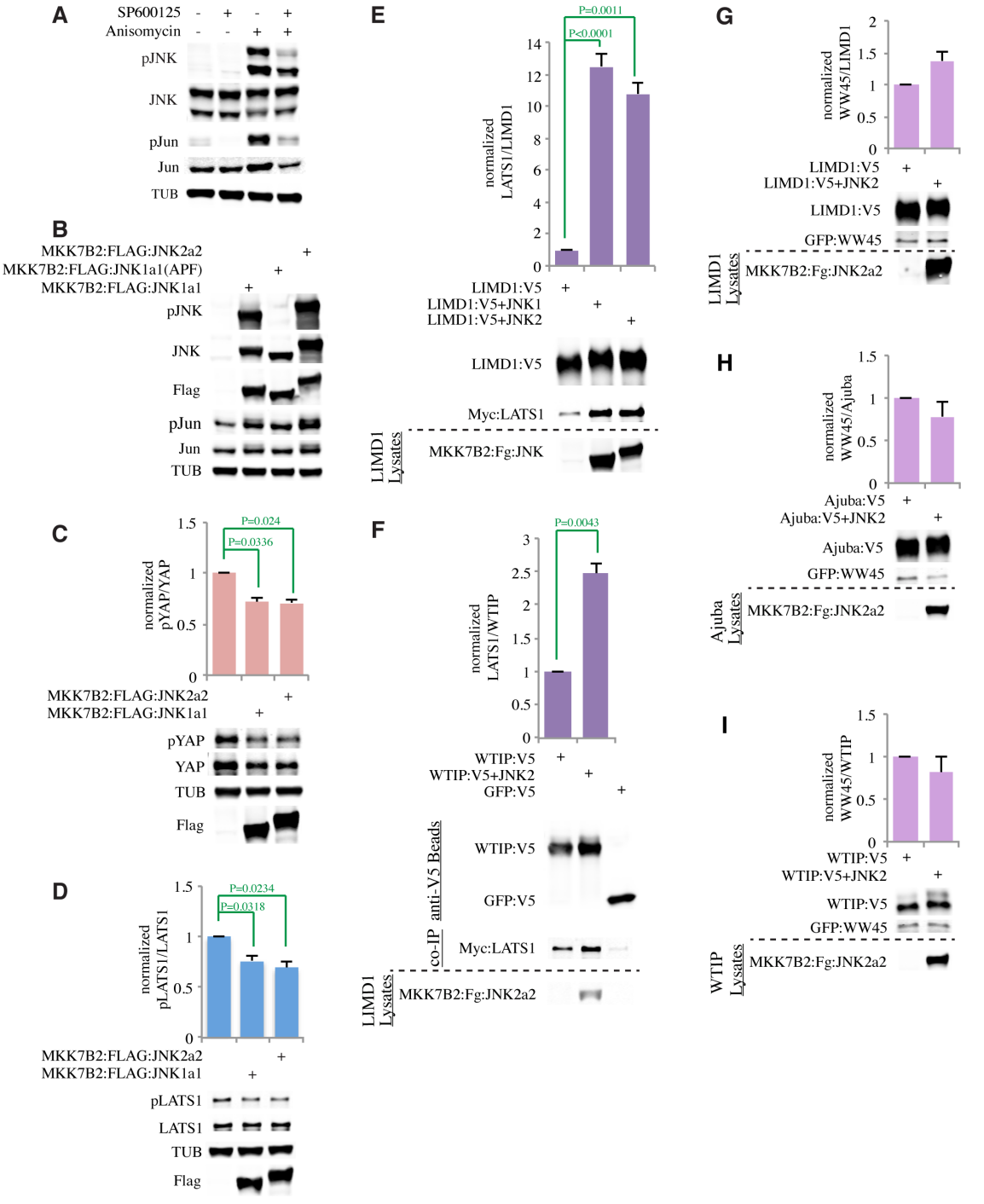
A
SP600125 - + - +
Anisomycin - - + +
pJNK
JNK
pJun
Jun
TUB
B
MKK7B2:FLAG:JNK2a2 +
MKK7B2:FLAG:JNK1a1(APF) +
MKK7B2:FLAG:JNK1a1 +
pJNK
JNK
Flag
pJun
Jun
TUB
C
P=0.024
P=0.0336
normalized pYAP/YAP
MKK7B2:FLAG:JNK2a2 +
MKK7B2:FLAG:JNK1a1 +
pYAP
YAP
TUB
Flag
D
P=0.0234
P=0.0318
normalized pLATS1/LATS1
MKK7B2:FLAG:JNK2a2 +
MKK7B2:FLAG:JNK1a1 +
pLATS1
LATS1
TUB
Flag
E
P=0.0011
P<0.0001
normalized LATS1/LIMD1
LIMD1:V5 +
LIMD1:V5+JNK1 +
LIMD1:V5+JNK2 +
LIMD1:V5
Myc:LATS1
LIMD1 Lysates
MKK7B2:Fg:JNK
F
P=0.0043
normalized LATS1/WTIP
WTIP:V5 +
WTIP:V5+JNK2 +
GFP:V5 +
WTIP:V5
anti-V5 Beads
GFP:V5
co-IP
Myc:LATS1
LIMD1 Lysates
MKK7B2:Fg:JNK2a2
G
normalized WW45/LIMD1
LIMD1:V5 +
LIMD1:V5+JNK2 +
LIMD1:V5
GFP:WW45
LIMD1 Lysates
MKK7B2:Fg:JNK2a2
H
normalized WW45/Ajuba
Ajuba:V5 +
Ajuba:V5+JNK2 +
Ajuba:V5
GFP:WW45
Ajuba Lysates
MKK7B2:Fg:JNK2a2
I
normalized WW45/WTIP
WTIP:V5 +
WTIP:V5+JNK2 +
WTIP:V5
GFP:WW45
WTIP Lysates
MKK7B2:Fg:JNK2a2

Fig S4. Phosphorylation of Ajuba family proteins by JNK and mapping of phosphorylation sites in LIMD1.

A) Western blots on lysates of S2 cells transfected to express FLAG:Jub with or without Hep.CA and Bsk. The upper blot shows a standard 4-15% gradient gel, and the lower blot shows a Phos-tag gel. JNK activity in lysates is shown in pJNK and JNK blots. N=3 biological replicates. B) Western blot on Phos-tag gel of FLAG:Jub purified from S2 cells and where indicated phosphorylated in vitro by Jnk. N=3 biological replicates. C) LIMD1 phosphopeptides identified by mass spectrometry with increased phosphorylation in the presence of JNK2 co-expression, as indicated, phosphorylated residues are in bold. D-E) Results of in vitro binding assays comparing binding of wild type LIMD1 and LIMD1^{4SA} mutant (D), or LIMD1^{8A} mutant (E) to LATS1. Anti-V5 beads blot shows LIMD1, LIMD1 mutant or GFP (control) protein on beads. Co-IP shows Myc:LATS1 bound to wild type or mutant LIMD1. Expression of transfected activated JNK2 in LIMD1 lysates is shown in LIMD1 Lysates blot. The histogram above shows the average LATS1/LIMD1 ratio from three independent experiments, normalized to the ratio in wild-type LIMD1 control. F) Results of in vitro binding assay evaluating the effect of JNK on C-terminal of LIMD1 (LIMD1-C) binding to LATS1. The blots showed LIMD1:V5-C and Myc:LATS1 proteins pulled down by beads. Histogram above shows average ratio of LATS1/LIMD1-C from three biological replicates, normalized to the ratio in controls. In all panels, error bars show standard error. P values less than 0.05 are listed.

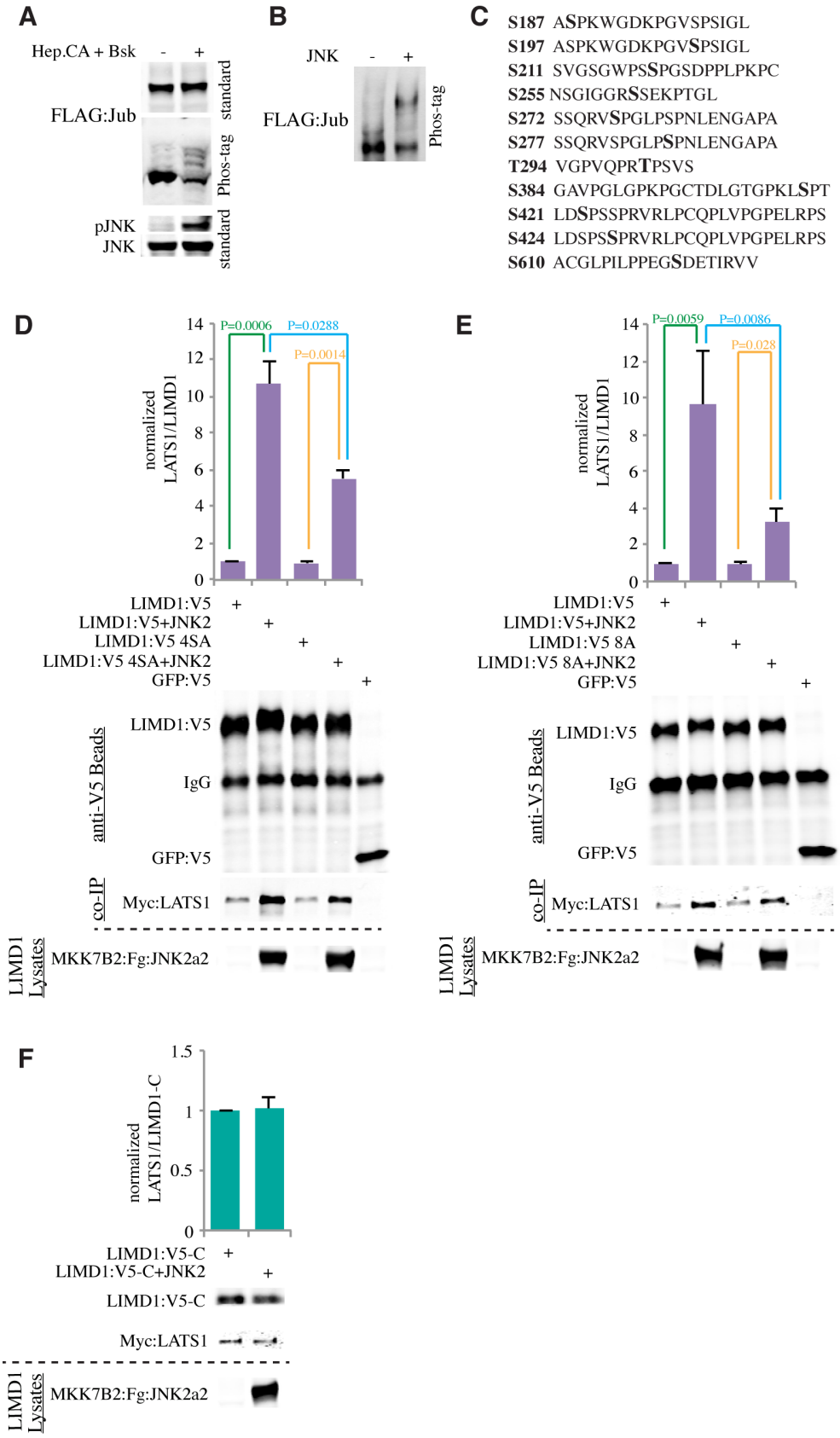
A
Hep.CA + Bsk - +
FLAG:Jub
standard
Phos-tag
pJNK
JNK
standard
B
JNK - +
FLAG:Jub
Phos-tag
C
S187 ASPKWGDKPGVSPSIGL
S197 ASPKWGDKPGVSPSIGL
S211 SVGSGWPSSPGSDPPLPKPC
S255 NSGIGGRSSEKPTGL
S272 SSQRVSPGLPSPNLENGAPA
S277 SSQRVSPGLPSPNLENGAPA
T294 VGPVQPRTPSVS
S384 GAVPGLGPKPGCTDLGTGPKLSPT
S421 LDSPSSPRVRLPCQPLVPGPELRPS
S424 LDSPSSPRVRLPCQPLVPGPELRPS
S610 ACGLPILPPEGSDETIRVV
D
normalized LATS1/LIMD1
P=0.0006
P=0.0288
P=0.0014
LIMD1:V5 +
LIMD1:V5+JNK2 +
LIMD1:V5 4SA +
LIMD1:V5 4SA+JNK2 +
GFP:V5 +
anti-V5 Beads
LIMD1:V5
IgG
GFP:V5
co-IP
Myc:LATS1
LIMD1 Lysates
MKK7B2:Fg:JNK2a2
E
normalized LATS1/LIMD1
P=0.0059
P=0.0086
P=0.028
LIMD1:V5 +
LIMD1:V5+JNK2 +
LIMD1:V5 8A +
LIMD1:V5 8A+JNK2 +
GFP:V5 +
anti-V5 Beads
LIMD1:V5
IgG
GFP:V5
co-IP
Myc:LATS1
LIMD1 Lysates
MKK7B2:Fg:JNK2a2
F
normalized LATS1/LIMD1-C
LIMD1:V5-C +
LIMD1:V5-C+JNK2 +
LIMD1:V5-C
Myc:LATS1
LIMD1 Lysates
MKK7B2:Fg:JNK2a2

CHAPTER IV

Regulation of Ajuba proteins by Jun kinase, Ras, and actomyosin tension

Summary

Ras, c-Jun N-terminal kinase (JNK), and cytoskeletal tension are important factors participating in tumorigenesis. Ras, JNK and the cytoskeleton have been reported as Hippo pathway regulators in both *Drosophila* and mammals. Hippo signaling translates these oncogenic signals to proliferation regulation. Both Ras and JNK suppress Hippo signaling through Ajuba proteins, suggesting an important role of Ajuba proteins in Hippo signaling regulation in human cancers. In this chapter, using mammalian cell culture, we found activation of RhoA, a GTPase regulating cytoskeleton dynamics, suppresses LATS, a core kinase in Hippo signaling, activates YAP, the downstream effector of Hippo signaling, and increases the binding between LATS and one mammalian Ajuba protein WTIP. Ras, JNK, and activation of RhoA regulate WTIP through different mechanisms. In accordance with this, we observed synergistic regulation of YAP activity and the binding between WTIP and LATS by Ras, JNK, and activated RhoA. In this study, we also found an intramolecular binding between the N-terminus and the C-terminus of Ajuba proteins, which might explain the regulation of Ajuba proteins by different signals.

Introduction

The progression of cancer involves multiple processes including gaining oncogenic mutations, loss of epithelial structure, cytoskeleton remodeling and increased cell proliferation and cell motility. JNK, Ras, and cytoskeletal contraction are all important factors in tumorigenesis. In *Drosophila* epithelia, activation of Ras signaling by overexpression of the oncogenic Ras^{V12} causes non-invasive tissue overgrowth. Activation of JNK in combination with overexpression of Ras^{V12} results in stronger tissue overgrowth and metastasis of the tumors[31]. The dramatic tissue overgrowth induced by the cooperation of Ras and JNK requires suppression of Hippo signaling and Yki activation[195]. The GTP exchange factor RhoGEF2 also cooperates with activated Ras to promote neoplastic tumor growth. Activation of the downstream effectors of RhoGEF2, Rho kinase or Myosin II is sufficient to induce neoplastic tumors together with Ras, suggesting it is the cytoskeletal contraction that contributes to tumor growth. The cooperation of the increased actomyosin tension and Ras promote growth through JNK activation[196, 197].

Ras is an oncogene activated in many human cancers. The role of JNK in the Ras-driven cancers is controversial, but at least in some tissues, JNK is required for the Ras-initiated tumorigenesis[198, 199]. The cell tension molecule, Rho-associated kinase, also participates in the development of human cancers, and is a potential therapeutic target[200]. Thus, understanding how JNK, Ras, and cell tension cooperate and how the cooperation leads to tumor formation and development is important for cancer research and therapy.

Jub is a LIM domain protein that suppresses Hippo signaling activity by inhibiting Warts (Wts) activity. In the past two years, the importance of Jub in Hippo signaling has been unveiled through studying the regulation of Hippo signaling by other signaling pathways. In Chapter III, we have shown that JNK regulates Hippo signaling through Jub during tissue regeneration and neoplastic tumor growth in *Drosophila*. And EGFR-Ras-ERK signaling also regulates Hippo signaling through Jub to promote glial cell proliferation[119]. Increase in actomyosin tension in epithelial cells activates Yki through Jub (unpublished data from our lab). These data indicate Jub is an important hub mediating the integration of other signals to Hippo signaling. These studies, together with the importance of JNK, Ras and tension in cancer, imply a model that the cooperation of JNK, Ras and actomyosin tension promotes neoplastic tumor growth through Jub and Yki. In human, YAP and TAZ are oncogenes related to many cancers, whereas mutations in the known upstream tumor suppressors in Hippo pathway have rarely been identified[47]. In mammalian cells, JNK and Ras can both regulate Ajuba proteins. So Ajuba proteins may bridge the upstream oncogenic signals and YAP/TAZ activation in human cancers.

In this chapter, using mammalian cell culture, we analyzed the regulation of WTIP and YAP by a cytoskeleton regulator, RhoA, and the synergistic effect of JNK, Ras, and RhoA on WTIP affinity to LATS and YAP activation. We also examined the relationship among the conformation, the post-translational modification, and the activity of Ajuba proteins in both mammalian cells and *Drosophila* imaginal discs.

Results and discussion

The synergistic regulation of Hippo signaling by JNK and Ras^{V12}

Ras activates Hippo signaling through ERK. ERK and JNK both belong to the MAPK family, and they have a common target within the Hippo signaling pathway, WTIP. ERK promotes the binding between WTIP and LATS through phosphorylating the Ser422 site in the C-terminus[119], but this site is not regulated by JNK (Fig 1A). So we tested if JNK and Ras-ERK signaling have a synergistic effect on Hippo signaling activity. To activate JNK signaling and Ras-ERK signaling, constitutively activated JNK1 and an activated mutant of Ras, Ras^{V12}, were transfected into HEK293 cells together or separately, and the phosphorylation of YAP was used as a readout for Hippo pathway activity. As reported, overexpression of active JNK1 or Ras^{V12} alone led to a reduction in YAP phosphorylation. The effect of JNK activation is stronger than that of Ras^{V12}. Co-expression of JNK and Ras^{V12} resulted in further reduction in YAP phosphorylation (Fig 1B). This is consistent with the previous report in *Drosophila* imaginal discs that co-expressing *egr* and *ras^{V12}* induces strong increase in Yki activation compared with expressing *egr* or *ras^{V12}* alone[195]. Furthermore, transfection of Ras^{V12} into HEK293 cells only caused a slight increase in the WTIP-LATS binding, but co-transfection of Ras^{V12} and activated JNK1 resulted in stronger binding between WTIP and LATS, even stronger than the binding when activated JNK1 was expressed alone (Fig 1C). Thus, JNK and Ras^{V12} may synergistically regulate YAP activity by promoting stronger binding between WTIP and LATS.

Regulation of Hippo signaling by Rho GTPase

To test the cytoskeletal regulation of WTIP, a constitutively active form of the Rho GTPase, RhoA-Q63L, was expressed in HEK293 cells. Overexpression of RhoA-Q63L resulted in strong reduction in YAP phosphorylation and LATS phosphorylation, indicating the suppression of LATS activity and activation of YAP (Fig 2A). Moreover, overexpression of RhoA-Q63L led to an increased binding between WTIP and LATS (Fig 2B). The influence on WTIP-LATS binding caused by RhoA-Q63L overexpression was stronger than that caused by JNK activation. Expression of RhoA-Q63L did not induce obvious gel shift of WTIP, suggesting the phosphorylation status of WTIP may not be affected, which is different from JNK regulation of WTIP. Thus, activated RhoA may regulate WTIP-LATS binding through a different mechanism.

We also examined if activated RhoA can cooperate with JNK or Ras^{V12} to promote stronger YAP activation and WTIP-LATS binding. Though overexpression of RhoA-Q63L causes reduced YAP phosphorylation and increased WTIP-LATS binding, co-expression of RhoA-Q63L with activated JNK or Ras^{V12} increased YAP activation and WTIP-LATS binding to a more dramatic extent (Fig 2C and D). Therefore, activated JNK, Ras, and Rho GTPase can cooperate to regulate Hippo signaling activity.

The N-terminus and C-terminus of Ajuba proteins bind each other

JNK, Ras, and Rho GTPase can all regulate the binding between Ajuba proteins and LATS, but the mechanisms are different. JNK and Ras regulate Ajuba proteins both through phosphorylation, but the phosphorylation sites are distinct. JNK phosphorylates the N-terminal part and Ras phosphorylates the C-terminal part. The fact that activated RhoA can increase WTIP-LATS binding without affecting the phosphorylation of WTIP

suggests a phosphorylation-independent regulation of Ajuba proteins. At the end of Chapter III, we proposed a model that phosphorylation-induced conformation change favors the binding of Ajuba proteins to LATS. Activated RhoA influences cytoskeleton dynamics[201], and Ajuba proteins associate with cytoskeletons through α-catenin[62]. So it is likely that activated RhoA affects Ajuba proteins conformation without changing its phosphorylation status through changing the cytoskeleton. Under this hypothesis, the conformation of Ajuba proteins is the key to their Hippo pathway activity. We then examined the relationship between the conformation and the activity of Ajuba proteins.

Constructs expressing the N-terminus and the C-terminus of LIMD1 were co-transfected into HEK293 cells, and the interaction between the N-terminus and the C-terminus was tested through co-immunoprecipitation. The N-terminus can be pulled down by the C-terminus, suggesting the existence of a binding between the N-terminus and the C-terminus of LIMD1 (Fig 3A). We then checked the influence of JNK on the binding between the N-terminus and the C-terminus of LIMD1, and found co-transfection of the constitutively active JNK2 reduced the binding between the N-terminus and the C-terminus (Fig 3A). Similar binding was also observed between the N-terminus and the C-terminus of Ajuba, WTIP, and Jub, and the binding can all be disrupted by JNK activation (Fig 3B-D). We also conducted *in vitro* binding assays in which the N-terminus and the C-terminus of LIMD1 were expressed in separate cells with or without JNK, then the C-terminus was purified and applied to lysates containing the N-terminus. When JNK was expressed together with the N-terminus, the binding between the N-terminus and the C-terminus was abolished, and a clear gel shift of the N-terminus was observed, suggesting phosphorylation of the N-terminus by JNK promotes its

dissociation from the C-terminus. All these data favor the model we proposed in the Fig. 4E in Chapter III.

To test if the N-C interaction occurs *in vivo*, we adopted the bimolecular fluorescence complementation (BiFC) system[202]. The N-terminus and the C-terminus of Jub were fused to the N-terminus and the C-terminus of Venus, respectively. And the fusion proteins Jub-N:VN and Jub-C:VC were expressed in the wing discs under the control of the GAL4-UAS system. When expressed alone, Jub-N:VN or Jub-C:VC did not emit any fluorescence (Fig 4B and C). However, when these two proteins were co-expressed, Venus signal was observed, indicating the interaction between the N-terminus and the C-terminus of Jub (Fig 4A). The complex formed by the Jub-N:VN and Jub-C:VC (the N-C complex) was found concentrated in the apical membrane, co-localized with E-cad (Fig 4A and D), which is similar to the endogenous Jub (Fig 4E). However, the endogenous Jub forms bright puncta at the adherens junction, whereas the N-C complex did not form puncta at the junction. This may indicate Jub at the E-cadherin-dependent junction and Jub at the junction-associated puncta have different activity. We also observed some N-C complexes existed in the cytoplasm (Fig 4A), which is possibly caused by the aggregation of the excessively expressed proteins.

Materials and methods

Fly stocks

The fly stocks used were as follows: *en-Gal4 UAS-mRFP/CyO; tub-Gal80ts UAS-dcr2/TM6B*, *jub:GFP/TM2*[194].

The N-terminus and the C-terminus of *jub* were cloned and inserted into pBiFC-VN173 and pBiFC-VC155 vectors, respectively. The *jub-N:VN173* and *jub-C:VC155* were then transferred to the PUAST-attB vector. *UAS-jub-N:VN173* was inserted at the 68A site on the third chromosome, and *UAS-jub-C:VC155* was inserted at the 25C site on the second chromosome.

Plasmids

V5-tagged Ajuba-N, LIMD1-C, WTIP-C were generated by PCR using Ajuba or LIMD1, or WTIP cDNA (Open Biosystems) as templates and inserting into pCDNA3.1-V5:His B vector (Life Technologies). FLAG-tagged Ajuba-C, LIMD1-N, and WTIP-N were generated by PCR using Ajuba or LIMD1, or WTIP cDNA (Open Biosystems) as templates and inserting into pUAST-3XFLAG vector first, then transferred to pCDNA3.1 vector. The C-terminus of *jub* was inserted into pAc5.1-V5:His (Life Technologies) first, then transferred to PUAST-attB vector. Other plasmids used in this paper includes pBabe-puro-HRasV12 (Addgene 1768), pRK5-myc:RhoA-Q63L (Addgene 12964), pCDNA3-MKK7B2:flag:Jnk1a1 (Addgene 19731), pCDNA3-MKK7B2:flag:Jnk2a2(Addgene 19727), pCDNA3-WTIP:V5, pCDNA3-WTIP:V5 S422A, PUAST-3XFLAG:jub-N[119].

Cell culture, transfection and treatment

Drosophila S2 cells were cultured in Schneider's *Drosophila* medium (Life Technologies) supplemented with 10% FBS (Sigma) and Antibiotic-Antimycotic (Life Technologies) at 25°C. HEK293 cells were cultured in DMEM medium (Life Technologies) supplemented with 10% FBS and Antibiotic-Antimycotic at 37°C and 5% CO_2. S2 cells were transfected with Cellfectin II (Life Technologies), and HEK293 cells were transfected with Lipofectamine 2000 (Life Technologies) according to manufacturer's protocols, and harvested 24h after transfection.

Immunoblotting and immunoprecipitation

Cells were lysed in lysis buffer (50mM Tris·HCl pH7.4, 150mM NaCl, 1% Triton X-100, 0.1% CHAPS, 0.1% NP-40, 1mM EDTA, 5% glycerol) supplemented with protease inhibitor cocktail (Roche) and phosphatase inhibitor cocktail (Calbiochem). Protein samples were applied to 4-15% gradient gels (Bio-rad). For immunoprecipitation, protein samples were incubated with mouse anti-V5 agarose affinity gel (Sigma) overnight at 4°C. Antibodies used for immunoblotting include rabbit anti-Lats1 (1:2000, Cell Signaling Technology), rabbit anti-phospho-Lats1(T1079) (1:2000, Cell Signaling Technology), rabbit anti-phospho-Yap(S127) (1:4000, Cell Signaling Technology), rabbit anti-Yap (1:2000, Epitomics), mouse anti-V5 (1:10000, Life Technologies), rabbit anti-V5 (1:2000, Bethyl Laboratories), mouse anti-FLAG (1:2000, M2, Sigma), mouse anti-tubulin (1:8000, Sigma). Blots were visualized and quantified using fluorescent-conjugated secondary antibodies (Li-Cor Biosciences) and Odyssey Imaging System (Li-Cor Biosciences).

In vitro binding assay

V5-tagged LIMD1-C was transfected into HEK293 cells. Cells were lysed in lysis buffer (50mM Tris·HCl pH7.4, 150mM NaCl, 1% Triton X-100, 0.1% CHAPS, 0.1% NP-40, 1mM EDTA, 5% glycerol) supplemented with protease inhibitor cocktail (Roche) and phosphatase inhibitor cocktail (Calbiochem). Lysates were incubated with mouse anti-V5 agarose (Sigma) for 3h at 4°C, then washed with lysis buffer 4 times. The beads with V5-tagged proteins were incubated with cell lysates containing FLAG-tagged LIMD1-N with or without MKK7B2:FLAG:Jnk2a2 overnight at 4°C. Beads were then washed with lysis buffer 6 times, and applied to SDS-PAGE.

Immunostaining

Inverted anterior part of *Drosophila* larvae were fixed in 4% PFA for 10min at room temperature, then washed with PBS containing 1% BSA and 0.1% Triton X-100 and blocked by 5% Donkey serum. Antibodies used for immunostaining include rat anti-E-cadherin (1:200, DHSB).

Figures

Fig 1. The synergistic effect of Ras and JNK on Hippo signaling

A) Mutation of WTIP S422 site does not affect the binding of WTIP to LATS when JNK is activated. V5-tagged wild type or S422A mutant WTIP was transfected into HEK293 cells with or without constitutively activated JNK1. WTIP was then precipitated with mouse anti-V5 beads, and the amount of LATS co-precipitated with WTIP was evaluated. B) The level of pYAP and YAP with active JNK1, active Ras, or active JNK1 and Ras is shown in the blots. Tubulin (TUB) was used as a loading control. The histogram in the lower panel shows the average ratio of pYAP over YAP from three independent experiments. The error bars present standard error. Active JNK1 and Ras have an additive effect on YAP phosphorylation. C) The binding of WTIP to LATS with active JNK1, active Ras, or active JNK1 and Ras was tested through co-immunoprecipitation with the agarose beads recognizing the V5-tagged WTIP. The blots show the level of LATS and WTIP in the input and the precipitate. The histogram shows the average amount of LATS precipitated with WTIP from three independent experiments. The error bar presents standard error. Active JNK1 and Ras have an additive effect on the binding of WTIP to LATS.

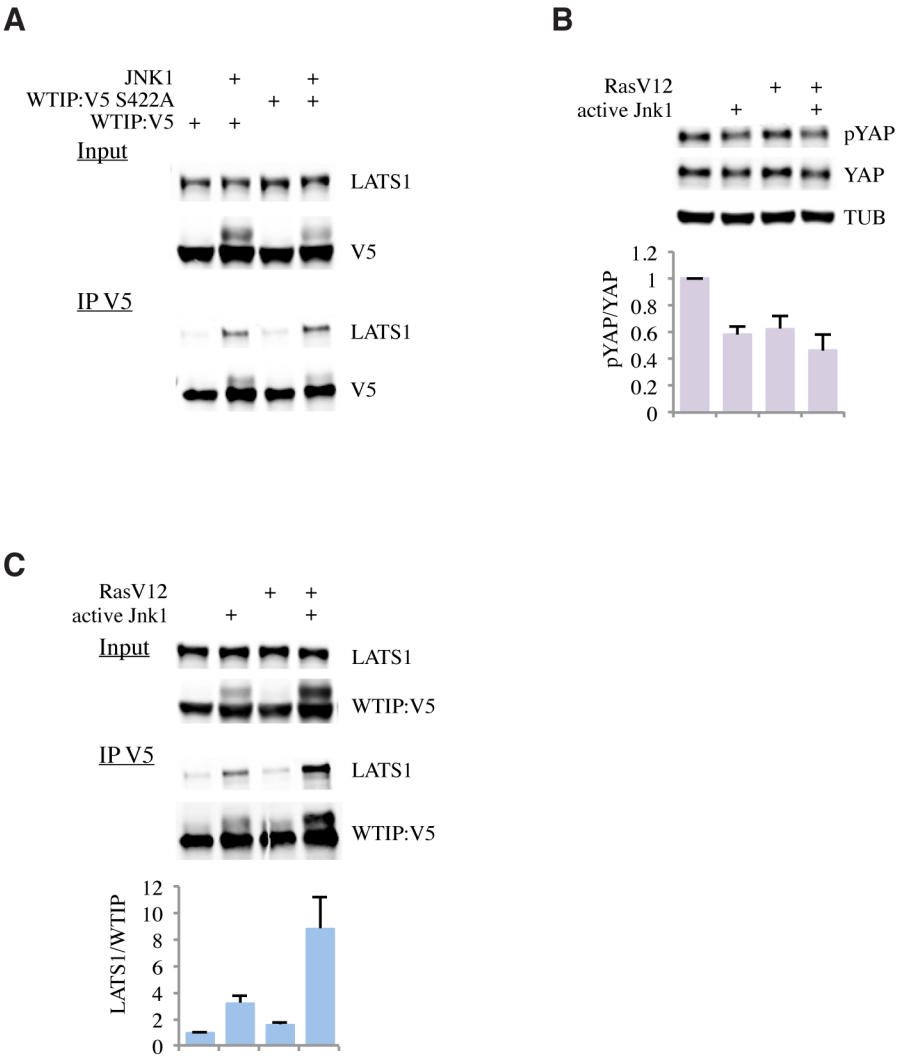
A
JNK1 + +
WTIP:V5 S422A + +
WTIP:V5 + +
Input
LATS1
V5
IP V5
LATS1
V5
B
RasV12 + +
active Jnk1 + +
pYAP
YAP
TUB
pYAP/YAP
1.2
1
0.8
0.6
0.4
0.2
0
C
RasV12 + +
active Jnk1 + +
Input
LATS1
WTIP:V5
IP V5
LATS1
WTIP:V5
LATS1/WTIP
12
10
8
6
4
2
0

Fig 2. Active RhoA is a Hippo signaling regulator and can cooperate with Ras and JNK to suppress Hippo signaling activity.

A) The level of pYAP, YAP, pLATS1, LATS in cells transfected with constitutively active form of RhoA, RhoA-Q63L, and in the control cells is shown on the blots. Tubulin (TUB) was used as a loading control. Active RhoA increases the phosphorylation of YAP and LATS1. B) Binding of WTIP to LATS is increased by active RhoA (RhoA-Q63L). V5-tagged WTIP was transfected into HEK293 cells with or without RhoA-Q63L, and precipitated with anti-V5 beads. The blots show the level of LATS and WTIP in the input and in the precipitate. C) The level of pYAP, YAP, and TUB in control cells, cells transfected with RhoA-Q63L, active JNK1, or Ras^{V12} alone, and cells transfected with RhoA-Q63L together with active JNK1 or Ras^{V12} is shown on the blots. The histogram shows the average ratio of pYAP over YAP from three independent experiments. The error bars present standard error. RhoA-Q63L and active JNK1 or Ras^{V12} have additive effect on YAP activity. D) The binding of WTIP to LATS in control cells, cells transfected with RhoA-Q63L, active JNK1, or Ras^{V12} alone, and cells transfected with RhoA-Q63L together with active JNK1 or Ras^{V12} was tested through co-immunoprecipitation with the agarose beads recognizing the V5-tagged WTIP. The blots show the level of LATS and WTIP in the input and the precipitate. The histogram shows the average amount of LATS precipitated with WTIP from three independent experiments. The error bar presents standard error. RhoA-Q63L cooperate with active JNK1 or Ras to promote the binding of WTIP to LATS.

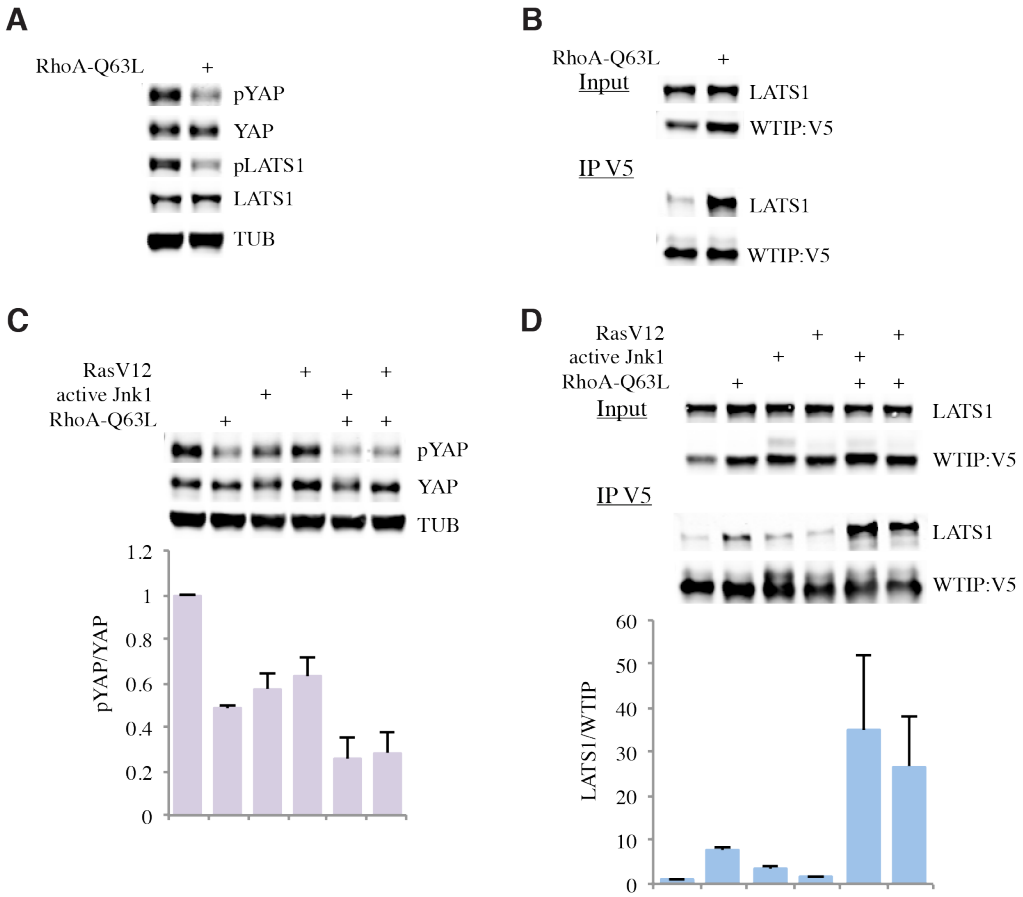
A
RhoA-Q63L +
pYAP
YAP
pLATS1
LATS1
TUB
B
RhoA-Q63L +
Input
LATS1
WTIP:V5
IP V5
LATS1
WTIP:V5
C
RasV12 + +
active Jnk1 + +
RhoA-Q63L + + +
pYAP
YAP
TUB
pYAP/YAP
1.2
1
0.8
0.6
0.4
0.2
0
D
RasV12 + +
active Jnk1 + +
RhoA-Q63L + + +
Input
LATS1
WTIP:V5
IP V5
LATS1
WTIP:V5
LATS1/WTIP
60
50
40
30
20
10
0

Fig 3. JNK activation disrupts the binding between the N-terminus and the C-terminus of Ajuba proteins.

The binding between the N-terminus and the C-terminus of LIMD1 (A), WTIP (B), Ajuba (C), and Jub (D) was tested in cells with or without JNK activation. The N-terminus and the C-terminus were tagged with V5 or FLAG and transfected into HEK293 cells or S2 cells (Jub). JNK activation was achieved by transfecting a constitutively active JNK1 or JNK2 into HEK293 cells or *bsk* together with *hep.CA* into S2 cells. Co-immunoprecipitation was conducted with anti-V5 beads, and the amount of the N-terminus and the C-terminus in the input and the precipitate is shown on the blots. The binding between the N-terminus and the C-terminus of LIMD1 (A), WTIP (B), Ajuba (C), or Jub (D) is reduced when JNK activated. E) The *in vitro* binding between the N-terminus and the C-terminus of LIMD1. The C-terminus of LIMD1 was transfected into HEK293 cells, purified with anti-V5 beads, and applied to cell lysates containing the N-terminus of LIMD1 alone or with active JNK2. The upper two blots show the level of the N-terminus and the C-terminus in the precipitate after *in vitro* binding, and the lower Lysates blot shows the relative level of the N-terminus in the input lysates. When JNK2 was co-expressed with the N-terminus, the binding of the C-terminus to the N-terminus was abolished.

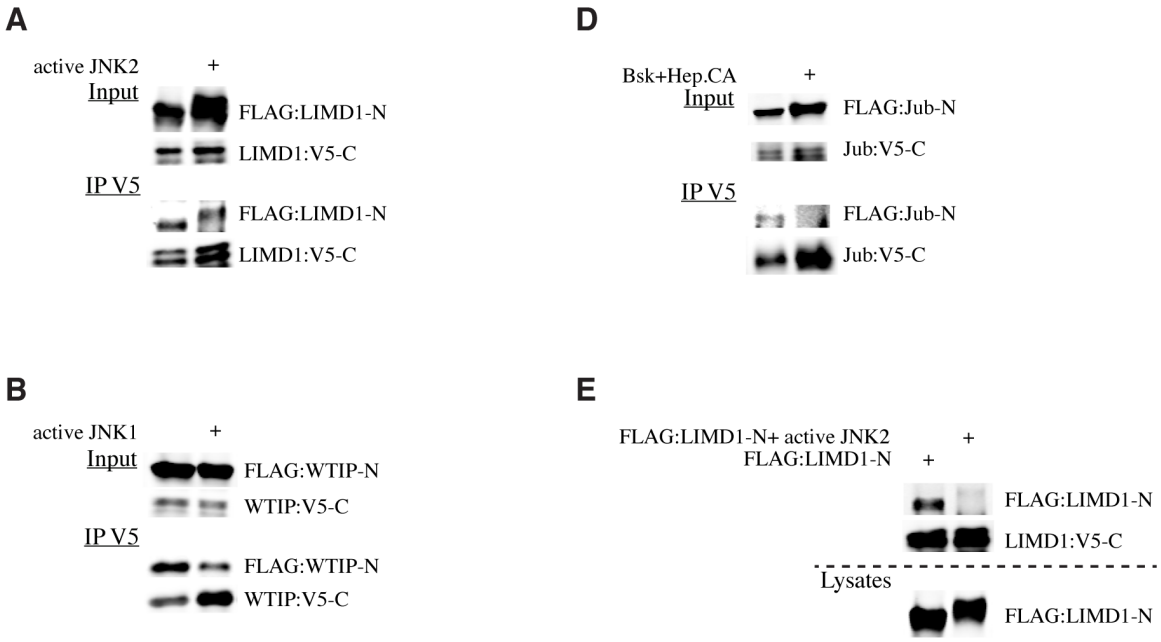
A
active JNK2
+
Input
FLAG:LIMD1-N
LIMD1:V5-C
IP V5
FLAG:LIMD1-N
LIMD1:V5-C
D
Bsk+Hep.CA
+
Input
FLAG:Jub-N
Jub:V5-C
IP V5
FLAG:Jub-N
Jub:V5-C
B
active JNK1
+
Input
FLAG:WTIP-N
WTIP:V5-C
IP V5
FLAG:WTIP-N
WTIP:V5-C
E
FLAG:LIMD1-N+ active JNK2
+
FLAG:LIMD1-N
+
FLAG:LIMD1-N
LIMD1:V5-C
Lysates
FLAG:LIMD1-N
C
active JNK1
+
Input
FLAG:Ajuba-C
Ajuba:V5-N
IP V5
FLAG:Ajuba-C
Ajuba:V5-N

Fig 4. The N-terminus and the C-terminus of Jub interact in the wing disc.

A-C) *UAS-jub-N:VN* and *UAS-jub-C:VC* were expressed separately or together in the posterior wing disc under the control of *en-Gal4* as indicated. The figures show the apical view of the wing disc epithelia. The green is the Venus signal, and the red is the staining for E-cadherin (E-cad). The panels labeled with prime show the separate channel to the left. Venus signal was only seen when *UAS-jub-N:VN* and *UAS-jub-C:VC* were co-expressed. D) The z-section view of the disc *en-Gal4 UAS-jub-N:VN UAS-jub-C:VC*. The green is Venus and the red is E-cad. The panels marked with prime show the separate channel. Venus signal is co-localized with E-cad. E) Localization of endogenous Jub tagged with GFP in the wing disc. The green is GFP.

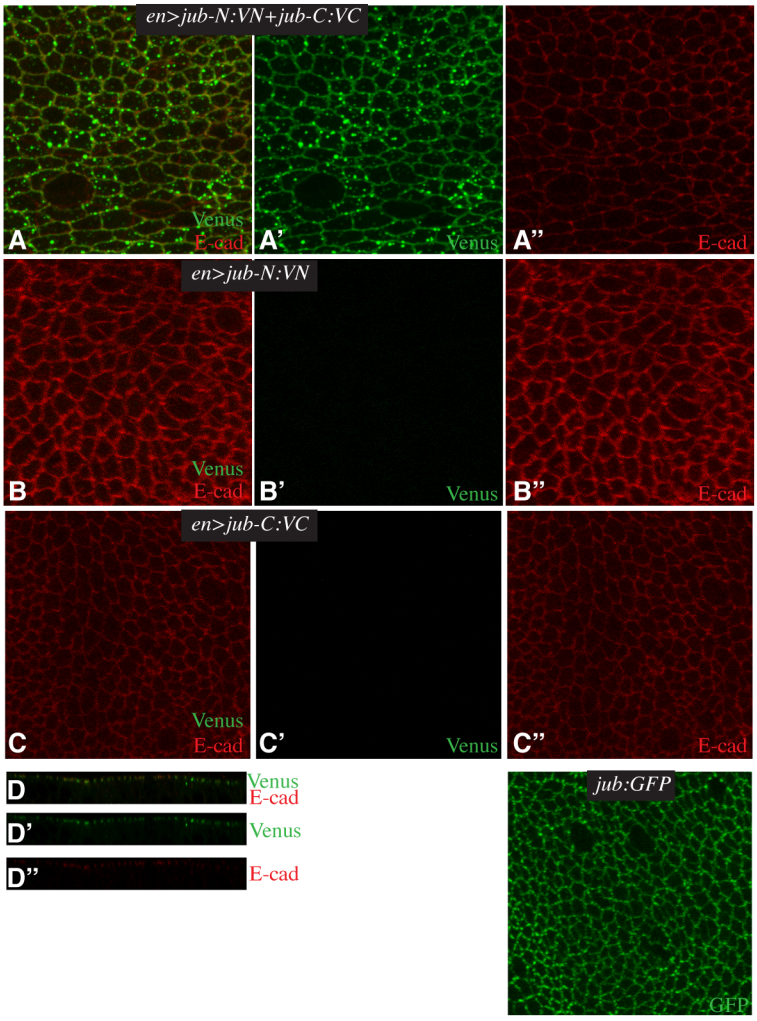
en>jub-N:VN+jub-C:VC
A
Venus
E-cad
A'
Venus
A''
E-cad
en>jub-N:VN
B
Venus
E-cad
B'
Venus
B''
E-cad
en>jub-C:VC
C
Venus
E-cad
C'
Venus
C''
E-cad
D
Venus
E-cad
D'
Venus
D''
E-cad
jub:GFP
GFP

CHAPTER V

General discussion

Ajuba proteins

The mammalian Ajuba proteins regulate cell-cell contact, cell-matrix interaction, cell migration, and gene expression, acting as adaptor or scaffold proteins[62, 63, 203-208]. The only *Drosophila* Ajuba homolog, Jub, was first identified in 2010. Reduced Jub expression results in defect in wing growth[64]. Our study in *Drosophila* wing imaginal discs showed Jub is required for growth during regeneration, and in neoplastic tumors[209]. Jub promotes growth through suppression of Hippo signaling, and a physical interaction between Wts and Jub exists. Interaction with LATS has also been found in the mammalian Ajuba proteins. Overexpression of Ajuba, LIMD1, or WTIP suppresses the phosphorylation on YAP S127 site, indicating a suppression of LATS activity[64]. LATS activation requires phosphorylation on two sites. Phosphorylation on the site in the activation loop requires MOB1 binding, and the site in the hydrophobic motif is the target of MST. Neither overexpression of LIMD1 nor activation of JNK which increases the activity of Ajuba proteins affects the binding between LATS and MOB1 (data not shown), but in our study on different signals that regulate Hippo signaling through Ajuba proteins, we observed a reverse correlation between the strength of the binding of Ajuba proteins to LATS and the phosphorylation of LATS by MST, suggesting Ajuba proteins bind to LATS/Wts to block its activation by MST/Hpo. This may be achieved by preventing Wts from forming complex with Hpo, Sav or Mats. Instead of forming stable direct interaction, Hpo/MST and Wts/LATS are brought together by the scaffold protein Sav. Thus Ajuba proteins may inhibit Hippo signaling activity by competing with Sav binding to Wts/LATS.

The observation that suppression of Hippo signaling by Jub is conserved in mammalian cells indicates a growth promotion role of the mammalian Ajuba proteins. However, this contradicts with the previous studies on LIMD1, which proposed LIMD1 as a tumor suppressor. LIMD1 is encoded in a region commonly deleted in many cancers. Gene alteration or the reduced expression of LIMD1 has been found in patients with lung cancer[210], head and neck squamous cell carcinoma[211], and breast cancer[212]. Overexpression of LIMD1 inhibits cell proliferation, delays tumor growth, and reduces tumor metastasis in vivo[207]. The growth inhibition effect of LIMD1 is through interaction with the retinoblastoma protein (Rb), a classical tumor suppressor. The activity of Hippo pathway in these specific tumors and cell lines is not clear. It is possible that Ajuba proteins have the capacity to interact with proteins with distinct functions. The ultimate biological effect exhibited depending on which interaction is dominant in the cells. This may depend on the cell type, cell fate, and the extracellular and intracellular signals. In the paper from *Sharp et al.* (2004), high level of Rb in the tumor cells may occupy the majority of LIMD1, leaving few for LATS interaction, thus LIMD1 overexpression causes growth inhibition.

Ajuba proteins interact with LATS, which is proposed as the mechanism how Ajuba proteins suppress Hippo signaling. As I mentioned, this assumption is mainly based on the correlation between the LATS-Ajuba proteins interaction and the phosphorylation of LATS and YAP. Till now, there is no direct evidence showing the binding suppresses LATS activity. Other people from our lab analyzed the subcellular localization of the Hippo pathway components in wing discs, and found though most of the components are at the apical membrane, the proteins that activate Wts are not co-

localized with Jub. Wts co-localize with either the activation complex or Jub, depending on the activity of Hippo signaling. And Jub is not co-localized with phospho-Wts, suggesting Jub is more likely a Wts suppressor *in vivo* (unpublished data from our lab). However, the binding between Ajuba proteins and Wts/LATS may have different functions in regulation of Hippo signaling in different contexts. A very recent report on Ajuba in malignant mesothelioma confirmed a genetic interaction between Ajuba and LATS in the malignant mesothelioma cells, but claimed a completely opposite effect on the Hippo pathway activity. In malignant mesothelioma cell lines, Ajuba suppresses YAP activity, demonstrated both by overexpression of Ajuba and by knocking down the endogenous Ajuba. And this suppression of YAP by Ajuba requires LATS activity, suggesting in these cells, Ajuba promotes LATS activation[213]. When studying Jub in *Drosophila* wing discs, we found overexpression of Jub has no growth-promoting effect, though reduction in the endogenous Jub level shows strong growth defect. Instead, overexpression of Jub exhibits a very weak dominant-negative effect on growth and Yki activity. The *jub*-overexpressing wings are about 10% smaller than wild type wings (Fig 1A-C), and expression of *jub* results in slight decrease in the expression of Yki target gene, *ex-lacz* (Fig 1D). The overexpressed Jub is enriched at the apical domain (Fig 1E), and removes the endogenous Jub from the adherens junctions (Fig 1F), suggesting the overexpressed Jub has the ability to associate to the adherens junctions and can compete with endogenous Jub for apical localization. Interestingly, it seems the overexpressed Jub remains the ability to bind to Wts as overexpression of Jub brings more Wts to the adherens junctions (Fig 1G). The overexpressed Jub in *Drosophila* wing discs functions like Ajuba in the malignant mesothelioma cells: binds to Wts but does not suppress

Hippo signaling activity. The distinct effects of the binding between Wts/LATS and Ajuba proteins on Hippo signaling activity suggest regulation of Hippo signaling by Ajuba proteins may consist of two steps, the binding of Ajuba proteins to Wts/LATS, and the regulation of the activity of Ajuba proteins. Binding to Wts/LATS is only the way Ajuba proteins exert influence on Hippo signaling, but whether the influence is positive or negative might depend on the activity of Ajuba proteins. Ajuba proteins suppress Hippo signaling only when "active" Ajuba proteins bind to Wts/LATS; otherwise binding of Ajuba proteins to Wts/LATS has no effect on or increases Hippo signaling activity. How Ajuba proteins are "activated" is a key question in understanding the regulation of Hippo signaling, especially considering the important role of Ajuba proteins in integration of other signaling pathways to Hippo signaling. Since Ajuba proteins do not have any catalytic domains, the activity of Ajuba proteins may be regulated through changing their conformation. We found a binding between the N-terminus and the C-terminus of Ajuba proteins both in mammalian cell culture and in *Drosophila* wing discs. Though the function of this intramolecular binding is not clear, analyzing the N-C binding in the tissues with different Hippo signaling activity and the function of different parts of Ajuba proteins may give us some clues on the regulation of Ajuba proteins activity.

Hippo signaling in neoplastic tumors

The development of cancer is a complex process. One important early step is disruption of cell polarity, which removes the restriction on epithelial cell proliferation. The *Drosophila* imaginal disc has been established as a good model for epithelial tumor research because of its simple structure and the ease of genetic manipulation in flies. In *Drosophila*, the apical-basal polarity is controlled by three polarity modules. Disturbance of either module leads to disruption of cell polarity and deregulation of cell proliferation. Components of one polarity module, Scrib, Lgl, and Dlg, are well-established neoplastic tumor suppressors. Loss of function mutation in either gene results in massive tissue overgrowth in imaginal discs and brains[214]. How loss of cell polarity drives the massive cell proliferation is a key question in cancer research. Our study and work from other groups have shown Hippo signaling links the cell polarity to cell proliferation. In our study, we reported activation of Yki in wing discs with knocking down *lgl* in the whole posterior compartment, and this activation of Yki requires JNK activity. Yki activation in *lgl* or *scrib* mutant is also observed in eye discs[107, 215], but in eye discs, the Yki activation caused by loss of cell polarity does not require JNK activity[215]. This is consistent with our finding that JNK has little effect on Yki activity in eye discs. Thus, cell polarity may regulate Hippo signaling through both JNK-dependent and JNK-independent pathways, depending on the tissues. The JNK-dependent regulation requires the LIM domain protein Jub, but the JNK-independent regulation involves Hpo mislocalization and the interaction between Hpo and dRASSF[107].

A paper published after ours on Hippo signaling in loss of *scrib* clones identified a different effect of JNK on Hippo signaling, suggesting the interaction among cell

polarity, JNK signaling and Hippo signaling is more complicated. Due to the cell competition, the expansion of *scrib* mutant clones is inhibited by the surrounding wild type cells. Chen et al. found Yki suppression in *scrib* mutant clones, and suppression of Yki is JNK-dependent, as blocking JNK leads to Yki activation in the mutant clones, which seems contradictory with our model that JNK activates Yki[124]. This may be due to the difference between the system we used and the one used in Chen et al (2012). In our system, *lgl* is knocked down from the embryo stage in the whole compartment. The mutant cells do not face cell competition, so the dominant signal the mutant cells receive is pro-growth signal, and JNK is switched to a pro-proliferation status. In Chen et al (2012), *scrib* is mutated in clones during larval stage. The mutant cells face cell competition with the neighboring wild type cells. Because of the growth disadvantage, the mutant cells are sacrificed, and JNK is switched to a pro-apoptosis status. Thus, it is very likely that whether JNK activates or inhibits Yki depends on whether JNK is at pro-proliferation status or at pro-apoptosis status.

Hippo signaling in regeneration

The Hippo pathway is an essential growth control pathway in development and tumorigenesis. Our study found *Drosophila* wing disc regeneration requires activity of Yki, a downstream effector of Hippo signaling. Yki activation in the regenerating wing discs is mainly in the unwounded cells surrounding apoptotic cells, and drives the compensatory cell proliferation in the surrounding cells. We also observed Yki activation in some cells expressing apoptotic genes. At the end of cell ablation, these cells remain in the epithelia, suggesting Yki activation slows down the removal of these apoptotic cells. This may be due to the increased expression of DIAP1 (*Drosophila* inhibitor of apoptosis 1), which is a target of Yki. Yki is activated in the regenerating wing discs through JNK regulation of Jub.

Hippo signaling also participates in regeneration in the *Drosophila* midgut, a tissue equivalent to the mammalian intestine. Different from the wing discs that only contain epithelial cells, the midguts consist of multiple cell types, and the renewal of the epithelial cells enterocytes (ECs) is based on the amplification and differentiation of the intestine stem cells (ISCs). Infection or toxin damage in ECs results in Yki activation, which induces the secretion of the ligand for JAK-STAT pathway and EGFR pathway to promote proliferation of ISCs[33, 87]. Some studies also found damage of the midgut activates Yki in ISCs and Yki activation autonomously promotes ISCs proliferation[86]. Whether Hippo signaling regulates ISCs in the autonomous or non-autonomous manner may depend on the injury reagents adopted in the experiments.

Two groups have studied the role of Hippo signaling in mice intestine using different damage reagents, and got distinct effects in mammalian intestine regeneration.

Cai et al. found increased YAP, mammalian homolog of Yki, in intestine crypts after feeding mice with dextran sodium sulfate (DSS). Mice with conditional deletion of YAP in epithelium of the small intestine and colon have normal intestine development and homeostasis, but after DSS treatment showed higher mortality rate, decrease of body weight, significant loss of crypts and scattered colonic epithelial cells[216]. Barry et al. found overexpression of activated YAP in intestine caused loss of crypts, which identifies YAP as a growth suppressor. Moreover, YAP suppresses intestine regeneration after whole body irradiation, as YAP-deficient mice exhibited crypt hyperplasia and formation of microadenomas[217]. The opposite roles of YAP in intestine regeneration found by these two groups may attribute to the way used to induce damage. The suppressive effect of YAP on intestinal stem cell proliferation is through antagonizing Wnt signaling which may not be important in DSS-induced regeneration.

The mammalian Hippo signaling pathway also participates in the compensatory cell proliferation of parenchymal cells during regeneration. YAP promotes proliferation of cardiomyocytes during the neonatal heart regeneration. Overexpression of the active YAP stimulates regeneration of the adult heart, an organ that is normally hard to regenerate[218]. YAP activation is also required for the regenerative proliferation of cholangiocytes and hepatocytes after cholestatic injury in liver[219].

The strength of Hippo signaling activity needs to be precisely modulated during regeneration. We found the regenerating tissues require higher activity of Yki and Jub. Loss of one copy of *yki* or *jub* is sufficient to impair regeneration, but does not result in any developmental defect. On the other hand, Yki activation must be turned off and the Hippo signaling has to be re-activated when regeneration finishes to prevent tissue

overgrowth. We observed a nice correlation between Yki activation and the progression of wing disc regeneration. When wing disc regeneration ends, Yki activity returns to the normal level. What stops Yki activation and reactivates Hippo signaling is an unknown but important question in tissue regeneration. At the end stage of regeneration, the cell-cell contact and cell junctions are restored. The cell-cell contact and cell junctions are both the upstream activators of Hippo signaling, may contribute to stop the regenerative growth. The tension sensed by the proliferating cells is also changed with the regeneration progresses, which may also contribute to the reactivation of Hippo signaling. Further studies are needed to figure out the mechanism underlying the reactivation of Hippo signaling and inhibition of growth at the end of regeneration. Deregulation of Hippo signaling is also observed in many human cancers. So understanding how Hippo signaling is reactivated during the termination of regeneration may shed some light on cancer therapy.

Figure

Fig 1. Overexpression of Jub brings more Wts to apical junctions but cannot suppress Hippo signaling.

A-B) The representative wing of *nub-Gal4 UAS-dcr2* (A) and *nub-Gal4 UAS-dcr2 UAS-3Xflag:jub* (B). C) The average wing size of *nub-Gal4 UAS-dcr2* (n=27) and *nub-Gal4 UAS-dcr2 UAS-3Xflag:jub* (n=23). The error bar presents standard error. D) The level of Yki target *ex-lacz* in the disc *ex-lacz en-Gal4 UAS-GFP UAS-dcr2 UAS-jub:V5*. The red is ex-lacz, and the green is GFP, marking the *en-Gal4*-expressing region. E) The localization of overexpressed Jub:V5 in the wing disc *nub-Gal4 UAS-dcr2 UAS-jub:V5*. The red is V5. F) Jub:GFP in the wing disc *en-Gal4 UAS-mRFP UAS-jub:V5 jub:GFP*. The green is Jub:GFP, and *en-Gal4* expressing region is marked by RFP (blue). G) Wts:GFP in the wing disc *en-Gal4 UAS-mRFP UAS-jub:V5 wts:GFP*. The green is Wts:GFP, and *en-Gal4* expressing region is marked by RFP (blue). The panels marked prime shows the separate channel to the left.

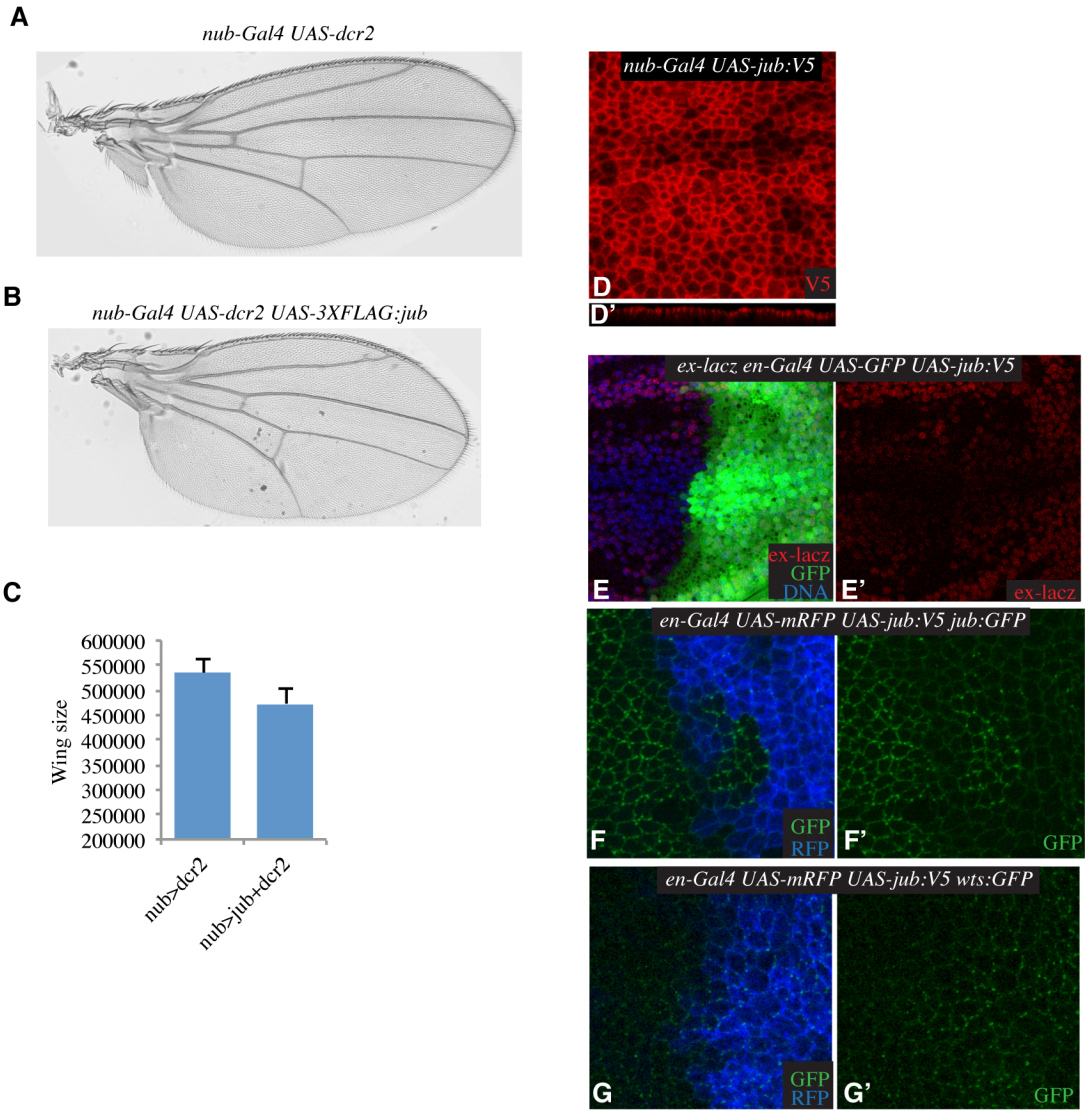
A
nub-Gal4 UAS-dcr2
B
nub-Gal4 UAS-dcr2 UAS-3XFLAG:jub
C
Wing size
600000
550000
500000
450000
400000
350000
300000
250000
200000
nub>dcr2
nub>jub+dcr2
nub-Gal4 UAS-jub:V5
D
V5
D'
ex-lacz en-Gal4 UAS-GFP UAS-jub:V5
ex-lacz
GFP
DNA
E
E'
ex-lacz
en-Gal4 UAS-mRFP UAS-jub:V5 jub:GFP
GFP
RFP
F
F'
GFP
en-Gal4 UAS-mRFP UAS-jub:V5 wts:GFP
GFP
RFP
G
G'
GFP

APPENDICES

1. JNK phosphorylation of protein 14-3-3

The 14-3-3 protein family is a group of highly conserved, ubiquitously expressed proteins that bind to a phospho-serine or phospho-threonine motif. In humans, there are 7 isoforms of protein 14-3-3 (β, γ, ε, ζ, τ, σ, η), and in *Drosophila* there are only two (ε and ζ). They participate in many biological processes through a large set of interacting proteins. Their major function is to sequester their partners in certain subcellular locations[220]. As for Hippo signaling, protein 14-3-3 is a cytoplasmic Yki/YAP binding partner that contributes to the majority of the cytoplasmic retention of Yki/YAP[66]. Reduced level of 14-3-3 protein induced nuclear localized Yki[82]. The binding between the 14-3-3 proteins and their partners are regulated by the phosphorylation status of the binding partners. However, modifications on protein 14-3-3 can also affect its binding to the targets. In mammalian cells, JNK has been reported to phosphorylate protein 14-3-3, which causes the dissociation of c-Abl or Bax from protein 14-3-3[221, 222]. The JNK phosphorylation site on mammalian protein 14-3-3 is conserved in *Drosophila* protein 14-3-3, so we tested if in *Drosophila* JNK can also phosphorylate protein 14-3-3 and if this phosphorylation affects the binding between protein 14-3-3 and Yki.

V5-tagged protein 14-3-3ζ was transfected into *Drosophila* S2 cells. To activate JNK, *bsk* and *hep.CA* were co-transfected. The protein samples were applied to Phos-tag gels. Activation of JNK resulted in a new band of protein 14-3-3ζ with slower migration in Phos-tag gel, indicating JNK activation induces the phosphorylation of protein 14-3-3 (Fig 1A). According to the phosphorylation site on mammalian protein 14-3-3, we made

a mutant of *Drosophila* protein 14-3-3ζ (14-3-3ζ^{S187A}), and found JNK no longer phosphorylated the mutant (Fig 1A). We then tested if JNK phosphorylation of protein 14-3-3ζ affects its binding to Yki. The activity of endogenous Hippo signaling in S2 cells is very weak, so *wts* and *hpo* were co-transfected into S2 cells to increase the basal binding between Yki and protein 14-3-3ζ. With the presence of Hpo and Wts, activation of JNK disrupted the binding between Yki and protein 14-3-3ζ. Without JNK activation, the 14-3-3ζ^{S187A} mutant exhibited stronger binding to Yki than the wild type. However, the binding between the 14-3-3ζ^{S187A} mutant and Yki was also reduced by JNK (Fig 1B). These data suggest JNK phosphorylation of protein 14-3-3 affects the ability of protein 14-3-3 to sequester Yki, but this is not the major mechanism underlying JNK regulation of Yki.

2. JNK phosphorylation of Yki

Two reports have shown JNK phosphorylates YAP in mammalian cells to regulate apoptosis, but the phosphorylation sites they identified and the function of the phosphorylation are distinct[121, 122]. In *Drosophila* S2 cells, we found activation of JNK by co-transfection of *bsk* and *hep.CA* led to Yki phosphorylation, indicated by the gel shift in Phos-tag gel (Fig 2A). Phosphorylation of Yki induced by JNK activation is not through Wts, as the JNK-induced gel shift also occurred on Yki with all Wts phosphorylation sites mutated (Yki^{3SA}) (Fig 2B). There are 6 JNK consensus sites in Yki. To map the phosphorylation sites on Yki, we mutated the 6 JNK consensus sites in different combination (Table 1). To exclude the influence of Wts phosphorylation, all mutation was made on Yki^{3SA} mutant. The phosphorylation status of the Yki mutants when JNK activated was tested on Phos-tag gel. Finally we found mutation of T100, S140, S255 sites abolishes the gel shift of Yki^{3SA} in Phos-tag gel (Fig 2B). Thus JNK phosphorylates Yki on the sites T100, S140, S255.

Figures

Fig 1. JNK phosphorylates protein 14-3-3, but the phosphorylation is not the major cause of the disruption of the binding of Yki to protein 14-3-3 by JNK.

A) The Phos-tag gel result of the wild type and the mutant protein 14-3-3ζ with or without JNK activation. V5-tagged protein 14-3-3ζ or protein 14-3-3ζ^{S187A} was transfected into S2 cells with or without *bsk* and *hep.CA*. JNK activation causes the gel shift of the wild type protein 14-3-3ζ but not the S187A mutant. B) The binding of Yki to protein 14-3-3ζ or protein 14-3-3ζ^{S187A} with or without JNK activation. GFP was used as a negative control. Protein 14-3-3ζ or GFP was precipitated with anti-V5 beads. The blots show the level of protein 14-3-3ζ, protein 14-3-3ζ^{S187A}, GFP, and Yki in the input and the precipitate. Without JNK activation, protein 14-3-3ζ^{S187A} shows stronger binding to Yki compared with the wild type. JNK activation disrupts Yki binding to both the wild type and the mutant protein 14-3-3ζ.

A

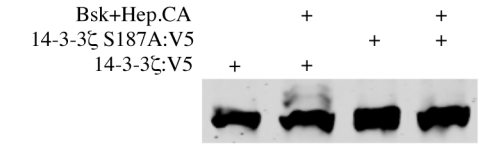
Bsk+Hep.CA + +
14-3-3ζ S187A:V5 + +
14-3-3ζ:V5 + +

B

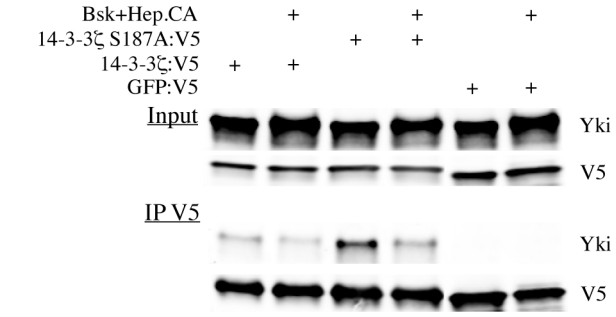
Bsk+Hep.CA + + +
14-3-3ζ S187A:V5 + +
14-3-3ζ:V5 + +
GFP:V5 + +
Input
Yki
V5
IP V5
Yki
V5

Fig 2. JNK phosphorylates Yki.

A) The Phos-tag gel result of Yki with or without JNK activation. *bsk* and *hep.CA* were co-transfected into S2 cells to activate JNK. JNK activation results in slower migration bands of Yki on Phos-tag gel. B) The Phos-tag gel results of Yki mutants with or without JNK activation. JNK activation results in slower migration bands of Yki^{3SA} (S111A, S168A, S250A) but not Yki mutI (S111A, S168A, S250A, T100A, S140A, S255A) on Phos-tag gels.

A

Bsk+Hep.CA +

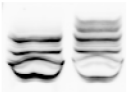

Yki

B

Bsk+Hep.CA + +
Yki:V5 mutI + +
Yki:V5 3SA + +

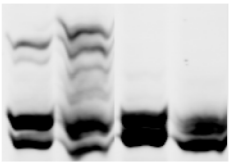

V5

Table 1. The Yki mutants

Mutant name	Mutated sites
Yki^{3SA}	S111A S168A S250A
Yki mutA	S111A S168A S169A S250A S255A
Yki mutB	T100A S111A S140A S168A S169A S250A S255A
Yki mutC	S49A T100A S111A S140A S153A S168A S169A S250A S255A
Yki mutD	S49A T100A S111A S140A S153A S168A S250A S255A
Yki mutE	T100A S111A S140A S168A S250A
Yki mutF	T100A S111A S168A S250A S255A
Yki mutG	S111A S140A S168A S250A S255A
Yki mutH	S111A S140A S168A S250A
Yki mutI	T100A S111A S140A S168A S250A S255A

REFERENCES

1. Klein, T., *Wing disc development in the fly: the early stages.* Curr Opin Genet Dev, 2001. **11**(4): p. 470-5.
2. Worley, M.I., L. Setiawan, and I.K. Hariharan, *Regeneration and transdetermination in Drosophila imaginal discs.* Annu Rev Genet, 2012. **46**: p. 289-310.
3. Morgan, T.H., *Regeneration and Liability to Injury.* Science, 1901. **14**(346): p. 235-48.
4. Reddien, P.W. and A. Sanchez Alvarado, *Fundamentals of planarian regeneration.* Annu Rev Cell Dev Biol, 2004. **20**: p. 725-57.
5. Brockes, J.P. and A. Kumar, *Comparative aspects of animal regeneration.* Annu Rev Cell Dev Biol, 2008. **24**: p. 525-49.
6. Yokoyama, H., *Initiation of limb regeneration: the critical steps for regenerative capacity.* Dev Growth Differ, 2008. **50**(1): p. 13-22.
7. Carlson, B.M., *Some principles of regeneration in mammalian systems.* Anat Rec B New Anat, 2005. **287**(1): p. 4-13.
8. Bergantinos, C., et al., *Imaginal discs: Renaissance of a model for regenerative biology.* Bioessays, 2010. **32**(3): p. 207-17.
9. Haynie, J.L. and P.J. Bryant, *Intercalary regeneration in imaginal wing disk of Drosophila melanogaster.* Nature, 1976. **259**(5545): p. 659-62.
10. Smith-Bolton, R.K., et al., *Regenerative growth in Drosophila imaginal discs is regulated by Wingless and Myc.* Dev Cell, 2009. **16**(6): p. 797-809.
11. Sun, G. and K.D. Irvine, *Regulation of Hippo signaling by Jun kinase signaling during compensatory cell proliferation and regeneration, and in neoplastic tumors.* Dev Biol, 2011. **350**(1): p. 139-51.
12. Herrera, S.C., R. Martin, and G. Morata, *Tissue homeostasis in the wing disc of drosophila melanogaster: immediate response to massive damage during development.* PLoS Genet, 2013. **9**(4): p. e1003446.
13. Grusche, F.A., et al., *The Salvador/Warts/Hippo pathway controls regenerative tissue growth in Drosophila melanogaster.* Dev Biol, 2011. **350**(2): p. 255-66.
14. Fan, Y. and A. Bergmann, *Apoptosis-induced compensatory proliferation. The Cell is dead. Long live the Cell!* Trends in Cell Biology, 2008. **18**(10): p. 467-473.
15. Kondo, S., et al., *DRONC coordinates cell death and compensatory proliferation.* Mol Cell Biol, 2006. **26**(19): p. 7258-68.
16. Ryoo, H.D., T. Gorenc, and H. Steller, *Apoptotic cells can induce compensatory cell proliferation through the JNK and the Wingless signaling pathways.* Dev Cell, 2004. **7**(4): p. 491-501.
17. Perez-Garijo, A., F.A. Martin, and G. Morata, *Caspase inhibition during apoptosis causes abnormal signalling and developmental aberrations in Drosophila.* Development, 2004. **131**(22): p. 5591-8.
18. Huh, J.R., M. Guo, and B.A. Hay, *Compensatory proliferation induced by cell death in the Drosophila wing disc requires activity of the apical cell death caspase Dronc in a nonapoptotic role.* Curr Biol, 2004. **14**(14): p. 1262-6.

19. Bosch, M., et al., *JNK signaling pathway required for wound healing in regenerating Drosophila wing imaginal discs.* Dev Biol, 2005. **280**(1): p. 73-86.
20. Bergantinos, C., M. Corominas, and F. Serras, *Cell death-induced regeneration in wing imaginal discs requires JNK signalling.* Development, 2010. **137**(7): p. 1169-79.
21. Morata, G., E. Shlevkov, and A. Perez-Garijo, *Mitogenic signaling from apoptotic cells in Drosophila.* Dev Growth Differ, 2011. **53**(2): p. 168-76.
22. Pahlavan, P.S., et al., *Prometheus' challenge: molecular, cellular and systemic aspects of liver regeneration.* J Surg Res, 2006. **134**(2): p. 238-51.
23. Moreno, E., M. Yan, and K. Basler, *Evolution of TNF signaling mechanisms: JNK-dependent apoptosis triggered by Eiger, the Drosophila homolog of the TNF superfamily.* Curr Biol, 2002. **12**(14): p. 1263-8.
24. Bosch, M., J. Baguna, and F. Serras, *Origin and proliferation of blastema cells during regeneration of Drosophila wing imaginal discs.* Int J Dev Biol, 2008. **52**(8): p. 1043-50.
25. Mattila, J., et al., *Role of Jun N-terminal Kinase (JNK) signaling in the wound healing and regeneration of a Drosophila melanogaster wing imaginal disc.* Int J Dev Biol, 2005. **49**(4): p. 391-9.
26. Perez-Garijo, A., E. Shlevkov, and G. Morata, *The role of Dpp and Wg in compensatory proliferation and in the formation of hyperplastic overgrowths caused by apoptotic cells in the Drosophila wing disc.* Development, 2009. **136**(7): p. 1169-77.
27. Yamanaka, T. and S. Ohno, *Role of Lgl/Dlg/Scribble in the regulation of epithelial junction, polarity and growth.* Front Biosci, 2008. **13**: p. 6693-707.
28. Wodarz, A., *Tumor suppressors: linking cell polarity and growth control.* Curr Biol, 2000. **10**(17): p. R624-6.
29. Ohsawa, S., et al., *Elimination of oncogenic neighbors by JNK-mediated engulfment in Drosophila.* Dev Cell, 2011. **20**(3): p. 315-28.
30. Brumby, A.M. and H.E. Richardson, *scribble mutants cooperate with oncogenic Ras or Notch to cause neoplastic overgrowth in Drosophila.* EMBO J, 2003. **22**(21): p. 5769-79.
31. Igaki, T., R.A. Pagliarini, and T. Xu, *Loss of cell polarity drives tumor growth and invasion through JNK activation in Drosophila.* Curr Biol, 2006. **16**(11): p. 1139-46.
32. Wu, M., J.C. Pastor-Pareja, and T. Xu, *Interaction between Ras(V12) and scribbled clones induces tumour growth and invasion.* Nature, 2010. **463**(7280): p. 545-8.
33. Staley, B.K. and K.D. Irvine, *Warts and Yorkie mediate intestinal regeneration by influencing stem cell proliferation.* Curr Biol, 2010. **20**(17): p. 1580-7.
34. Justice, R.W., et al., *The Drosophila tumor suppressor gene warts encodes a homolog of human myotonic dystrophy kinase and is required for the control of cell shape and proliferation.* Genes Dev, 1995. **9**(5): p. 534-46.
35. Xu, T., et al., *Identifying tumor suppressors in genetic mosaics: the Drosophila lats gene encodes a putative protein kinase.* Development, 1995. **121**(4): p. 1053-63.

36. Kango-Singh, M., et al., *Shar-pei mediates cell proliferation arrest during imaginal disc growth in Drosophila.* Development, 2002. **129**(24): p. 5719-30.
37. Tapon, N., et al., *salvador Promotes both cell cycle exit and apoptosis in Drosophila and is mutated in human cancer cell lines.* Cell, 2002. **110**(4): p. 467-78.
38. Harvey, K.F., C.M. Pfleger, and I.K. Hariharan, *The Drosophila Mst ortholog, hippo, restricts growth and cell proliferation and promotes apoptosis.* Cell, 2003. **114**(4): p. 457-67.
39. Pantalacci, S., N. Tapon, and P. Leopold, *The Salvador partner Hippo promotes apoptosis and cell-cycle exit in Drosophila.* Nat Cell Biol, 2003. **5**(10): p. 921-7.
40. Udan, R.S., et al., *Hippo promotes proliferation arrest and apoptosis in the Salvador/Warts pathway.* Nat Cell Biol, 2003. **5**(10): p. 914-20.
41. Wu, S., et al., *hippo encodes a Ste-20 family protein kinase that restricts cell proliferation and promotes apoptosis in conjunction with salvador and warts.* Cell, 2003. **114**(4): p. 445-56.
42. Jia, J., et al., *The Drosophila Ste20 family kinase dMST functions as a tumor suppressor by restricting cell proliferation and promoting apoptosis.* Genes Dev, 2003. **17**(20): p. 2514-9.
43. Lai, Z.C., et al., *Control of cell proliferation and apoptosis by mob as tumor suppressor, mats.* Cell, 2005. **120**(5): p. 675-85.
44. St John, M.A., et al., *Mice deficient of Lats1 develop soft-tissue sarcomas, ovarian tumours and pituitary dysfunction.* Nat Genet, 1999. **21**(2): p. 182-6.
45. Hisaoka, M., A. Tanaka, and H. Hashimoto, *Molecular alterations of h-warts/LATS1 tumor suppressor in human soft tissue sarcoma.* Lab Invest, 2002. **82**(10): p. 1427-35.
46. Zhao, B., et al., *Cell detachment activates the Hippo pathway via cytoskeleton reorganization to induce anoikis.* Genes Dev, 2012. **26**(1): p. 54-68.
47. Harvey, K.F., X. Zhang, and D.M. Thomas, *The Hippo pathway and human cancer.* Nat Rev Cancer, 2013. **13**(4): p. 246-57.
48. Colombani, J., et al., *Dmp53 activates the Hippo pathway to promote cell death in response to DNA damage.* Curr Biol, 2006. **16**(14): p. 1453-8.
49. Jin, Y., et al., *Dimerization and cytoplasmic localization regulate Hippo kinase signaling activity in organ size control.* J Biol Chem, 2012. **287**(8): p. 5784-96.
50. Deng, Y., et al., *Hippo activation through homodimerization and membrane association for growth inhibition and organ size control.* Dev Biol, 2013. **375**(2): p. 152-9.
51. Poon, C.L., et al., *The sterile 20-like kinase Tao-1 controls tissue growth by regulating the Salvador-Warts-Hippo pathway.* Dev Cell, 2011. **21**(5): p. 896-906.
52. Boggiano, J.C., P.J. Vanderzalm, and R.G. Fehon, *Tao-1 phosphorylates Hippo/MST kinases to regulate the Hippo-Salvador-Warts tumor suppressor pathway.* Dev Cell, 2011. **21**(5): p. 888-95.
53. Wei, X., T. Shimizu, and Z.C. Lai, *Mob as tumor suppressor is activated by Hippo kinase for growth inhibition in Drosophila.* EMBO J, 2007. **26**(7): p. 1772-81.

54. Chan, E.H., et al., *The Ste20-like kinase Mst2 activates the human large tumor suppressor kinase Lats1.* Oncogene, 2005. **24**(12): p. 2076-86.
55. Praskova, M., F. Xia, and J. Avruch, *MOBKL1A/MOBKL1B phosphorylation by MST1 and MST2 inhibits cell proliferation.* Curr Biol, 2008. **18**(5): p. 311-21.
56. Polesello, C., et al., *The Drosophila RASSF homolog antagonizes the hippo pathway.* Curr Biol, 2006. **16**(24): p. 2459-65.
57. Ribeiro, P.S., et al., *Combined functional genomic and proteomic approaches identify a PP2A complex as a negative regulator of Hippo signaling.* Mol Cell, 2010. **39**(4): p. 521-34.
58. Huang, H.L., et al., *Par-1 regulates tissue growth by influencing hippo phosphorylation status and hippo-salvador association.* PLoS Biol, 2013. **11**(8): p. e1001620.
59. Wehr, M.C., et al., *Salt-inducible kinases regulate growth through the Hippo signalling pathway in Drosophila.* Nat Cell Biol, 2013. **15**(1): p. 61-71.
60. Zheng, Q. and Y. Zhao, *The diverse biofunctions of LIM domain proteins: determined by subcellular localization and protein-protein interaction.* Biol Cell, 2007. **99**(9): p. 489-502.
61. Hirata, H., H. Tatsumi, and M. Sokabe, *Zyxin emerges as a key player in the mechanotransduction at cell adhesive structures.* Commun Integr Biol, 2008. **1**(2): p. 192-5.
62. Marie, H., et al., *The LIM protein Ajuba is recruited to cadherin-dependent cell junctions through an association with alpha-catenin.* J Biol Chem, 2003. **278**(2): p. 1220-8.
63. Nola, S., et al., *Ajuba is required for Rac activation and maintenance of E-cadherin adhesion.* J Cell Biol, 2011. **195**(5): p. 855-71.
64. Das Thakur, M., et al., *Ajuba LIM proteins are negative regulators of the Hippo signaling pathway.* Curr Biol, 2010. **20**(7): p. 657-62.
65. Rauskolb, C., et al., *Zyxin links fat signaling to the hippo pathway.* PLoS Biol, 2011. **9**(6): p. e1000624.
66. Huang, J., et al., *The Hippo signaling pathway coordinately regulates cell proliferation and apoptosis by inactivating Yorkie, the Drosophila Homolog of YAP.* Cell, 2005. **122**(3): p. 421-34.
67. Badouel, C., et al., *The FERM-domain protein Expanded regulates Hippo pathway activity via direct interactions with the transcriptional activator Yorkie.* Dev Cell, 2009. **16**(3): p. 411-20.
68. Oh, H., B.V. Reddy, and K.D. Irvine, *Phosphorylation-independent repression of Yorkie in Fat-Hippo signaling.* Dev Biol, 2009. **335**(1): p. 188-97.
69. Dong, J., et al., *Elucidation of a universal size-control mechanism in Drosophila and mammals.* Cell, 2007. **130**(6): p. 1120-33.
70. Oh, H. and K.D. Irvine, *In vivo regulation of Yorkie phosphorylation and localization.* Development, 2008. **135**(6): p. 1081-8.
71. Oh, H. and K.D. Irvine, *In vivo analysis of Yorkie phosphorylation sites.* Oncogene, 2009. **28**(17): p. 1916-27.
72. Hao, Y., et al., *Tumor suppressor LATS1 is a negative regulator of oncogene YAP.* J Biol Chem, 2008. **283**(9): p. 5496-509.

73. Zhao, B., et al., *Inactivation of YAP oncoprotein by the Hippo pathway is involved in cell contact inhibition and tissue growth control.* Genes Dev, 2007. **21**(21): p. 2747-61.
74. Zhang, J., G.A. Smolen, and D.A. Haber, *Negative regulation of YAP by LATS1 underscores evolutionary conservation of the Drosophila Hippo pathway.* Cancer Res, 2008. **68**(8): p. 2789-94.
75. Zhao, B., et al., *A coordinated phosphorylation by Lats and CK1 regulates YAP stability through SCF(beta-TRCP).* Genes Dev, 2010. **24**(1): p. 72-85.
76. Liu, C.Y., et al., *The hippo tumor pathway promotes TAZ degradation by phosphorylating a phosphodegron and recruiting the SCF{beta}-TrCP E3 ligase.* J Biol Chem, 2010. **285**(48): p. 37159-69.
77. Thompson, B.J. and S.M. Cohen, *The Hippo pathway regulates the bantam microRNA to control cell proliferation and apoptosis in Drosophila.* Cell, 2006. **126**(4): p. 767-74.
78. Nolo, R., et al., *The bantam microRNA is a target of the hippo tumor-suppressor pathway.* Curr Biol, 2006. **16**(19): p. 1895-904.
79. Nicolay, B.N. and M.V. Frolov, *Context-dependent requirement for dE2F during oncogenic proliferation.* PLoS Genet, 2008. **4**(10): p. e1000205.
80. Neto-Silva, R.M., S. de Beco, and L.A. Johnston, *Evidence for a growth-stabilizing regulatory feedback mechanism between Myc and Yorkie, the Drosophila homolog of Yap.* Dev Cell, 2010. **19**(4): p. 507-20.
81. Zecca, M. and G. Struhl, *A feed-forward circuit linking wingless, fat-dachsous signaling, and the warts-hippo pathway to Drosophila wing growth.* PLoS Biol, 2010. **8**(6): p. e1000386.
82. Ren, F., L. Zhang, and J. Jiang, *Hippo signaling regulates Yorkie nuclear localization and activity through 14-3-3 dependent and independent mechanisms.* Dev Biol, 2010. **337**(2): p. 303-12.
83. Hamaratoglu, F., et al., *The tumour-suppressor genes NF2/Merlin and Expanded act through Hippo signalling to regulate cell proliferation and apoptosis.* Nat Cell Biol, 2006. **8**(1): p. 27-36.
84. Genevet, A., et al., *Kibra is a regulator of the Salvador/Warts/Hippo signaling network.* Dev Cell, 2010. **18**(2): p. 300-8.
85. Cosgrove, D.E. and G.S. Cox, *Effects of sodium butyrate and 5-azacytidine on DNA methylation in human tumor cell lines: variable response to drug treatment and withdrawal.* Biochim Biophys Acta, 1990. **1087**(1): p. 80-6.
86. Karpowicz, P., J. Perez, and N. Perrimon, *The Hippo tumor suppressor pathway regulates intestinal stem cell regeneration.* Development, 2010. **137**(24): p. 4135-45.
87. Ren, F., et al., *Hippo signaling regulates Drosophila intestine stem cell proliferation through multiple pathways.* Proc Natl Acad Sci U S A, 2010. **107**(49): p. 21064-9.
88. Zhou, D., et al., *Mst1 and Mst2 maintain hepatocyte quiescence and suppress hepatocellular carcinoma development through inactivation of the Yap1 oncogene.* Cancer Cell, 2009. **16**(5): p. 425-38.
89. Hall, C.A., et al., *Hippo pathway effector Yap is an ovarian cancer oncogene.* Cancer Res, 2010. **70**(21): p. 8517-25.

90. Xu, M.Z., et al., *Yes-associated protein is an independent prognostic marker in hepatocellular carcinoma.* Cancer, 2009. **115**(19): p. 4576-85.
91. Camargo, F.D., et al., *YAP1 increases organ size and expands undifferentiated progenitor cells.* Curr Biol, 2007. **17**(23): p. 2054-60.
92. Zhou, D., et al., *Mst1 and Mst2 protein kinases restrain intestinal stem cell proliferation and colonic tumorigenesis by inhibition of Yes-associated protein (Yap) overabundance.* Proc Natl Acad Sci U S A, 2011. **108**(49): p. E1312-20.
93. Lee, K.P., et al., *The Hippo-Salvador pathway restrains hepatic oval cell proliferation, liver size, and liver tumorigenesis.* Proc Natl Acad Sci U S A, 2010. **107**(18): p. 8248-53.
94. Schlegelmilch, K., et al., *Yap1 acts downstream of alpha-catenin to control epidermal proliferation.* Cell, 2011. **144**(5): p. 782-95.
95. Lamar, J.M., et al., *The Hippo pathway target, YAP, promotes metastasis through its TEAD-interaction domain.* Proc Natl Acad Sci U S A, 2012. **109**(37): p. E2441-50.
96. Jeong, G.O., et al., *TAZ mediates lysophosphatidic acid-induced migration and proliferation of epithelial ovarian cancer cells.* Cell Physiol Biochem, 2013. **32**(2): p. 253-63.
97. Strano, S., et al., *Physical interaction with Yes-associated protein enhances p73 transcriptional activity.* J Biol Chem, 2001. **276**(18): p. 15164-73.
98. Strano, S., et al., *The transcriptional coactivator Yes-associated protein drives p73 gene-target specificity in response to DNA Damage.* Mol Cell, 2005. **18**(4): p. 447-59.
99. Tumaneng, K., et al., *YAP mediates crosstalk between the Hippo and PI(3)K-TOR pathways by suppressing PTEN via miR-29.* Nat Cell Biol, 2012. **14**(12): p. 1322-9.
100. McCartney, B.M., et al., *The neurofibromatosis-2 homologue, Merlin, and the tumor suppressor expanded function together in Drosophila to regulate cell proliferation and differentiation.* Development, 2000. **127**(6): p. 1315-24.
101. Rouleau, G.A., et al., *Alteration in a new gene encoding a putative membrane-organizing protein causes neuro-fibromatosis type 2.* Nature, 1993. **363**(6429): p. 515-21.
102. Yu, J., et al., *Kibra functions as a tumor suppressor protein that regulates Hippo signaling in conjunction with Merlin and Expanded.* Dev Cell, 2010. **18**(2): p. 288-99.
103. Baumgartner, R., et al., *The WW domain protein Kibra acts upstream of Hippo in Drosophila.* Dev Cell, 2010. **18**(2): p. 309-16.
104. Yin, F., et al., *Spatial organization of Hippo signaling at the plasma membrane mediated by the tumor suppressor Merlin/NF2.* Cell, 2013. **154**(6): p. 1342-55.
105. Chen, C.L., et al., *The apical-basal cell polarity determinant Crumbs regulates Hippo signaling in Drosophila.* Proc Natl Acad Sci U S A, 2010. **107**(36): p. 15810-5.
106. Ling, C., et al., *The apical transmembrane protein Crumbs functions as a tumor suppressor that regulates Hippo signaling by binding to Expanded.* Proc Natl Acad Sci U S A, 2010. **107**(23): p. 10532-7.

107. Grzeschik, N.A., et al., *Lgl, aPKC, and Crumbs regulate the Salvador/Warts/Hippo pathway through two distinct mechanisms.* Curr Biol, 2010. **20**(7): p. 573-81.
108. Robinson, B.S., et al., *Crumbs regulates Salvador/Warts/Hippo signaling in Drosophila via the FERM-domain protein Expanded.* Curr Biol, 2010. **20**(7): p. 582-90.
109. Varelas, X., et al., *The Crumbs complex couples cell density sensing to Hippo-dependent control of the TGF-beta-SMAD pathway.* Dev Cell, 2010. **19**(6): p. 831-44.
110. Kim, N.G., et al., *E-cadherin mediates contact inhibition of proliferation through Hippo signaling-pathway components.* Proc Natl Acad Sci U S A, 2011. **108**(29): p. 11930-5.
111. Silvis, M.R., et al., *alpha-catenin is a tumor suppressor that controls cell accumulation by regulating the localization and activity of the transcriptional coactivator Yap1.* Sci Signal, 2011. **4**(174): p. ra33.
112. Zhao, B., et al., *Angiomotin is a novel Hippo pathway component that inhibits YAP oncoprotein.* Genes Dev, 2011. **25**(1): p. 51-63.
113. Paramasivam, M., et al., *Angiomotin family proteins are novel activators of the LATS2 kinase tumor suppressor.* Mol Biol Cell, 2011. **22**(19): p. 3725-33.
114. Willecke, M., et al., *The fat cadherin acts through the hippo tumor-suppressor pathway to regulate tissue size.* Curr Biol, 2006. **16**(21): p. 2090-100.
115. Silva, E., et al., *The tumor-suppressor gene fat controls tissue growth upstream of expanded in the hippo signaling pathway.* Curr Biol, 2006. **16**(21): p. 2081-9.
116. Bennett, F.C. and K.F. Harvey, *Fat cadherin modulates organ size in Drosophila via the Salvador/Warts/Hippo signaling pathway.* Curr Biol, 2006. **16**(21): p. 2101-10.
117. Feng, Y. and K.D. Irvine, *Fat and expanded act in parallel to regulate growth through warts.* Proc Natl Acad Sci U S A, 2007. **104**(51): p. 20362-7.
118. Yu, F.X., et al., *Regulation of the Hippo-YAP pathway by G-protein-coupled receptor signaling.* Cell, 2012. **150**(4): p. 780-91.
119. Reddy, B.V. and K.D. Irvine, *Regulation of Hippo signaling by EGFR-MAPK signaling through Ajuba family proteins.* Dev Cell, 2013. **24**(5): p. 459-71.
120. Fan, R., N.G. Kim, and B.M. Gumbiner, *Regulation of Hippo pathway by mitogenic growth factors via phosphoinositide 3-kinase and phosphoinositide-dependent kinase-1.* Proc Natl Acad Sci U S A, 2013. **110**(7): p. 2569-74.
121. Tomlinson, V., et al., *JNK phosphorylates Yes-associated protein (YAP) to regulate apoptosis.* Cell Death Dis, 2010. **1**: p. e29.
122. Lee, K.K. and S. Yonehara, *Identification of mechanism that couples multisite phosphorylation of Yes-associated protein (YAP) with transcriptional coactivation and regulation of apoptosis.* J Biol Chem, 2012. **287**(12): p. 9568-78.
123. Enomoto, M. and T. Igaki, *Src controls tumorigenesis via JNK-dependent regulation of the Hippo pathway in Drosophila.* EMBO Rep, 2013. **14**(1): p. 65-72.
124. Chen, C.L., et al., *Tumor suppression by cell competition through regulation of the Hippo pathway.* Proc Natl Acad Sci U S A, 2012. **109**(2): p. 484-9.

125. Dupont, S., et al., *Role of YAP/TAZ in mechanotransduction.* Nature, 2011. **474**(7350): p. 179-83.
126. Aragona, M., et al., *A mechanical checkpoint controls multicellular growth through YAP/TAZ regulation by actin-processing factors.* Cell, 2013. **154**(5): p. 1047-59.
127. Wada, K., et al., *Hippo pathway regulation by cell morphology and stress fibers.* Development, 2011. **138**(18): p. 3907-14.
128. Fernandez, B.G., et al., *Actin-Capping Protein and the Hippo pathway regulate F-actin and tissue growth in Drosophila.* Development, 2011. **138**(11): p. 2337-46.
129. Sansores-Garcia, L., et al., *Modulating F-actin organization induces organ growth by affecting the Hippo pathway.* EMBO J, 2011. **30**(12): p. 2325-35.
130. Butler, M.J., et al., *Discovery of genes with highly restricted expression patterns in the Drosophila wing disc using DNA oligonucleotide microarrays.* Development, 2003. **130**(4): p. 659-70.
131. Fan, Y. and A. Bergmann, *Apoptosis-induced compensatory proliferation. The Cell is dead. Long live the Cell!* Trends Cell Biol, 2008. **18**(10): p. 467-73.
132. Haynie, J.L. and P.J. Bryant, *The effects of X-rays on the proliferation dynamics of cells in he imaginal wing disc of Drosophila melanogaster.* Roux's Archives, 1977. **183**: p. 85-100.
133. Bogoyevitch, M.A., et al., *c-Jun N-terminal kinase (JNK) signaling: recent advances and challenges.* Biochim Biophys Acta, 2010. **1804**(3): p. 463-75.
134. Igaki, T., *Correcting developmental errors by apoptosis: lessons from Drosophila JNK signaling.* Apoptosis, 2009. **14**(8): p. 1021-8.
135. Karin, M. and E. Gallagher, *From JNK to pay dirt: jun kinases, their biochemistry, physiology and clinical importance.* TBMB, 2005. **57**(4-5): p. 283-95.
136. Martin, P. and S.M. Parkhurst, *Parallels between tissue repair and embryo morphogenesis.* Development, 2004. **131**(13): p. 3021-34.
137. Kanda, H. and M. Miura, *Regulatory roles of JNK in programmed cell death.* J Biochem, 2004. **136**(1): p. 1-6.
138. Hariharan, I.K. and D. Bilder, *Regulation of imaginal disc growth by tumor-suppressor genes in Drosophila.* Annu Rev Genet, 2006. **40**: p. 335-61.
139. McEwen, D.G. and M. Peifer, *Puckered, a Drosophila MAPK phosphatase, ensures cell viability by antagonizing JNK-induced apoptosis.* Development, 2005. **132**(17): p. 3935-46.
140. Uhlirova, M. and D. Bohmann, *JNK- and Fos-regulated Mmp1 expression cooperates with Ras to induce invasive tumors in Drosophila.* EMBO J, 2006. **25**(22): p. 5294-304.
141. Bilder, D., M. Li, and N. Perrimon, *Cooperative regulation of cell polarity and growth by Drosophila tumor suppressors.* Science, 2000. **289**(5476): p. 113-6.
142. Agrawal, N., et al., *Neoplastic transformation and aberrant cell-cell interactions in genetic mosaics of lethal(2)giant larvae (lgl), a tumor suppressor gene of Drosophila.* Dev Biol, 1995. **172**(1): p. 218-29.
143. Froldi, F., et al., *The lethal giant larvae tumour suppressor mutation requires dMyc oncoprotein to promote clonal malignancy.* BMC Biol, 2010. **8**(1): p. 33.

144. Igaki, T., et al., *Intrinsic tumor suppression and epithelial maintenance by endocytic activation of Eiger/TNF signaling in Drosophila.* Dev Cell, 2009. **16**(3): p. 458-65.
145. Pagliarini, R.A. and T. Xu, *A genetic screen in Drosophila for metastatic behavior.* Science, 2003. **302**(5648): p. 1227-31.
146. Zhao, B., et al., *The Hippo-YAP pathway in organ size control and tumorigenesis: an updated version.* Genes Dev, 2010. **24**(9): p. 862-74.
147. Reddy, B.V. and K.D. Irvine, *The Fat and Warts signaling pathways: new insights into their regulation, mechanism and conservation.* Development, 2008. **135**(17): p. 2827-38.
148. Oh, H. and K.D. Irvine, *Yorkie: the final destination of Hippo signaling.* Trends Cell Biol, 2010: p. in press.
149. Menéndez, J., et al., *A tumor-suppressing mechanism in Drosophila involving cell competition and the Hippo pathway.* Proc Natl Acad Sci USA, 2010. **107**(33): p. 14651-6.
150. Goyal, L., et al., *Induction of apoptosis by Drosophila reaper, hid and grim through inhibition of IAP function.* EMBO J, 2000. **19**(4): p. 589-97.
151. Wang, S.L., et al., *The Drosophila caspase inhibitor DIAP1 is essential for cell survival and is negatively regulated by HID.* Cell, 1999. **98**(4): p. 453-63.
152. White, K., et al., *Genetic control of programmed cell death in Drosophila.* Science, 1994. **264**(5159): p. 677-83.
153. Igaki, T., et al., *Eiger, a TNF superfamily ligand that triggers the Drosophila JNK pathway.* EMBO J, 2002. **21**(12): p. 3009-18.
154. Feng, Y. and K.D. Irvine, *Processing and phosphorylation of the Fat receptor.* Proc Natl Acad Sci U S A, 2009. **106**(29): p. 11989-94.
155. Kauppila, S., et al., *Eiger and its receptor, Wengen, comprise a TNF-like system in Drosophila.* Oncogene, 2003. **22**(31): p. 4860-7.
156. Martín-Blanco, E., et al., *puckered encodes a phosphatase that mediates a feedback loop regulating JNK activity during dorsal closure in Drosophila.* Genes & Development, 1998. **12**(4): p. 557-70.
157. Adachi-Yamada, T., et al., *Distortion of proximodistal information causes JNK-dependent apoptosis in Drosophila wing.* Nature, 1999. **400**(6740): p. 166-9.
158. Wells, B.S., E. Yoshida, and L.A. Johnston, *Compensatory proliferation in Drosophila imaginal discs requires Dronc-dependent p53 activity.* Curr Biol, 2006. **16**(16): p. 1606-15.
159. Cho, E., et al., *Delineation of a Fat tumor suppressor pathway.* Nat Genet, 2006. **38**(10): p. 1142-50.
160. Cho, E. and K.D. Irvine, *Action of fat, four-jointed, dachsous and dachs in distal-to-proximal wing signaling.* Development, 2004. **131**(18): p. 4489-500.
161. Bennett, F.C. and K.F. Harvey, *Fat Cadherin Modulates Organ Size in Drosophila via the Salvador/Warts/Hippo Signaling Pathway.* Curr Biol, 2006. **16**: p. 2101-10.
162. Dietzl, G., et al., *A genome-wide transgenic RNAi library for conditional gene inactivation in Drosophila.* Nature, 2007. **448**(7150): p. 151-6.
163. Lee, C.-Y., K.J. Robinson, and C.Q. Doe, *Lgl, Pins and aPKC regulate neuroblast self-renewal versus differentiation.* Nature, 2006. **439**(7076): p. 594-8.

164. Rogulja, D., C. Rauskolb, and K.D. Irvine, *Morphogen control of wing growth through the Fat signaling pathway.* Dev Cell, 2008. **15**(2): p. 309-21.
165. Zhu, M., et al., *Activation of JNK signaling links lgl mutations to disruption of the cell polarity and epithelial organization in Drosophila imaginal discs.* Cell Res, 2010. **20**(2): p. 242-5.
166. Bilder, D., M. Schober, and N. Perrimon, *Integrated activity of PDZ protein complexes regulates epithelial polarity.* Nat Cell Biol, 2003. **5**(1): p. 53-8.
167. Buttitta, L.A., et al., *A double-assurance mechanism controls cell cycle exit upon terminal differentiation in Drosophila.* Dev Cell, 2007. **12**(4): p. 631-43.
168. Brand, A.H. and N. Perrimon, *Targeted gene expression as a means of altering cell fates and generating dominant phenotypes.* Development, 1993. **118**(2): p. 401-15.
169. Tanaka, E.M. and P.W. Reddien, *The cellular basis for animal regeneration.* Developmental Cell, 2011. **21**(1): p. 172-185.
170. Chen, F., *JNK-induced apoptosis, compensatory growth, and cancer stem cells.* Cancer Research, 2012. **72**(2): p. 379-386.
171. Bogoyevitch, M.A., et al., *c-Jun N-terminal kinase (JNK) signaling: recent advances and challenges.* Biochim Biophys Acta, 2010. **1804**(3): p. 463-75.
172. Iimuro, Y. and J. Fujimoto, *TLRs, NF-kappaB, JNK, and Liver Regeneration.* Gastroenterol Res Pract, 2010. **2010**.
173. Tasaki, J., et al., *Role of c-Jun N-terminal kinase activation in blastema formation during planarian regeneration.* Dev Growth Differ, 2011. **53**(3): p. 389-400.
174. Menendez, J., et al., *A tumor-suppressing mechanism in Drosophila involving cell competition and the Hippo pathway.* Proceedings of the National Academy of Sciences of the United States of America, 2010. **107**(33): p. 14651-6.
175. Pérez-Garijo, A., E. Shlevkov, and G. Morata, *The role of Dpp and Wg in compensatory proliferation and in the formation of hyperplastic overgrowths caused by apoptotic cells in the Drosophila wing disc.* Development (Cambridge, England), 2009.
176. Leong, G.R., et al., *scribble mutants promote aPKC and JNK-dependent epithelial neoplasia independently of Crumbs.* BMC Biology, 2009. **7**: p. 62.
177. Cordero, J.B., et al., *Oncogenic Ras diverts a host TNF tumor suppressor activity into tumor promoter.* Dev Cell, 2010. **18**(6): p. 999-1011.
178. Zhang, J.Y. and M.A. Selim, *The role of the c-Jun N-terminal Kinase signaling pathway in skin cancer.* Am J Cancer Res, 2012. **2**(6): p. 691-8.
179. Hui, L., et al., *Proliferation of human HCC cells and chemically induced mouse liver cancers requires JNK1-dependent p21 downregulation.* J Clin Invest, 2008. **118**(12): p. 3943-53.
180. Bogoyevitch, M.A. and B. Kobe, *Uses for JNK: the many and varied substrates of the c-Jun N-terminal kinases.* Microbiol Mol Biol Rev, 2006. **70**(4): p. 1061-95.
181. Staley, B.K. and K.D. Irvine, *Hippo signaling in Drosophila: recent advances and insights.* Dev Dyn, 2012. **241**(1): p. 3-15.
182. Irvine, K.D., *Integration of intercellular signaling through the Hippo pathway.* Semin Cell Dev Biol, 2012. **23**(7): p. 812-7.
183. Pan, D., *The hippo signaling pathway in development and cancer.* Dev Cell, 2010. **19**(4): p. 491-505.

184. Shaw, R.L., et al., *The Hippo pathway regulates intestinal stem cell proliferation during Drosophila adult midgut regeneration.* Development, 2010. **137**(24): p. 4147-58.
185. Kulshammer, E. and M. Uhlirova, *The actin cross-linker Filamin/Cheerio mediates tumor malignancy downstream of JNK signaling.* J Cell Sci, 2013. **126**(Pt 4): p. 927-38.
186. Ribeiro, P.S., et al., *Combined functional genomic and proteomic approaches identify a PP2A complex as a negative regulator of Hippo signaling.* Molecular Cell, 2010. **39**(4): p. 521-534.
187. Du, L., et al., *Inhibition of cell proliferation and cell cycle progression by specific inhibition of basal JNK activity: evidence that mitotic Bcl-2 phosphorylation is JNK-independent.* J Biol Chem, 2004. **279**(12): p. 11957-66.
188. Bennett, B.L., et al., *SP600125, an anthrapyrazolone inhibitor of Jun N-terminal kinase.* Proc Natl Acad Sci U S A, 2001. **98**(24): p. 13681-6.
189. Barancik, M., P. Htun, and W. Schaper, *Okadaic acid and anisomycin are protective and stimulate the SAPK/JNK pathway.* J Cardiovasc Pharmacol, 1999. **34**(2): p. 182-90.
190. Lei, K., et al., *The Bax subfamily of Bcl2-related proteins is essential for apoptotic signal transduction by c-Jun NH(2)-terminal kinase.* Mol Cell Biol, 2002. **22**(13): p. 4929-42.
191. Kinoshita, E., et al., *Phosphate-binding tag, a new tool to visualize phosphorylated proteins.* Mol Cell Proteomics, 2006. **5**(4): p. 749-57.
192. Dephoure, N., et al., *A quantitative atlas of mitotic phosphorylation.* Proc Natl Acad Sci U S A, 2008. **105**(31): p. 10762-7.
193. Abe, Y., et al., *LATS2-Ajuba complex regulates gamma-tubulin recruitment to centrosomes and spindle organization during mitosis.* FEBS Lett, 2006. **580**(3): p. 782-8.
194. Sabino, D., N.H. Brown, and R. Basto, *Drosophila Ajuba is not an Aurora-A activator but is required to maintain Aurora-A at the centrosome.* J Cell Sci, 2011. **124**(Pt 7): p. 1156-66.
195. Ohsawa, S., et al., *Mitochondrial defect drives non-autonomous tumour progression through Hippo signalling in Drosophila.* Nature, 2012. **490**(7421): p. 547-51.
196. Brumby, A.M., et al., *Identification of novel Ras-cooperating oncogenes in Drosophila melanogaster: a RhoGEF/Rho-family/JNK pathway is a central driver of tumorigenesis.* Genetics, 2011. **188**(1): p. 105-25.
197. Khoo, P., et al., *In Drosophila, RhoGEF2 cooperates with activated Ras in tumorigenesis through a pathway involving Rho1-Rok-Myosin-II and JNK signalling.* Dis Model Mech, 2013. **6**(3): p. 661-78.
198. Cellurale, C., et al., *Requirement of c-Jun NH(2)-terminal kinase for Ras-initiated tumor formation.* Mol Cell Biol, 2011. **31**(7): p. 1565-76.
199. Nielsen, C., et al., *c-Jun NH2-terminal kinase 2 is required for Ras transformation independently of activator protein 1.* Cancer Res, 2007. **67**(1): p. 178-85.

200. Rath, N. and M.F. Olson, *Rho-associated kinases in tumorigenesis: re-considering ROCK inhibition for cancer therapy.* EMBO Rep, 2012. **13**(10): p. 900-8.
201. Asparuhova, M.B., L. Gelman, and M. Chiquet, *Role of the actin cytoskeleton in tuning cellular responses to external mechanical stress.* Scand J Med Sci Sports, 2009. **19**(4): p. 490-9.
202. Shyu, Y.J., C.D. Suarez, and C.D. Hu, *Visualization of ternary complexes in living cells by using a BiFC-based FRET assay.* Nat Protoc, 2008. **3**(11): p. 1693-702.
203. Pratt, S.J., et al., *The LIM protein Ajuba influences p130Cas localization and Rac1 activity during cell migration.* J Cell Biol, 2005. **168**(5): p. 813-24.
204. Kisseleva, M., et al., *The LIM protein Ajuba regulates phosphatidylinositol 4,5-bisphosphate levels in migrating cells through an interaction with and activation of PIPKI alpha.* Mol Cell Biol, 2005. **25**(10): p. 3956-66.
205. Montoya-Durango, D.E., et al., *Ajuba functions as a histone deacetylase-dependent co-repressor for autoregulation of the growth factor-independent-1 transcription factor.* J Biol Chem, 2008. **283**(46): p. 32056-65.
206. Hou, Z., et al., *LIM protein Ajuba functions as a nuclear receptor corepressor and negatively regulates retinoic acid signaling.* Proc Natl Acad Sci U S A, 2010. **107**(7): p. 2938-43.
207. Sharp, T.V., et al., *LIM domains-containing protein 1 (LIMD1), a tumor suppressor encoded at chromosome 3p21.3, binds pRB and represses E2F-driven transcription.* Proc Natl Acad Sci U S A, 2004. **101**(47): p. 16531-6.
208. Kim, J.H., et al., *WT1-interacting protein (Wtip) regulates podocyte phenotype by cell-cell and cell-matrix contact reorganization.* Am J Physiol Renal Physiol, 2012. **302**(1): p. F103-15.
209. Sun, G. and K.D. Irvine, *Ajuba family proteins link JNK to Hippo signaling.* Sci Signal, 2013. **6**(292): p. ra81.
210. Sharp, T.V., et al., *The chromosome 3p21.3-encoded gene, LIMD1, is a critical tumor suppressor involved in human lung cancer development.* Proc Natl Acad Sci U S A, 2008. **105**(50): p. 19932-7.
211. Ghosh, S., et al., *LIMD1 is more frequently altered than RB1 in head and neck squamous cell carcinoma: clinical and prognostic implications.* Mol Cancer, 2010. **9**: p. 58.
212. Huggins, C.J., M. Gill, and I.L. Andrulis, *Identification of rare variants in the hLIMD1 gene in breast cancer.* Cancer Genet Cytogenet, 2007. **178**(1): p. 36-41.
213. Tanaka, I., et al., *LIM-domain protein AJUBA suppresses malignant mesothelioma cell proliferation via Hippo signaling cascade.* Oncogene, 2013.
214. Elsum, I., et al., *The Scribble-Dlg-Lgl polarity module in development and cancer: from flies to man.* Essays Biochem, 2012. **53**: p. 141-68.
215. Doggett, K., et al., *Loss of the Drosophila cell polarity regulator Scribbled promotes epithelial tissue overgrowth and cooperation with oncogenic Ras-Raf through impaired Hippo pathway signaling.* BMC Dev Biol, 2011. **11**: p. 57.
216. Cai, J., et al., *The Hippo signaling pathway restricts the oncogenic potential of an intestinal regeneration program.* Genes Dev, 2010. **24**(21): p. 2383-8.

217. Barry, E.R., et al., *Restriction of intestinal stem cell expansion and the regenerative response by YAP.* Nature, 2013. **493**(7430): p. 106-10.
218. Xin, M., et al., *Hippo pathway effector Yap promotes cardiac regeneration.* Proc Natl Acad Sci U S A, 2013. **110**(34): p. 13839-44.
219. Bai, H., et al., *Yes-associated protein regulates the hepatic response after bile duct ligation.* Hepatology, 2012. **56**(3): p. 1097-107.
220. Dougherty, M.K. and D.K. Morrison, *Unlocking the code of 14-3-3.* J Cell Sci, 2004. **117**(Pt 10): p. 1875-84.
221. Yoshida, K., et al., *JNK phosphorylation of 14-3-3 proteins regulates nuclear targeting of c-Abl in the apoptotic response to DNA damage.* Nat Cell Biol, 2005. **7**(3): p. 278-85.
222. Tsuruta, F., et al., *JNK promotes Bax translocation to mitochondria through phosphorylation of 14-3-3 proteins.* EMBO J, 2004. **23**(8): p. 1889-99.